12-2010

Late Paleozoic deformation in the Osgood Mountains and Dry Hills, northern Nevada

Samuel A. Siebenaler
University of Nevada, Las Vegas

LATE PALEOZOIC DEFORMATION IN THE OSGOOD MOUNTAINS AND DRY HILLS, NORTHERN NEVADA

by

Samuel Anthony Siebenaler

Bachelor of Science
Winona State University
2006

A thesis submitted in partial satisfaction
of the requirements for the

Master of Science in Geoscience
Department of Geoscience
College of Sciences

Graduate College
University of Nevada, Las Vegas
December 2010

UNIVERSITY OF NEVADA LAS VEGAS

THE GRADUATE COLLEGE

We recommend the thesis prepared under our supervision by

Samuel Anthony Siebenaler

entitled

Late Paleozoic Deformation in the Osgood Mountains and Dry Hills, Northern Nevada

be accepted in partial fulfillment of the requirements for the degree of

Master of Science in Geoscience

Wanda Taylor, Committee Chair

Patricia Cashman, Committee Member

Andrew Hanson, Committee Member

Eugene Smith, Committee Member
Chih-Hsiang, Graduate Faculty Representative

Ronald Smith, Ph. D., Vice President for Research and Graduate Studies
and Dean of the Graduate College

December 2010

ABSTRACT

Late Paleozoic Deformation in the Osgood Mountains and Dry Hills, Northern Nevada

by

Samuel Anthony Siebenaler

Dr. Wanda Taylor, Examination Committee Chair
Professor of Geoscience
University of Nevada, Las Vegas

Pennsylvanian (IP) and Permian (P) deposits (Etchart Formation) and structures in the northern Osgood Mountains and Dry Hills are identified and interpreted to reconstruct a late Paleozoic tectonic history for the time between the Antler and Sonoma orogenies. Mapping, field observations, fusulinid-based unit ages, and structural analysis are used to identify three fold and fault sets, a fault set, a fold set, and at least two angular unconformities: the C6 and P1 angular unconformities of Trexler et al. (2003). The N-S striking normal faults of fault set 1 are cut by WSW-ENE striking thrust faults (fault set 2). Sets 1 and 2 are cut by imbricated SW-NE striking thrust faults, the Golconda Thrust (fault set 3). Fault set 3 is offset in the southern Dry Hills by an oblique right-lateral normal fault zone (fault set 4), the Getchell Fault. This offset allows estimation of right-lateral offset of the Getchell Fault ranging from 1.7 km to 8 km and 600 m of throw, since the emplacement of the Golconda Allochthon.

Etchart members contain at least four fold sets. The oldest fold set (F1) is SW-trending, gentle, upright, sub horizontal to gently SW-plunging folds

constrained to Missourian time. F2 folds are WSW-to-ENE trending and gently plunging, open, upright folds. F3 folds are gentle to open, upright to steeply east inclined, NNW-trending and gently plunging. F2 and F3 folds are both interpreted to be Wolfcampian to Leonardian in age based on the age of the youngest unit folded by them. F4 folds are NE-trending and gently plunging, open, upright to steeply inclined folds.

Using crosscutting relationships and parallelism, the structures are interpreted to be the result of at least six deformational events during or after IP and P time. Timing of the oldest four of these deformations is between Atokan and Leonardian stages based on unit ages, stratigraphic relationships, and structural overprinting.

The unconformities along with additional lithologic evidence warrant division of the Etchart Formation into three separate informal members. Interbedded Permian age conglomerates that contain Atokan age clasts require reevaluation of the presence of Battle Formation in the area and indicate Permian uplift and erosion of Pennsylvanian age deposits. Lithologic characteristics of the Etchart members imply that increasing amounts of siliclastic material was shed into the Dry Hills basin from the IP to the early P, coinciding with increased frequency of tectonism and increasingly shallow depositional environments.

Correlation of units in the Dry Hills to those at Edna Mountain, Carlin Canyon, and the Pequop Mountains are used to fit the local structural history of the Dry Hills into the regional tectonic history. The structural and depositional history of

the Osgood Mountains and Dry Hills are plotted along with six other locations to fit a regional scale late Paleozoic deformational history. This analysis suggests relatively “major” regional shortening events in the Atokan and Missourian, resulting in largely parallel structures, and the C6 and P1 unconformities. Several other “lesser” contractional events occur in the region during the Desmoinesian, Wolfcampian, and Leonardian with scattered orientations

TABLE OF CONTENTS

CHAPTER 1

INTRODUCTION

Purpose of Study

Devonian and older sedimentary rocks in northeastern and north-central Nevada generally are considered off-shelf deposits tectonically emplaced atop the shelf rocks of a passive margin (miogeocline) during the Antler and Sonoma orogenies (Fig. 1) (Saller and Dickinson, 1982; Burchfiel et al., 1992). These two orogenies are thought to have occurred in the Late Devonian and Triassic time periods, with a period of quiescence between events early Mississippian to Permian time (Fig. 1). During this period of tectonic quiescence, the marine sedimentary rocks of the Antler Overlap Sequence (AOS) were deposited. Mounting evidence from various workers (cf., Crafford, 2008) argues that this interpretation is likely overly simplistic.

One of the problems with this interpretation is that numerous areas in northern and central Nevada contain documented Late Paleozoic deformation (Fig. 2), such as regionally continuous angular unconformities within the AOS (Fig. 3) (Theodore et al., 1998; Trexler et al., 2003, 2004; Villa, 2008). These unconformities commonly truncate underlying deformation such as thrust faults and folds (Trexler et al., 2003). These structures and their extent are not yet fully understood. The goal of this study is to continue the investigation of these structures to add to the growing evidence for Late Paleozoic tectonism and to assist in the understanding of their regional extent.

This research is significant as these structures formed after the traditionally inferred early Mississippian termination of the Antler Orogeny and prior to the traditional inferred mid-late Permian onset of the Sonoma Orogeny (Fig. 1) (Burchfiel et al., 1992). Several possibilities account for Pennsylvanian and Permian deformation: (a) the timing of one of the orogenies is not properly constrained, (b) the deformation is associated with the little-recognized Pennsylvanian-Permian age Humboldt Orogeny envisioned by Ketner (1977), or (c) the deformation is the result of a previously unrecognized tectonic event. This geologic problem has implications regarding the current interpretation of the Paleozoic geologic history of western North America.

The study area for this research is located in the Dry Hills of Humboldt County (Fig. 4). Northeast of the Osgood Mountains (Figs. 2 & 4) lies one of two lower-elevation outliers to the Osgood Range named the Dry Hills (Fig. 4). The second low-elevation outlier named the Dry Hills lies approximately 25 km north of the southernmost tip of the Osgood range, on the western side (Fig. 4). For clarification, Dry Hills to the northeast of the Osgood Mountains are referred to as the Dry Hills in this document. The Dry Hills to the west of the Osgood Mountains are not discussed further within this work.

Previous maps (Hotz and Willden, 1961; Carlisle and Nelson, 1964; Stewart and Carlson, 1977; Jones, 1991, 1993; Laravie, 2005) indicate that the Dry Hills contain a geologic unit named the Etchart Formation (Figs. 5 & 6) that is Pennsylvanian to Permian in age based on fusulinid derived ages (Hotz and Willden, 1964; Saller and Dickinson, 1982). In previous research, (Hotlz and

Willden, 1964; Stewart and Carlson, 1977; Saller and Dickinson, 1982; Jones, 1991) the Etchart Formation was treated as a single formation. Some researchers (e.g. Laravie, 2005) noted that the Etchart Formation could be informally separated into two units: upper and lower. Thoreson et al. (2000) noted that the Etchart Formation consists of three informal units of relatively equal thicknesses (Fig. 6). The Etchart Formation generally is described in these previous works as interbedded limestone, dolostone, chert, and siliceous conglomerates, with minor sandstone lenses of the Antler Overlap Sequence or tectonic domain.

Saller and Dickinson (1982) studied stratigraphy within the Etchart Formation (Fig. 6) and paleo-current interpretations derived from statistical analysis of imbricated clasts taken from locations at Lone Butte and the Dry Hills. They argue the Dry Hills is a regressive sequence of shelf facies, transitioning to a transgressive sequence of a flooded river delta into an inundated paleo-valley. Jones (1991) interpreted the Etchart Formation to be a part of an accreted terrane named the Dry Hills terrane that is a sub-member of a large tectonic domain, the Antler Overlap Domain (Figs. 7 & 8) (Crafford, 2008).

The Etchart Formation in the Dry Hills has not been investigated for structures or angular unconformities of Pennsylvanian and Permian age despite, being a tectonostratigraphically and tectonogeographically ideal location to do so. Previous structural studies of the area focused largely on the existence of structures as they relate to local ore deposits. Inconsistencies exist in the regional structural interpretations, and a general structural history is lacking for

the Dry Hills Etchart Formation due to its complexity. For these reasons, this research attempts to determine the Pennsylvanian to Permian structural history for this area using faults, folds, and angular unconformities. The hypotheses this research tests are that folds, faults and associated unconformities

1. can be documented in the Dry Hills to have formed during Pennsylvanian and Permian time;
2. record a sequence of multiple late Paleozoic structural events that can be used to infer the local structural history and shortening direction; and
3. represent one or more tectonic events that occurred at a greater-than-local scale, and thus can be correlated to other areas of Nevada.

To provide a regional context, correlations of the newly documented geologic history of the Dry Hills Etchart Formation are made to other locations in Nevada where Pennsylvanian and Permian deformation occurred.

Significance

This research is significant because the presence of Late Paleozoic deformation requires redefinition of our current understanding of the evolution of the western United States. Inaccuracies in our conceptions of this history inhibit accurate paleo-geographical and plate margin reconstructions. Recognition of tectonic events prior to the traditional timing of the Sonoma Orogeny may require a reevaluation of the tectonic model for emplacement the Golconda allochthon (Fig. 1).

The Dry Hills, the Osgood Mountains, and the surrounding area are locations of economic interest in northern Nevada. To the southeast of the Dry Hills, the Turquoise Ridge Joint Venture is operated by Barrick Gold Corporation and the Twin Creeks Mine operated by Newmont Gold Corporation (Fig. 4). Twin Creeks has mined Carlin-type gold deposits from the Etchart Formation (Fig. 4, 5, and 9) while both mine sites have extracted gold from the underlying Ordovician Valmy and Comus Formations. The ore deposits in the area are both structurally and stratigraphically controlled (Thoreson et al., 2000). Late Paleozoic deformation will also have deformed ore bearing areas of the older Valmy Formation and portions of the lower Etchart Formation. This research is significant on a local level, as a greater structural understanding of the units within this area is valuable for economic resource deposit exploration.

CHAPTER 2

BACKGROUND

The following background focuses on deposition and structural deformation between the Devonian and Triassic in western North America, which is relevant to the problem addressed herein. Younger deposition and structural deformations are mentioned but not thoroughly discussed. For a more complete background of western United States tectonic history see Burchfiel et al. (1992).

Antler Orogeny

The Antler Orogeny (Figs. 1 & 10) was first proposed by Roberts et al. (1958) to explain Ordovician basinal strata thrust over Ordovician to Devonian shelf to inner shelf strata as recognized by Merriam and Anderson (1942). This orogeny was originally proposed to occur from the Mississippian (based on the age of foreland basin deposits) to Late Pennsylvanian (based on the age of the oldest overlap sediments) (Roberts et al., 1958).

The Antler Orogeny has been defined by subsequent workers as a Devonian to Mississippian contractional event responsible for emplacing deep-ocean sedimentary and igneous rocks eastward over passive margin (miogeoclinal) strata (e.g., Kerr, 1962; Hotz and Willden, 1964; Burchfiel and Davis, 1972; Poole, 1974; Smith and Ketner, 1977). The rocks emplaced were mainly Cambrian to Ordovician deep-marine chert, argillite, greenstone, minor sandstone, quartzite, limestone, and mafic volcanic rocks (e.g., Roberts et al., 1958; Hotz and Willden, 1964). These eastward-thrust units are referred to as the Roberts Mountain allochthon (Figs. 1 & 11). The allochthon is estimated to

be up to 5 km thick with estimates of 100 to 200 km of lateral overlap in the modern geographical setting (Poole et al., 1992). Effects of the Antler Orogeny may reach as far north as the Canadian Cordillera (Nilson and Stewart, 1980; Gehrels and Smith, 1987; Turner et al., 1989; Smith et al., 1993). The main fault responsible for the emplacement of the Roberts Mountain Allochthon is named the Roberts Mountain thrust.

The timing of the Antler Orogeny is largely constrained by the ages of sediments within the foreland basin. Oldest sediments within the foreland basin indicate the Antler Orogeny started during latest Devonian time (Poole, 1977; Dickinson, 2001). As dated using conodont biogeochronology, the youngest sediments deposited in the foreland basin are Mississippian in age (Roberts et al., 1958; Dickinson, 2001). Timing of the orogeny is still debated due to poor exposures, scarcity of fossils, complex structural history subsequent to emplacement, and lack of consistently detailed maps.

Uplift of the Roberts Mountain Allochthon sub-aerially exposed a portion of the upper plate referred to as the Antler highlands (Poole, 1974; Poole and Sandberg, 1977). The related crustal loading resulted in flexural subsidence that created a foreland basin (Figs. 1& 10) filled with recycled orogenic sediments (Dickinson et al., 1983; Dickinson and Gehrels, 2000; Gehrels and Dickinson, 2000). The basin originated in the latest Devonian and continued into Mississippian time (e.g., Smith and Ketner, 1968; Poole, 1974; Dickinson, 2000). Conclusive evidence that the Antler Orogeny was accompanied by magmatism,

penetrative regional deformation, or metamorphism within the allochthon has been found (Speed and Sleep, 1982).

Timing uncertainties inhibit the definition of exactly what package of rocks actually composes the Antler thrust plate (Saucier, 1997). For example, “Antler-age” folds and thrusts are documented in carbonates below the RMA (Stewart and Palmer, 1967). Some believe this deformation is merely parautochthonous (Speed and Sleep, 1982; Jansma and Speed, 1993, 1995), inferring the traditional timing of deformation. Some have used this to argue the RMT as a “roof thrust” to a larger thrust complex. This interpretation enlarges the package of rocks considered to be a part of the RMA and stretches the timing of deformation later than Mississippian to account for deformation in rocks of these ages (Carpenter et al., 1993; Saucier, 1997).

Crafford (2008) argued that lithology, provenance, juxtaposition data, and depositional environment interpretations from throughout Nevada imply that the Roberts Mountain Allochthon is not a single allochthon emplaced during a single regional thrusting event. Rather, Crafford (2008) conceptualizes that rocks assigned to the Roberts Mountain Allochthon are actually the composite remnants of several tectonic domains emplaced into their current positions by multiple tectonic episodes throughout the Paleozoic and Mesozoic (Figs. 7 & 8). These include post-Antler Orogeny related events. To further support this interpretation, Crafford (2008) notes that structural studies indicate that upper Paleozoic and Mesozoic rocks in Nevada and California are displaced tens to

hundreds of kilometers along strike-slip faults during the Late Paleozoic to the Cretaceous.

In the modern-day continental configuration, exposure of the Roberts Mountain allochthon is limited due to erosion and burial (Fig. 8). The location of the Antler Allochthon is best defined by outcrops interpreted as sediments of the Antler Foreland Basin (Figs. 1 & 2). The western edge of the foreland basin trends generally north/south through central Nevada, terminating to the north in southern Idaho, and to the south in southern Nevada (Roberts et al., 1958; Poole, 1974).

In the Dry Hills, the Roberts Mountain Allochthon is represented by the Ordovician Valmy Formation. In the northern Osgood Mountains, the Valmy Formation is exposed over the Preble Formation. In the Dry Hills, the Valmy Formation unconformably underlies the Etchart Formation, and is sporadically exposed in the southernmost portions of the Dry Hills, where it is mined for its gold ore.

The eastern edge of the Antler thrust belt is ~140 km to the east of the Dry Hills (Fig. 11). The Osgood Mountains and Dry Hills host rocks interpreted to be from both the lower and upper plates of the Roberts Mountain Thrust (Figs. 5 & 9) (Berger, 1975; Boskie and Schweickert, 2001; Laravie, 2005). The Antler lower plate is interpreted to be composed of the Cambrian Preble and Ordovician Comus formations (Berger, 1975). These formations underlie the Etchart Formation and Havallah Sequence in the Dry Hills (Figs. 5 & 9). On the western side of the northern tip of the Osgood Mountains, the Etchart Formation overlies

the Preble Formation. The contact between the two units is either an angular unconformity or a fault contact.

The driving tectonic stresses and plate-boundary conditions responsible for the Antler Orogeny are still not thoroughly understood. Some authors (Burchfiel and Davis, 1972; Schweickert and Snyder; 1981; Miller and Hardwood, 1990; Poole, 1992) invoke a scenario (Fig. 1) in which subduction caused volcanic arc accretion and back arc contraction to emplace the Roberts Mountain Allochthon on the continental edge, as first proposed by Moore (1970). This model is the “classic’ model for the Antler Orogeny. However, there is no consensus about the origin of the Antler belt.

Nielson and Stewart (1990) noted that at least ten different models are proposed for the Antler Orogeny. A relatively popular model proposed by Speed and Sleep (1982) states the Roberts Mountain Allochthon was an accretionary prism emplaced in front of a volcanic arc that collided with western North America. This scenario (and others proposed) requires remnants of a volcanic arc west of the allochthon. These volcanic arc rocks have not yet been definitively located. Some suggest that the volcanic rocks within the lower Klamath Mountains are the remnants of the volcanic arc (Burchfiel and Davis, 1972; Davis et al., 1978; Schweickert and Snyder, 1981; Poole et al., 1992). Others dispute this suggestion, arguing that constraints on the paleogeography of these locations is insufficient and that the volcanic rocks currently in these locations originated much farther away (Jones, 1990; Stevens et al., 1990; Stevens et al., 1992; Crafford, 2008). Some researchers (Speed and Sleep,

1982; Burchfiel and Royden, 1991) suggest that the remnants of the arc are not exposed and that they are buried by either sediments or subsequent thrust sheets.

Crafford (2008) favors a model in which the Antler Orogeny was not actually a compressive orogeny, but the accretion of distinct terranes along one or more transpressive plate boundaries (Figs. 7 & 8). She favors initiation of subduction and arc volcanism in the Mesozoic. Transpression would have resulted in episodic thrusting and faulting, account for the spatial distribution of Devonian to Mississippian sediments as is observed, and does not require a subsided arc (Crafford, 2008). However, if this theory is correct, the Antler Foreland Basin is not a true foreland basin, and may have been misidentified due to the sporadic exposure of units assigned to the Antler Foreland Basin.

Much of the controversy regarding the Antler tectonic model is due to the fact that no one proposed model accounts for all aspects of the orogen (Burchfiel and Royden, 1991). Each proposed tectonic setting conflicts with geologic evidence from the Antler belt in some manner (Burchfiel and Royden, 1991)

Antler Overlap Sequence

Based on fossil ages from the Inskip Formation of the eastern Range, clastic and carbonate rocks began to be deposited unconformably above deformed Devonian-Ordovician rocks of the Antler orogenic belt or RMA during the Mississippian. These deposits were named the Antler Overlap Sequence (AOS) by Roberts et al. (1964). They suggested that these rocks were deposited such that they onlapped the RMA and overlapped lithologic assemblages both east

and west of the Antler Orogenic belt. This overlapping relationship demonstrates the end of the Antler Foreland Basin fill. Recently, in light of growing evidence, some researchers (Crafford, 2008) began suggesting that the AOS or portions of it constitute foreland basin sediments from tectonically emplaced terranes during Pennsylvanian and Permian time.

The AOS is a valuable age constraint for Antler-related deformation because the AOS laterally overlaps all previously deposited and emplaced units. Because the ages of its units are well known, the AOS represents the traditional or classic end of the Antler Orogeny.

From stratigraphically lowest to highest, the AOS consists of the Inskip Formation, or basal conglomerates such as the Iron Point and Battle Formation. Those units, where and if present, are overlain by Pennsylvanian and Permian limestone and dolostone given various names locally including the Highway, Ely, Etchart, Edna Mountain, Strathearn, and Buckskin Mountain formations as well as others (Fig. 12). Generally, the Pennsylvanian to Permian limestone and dolostone units in the upper AOS are thought to represent a continuous, long-lived, non-tectonically influenced depositional episode (Poole, 1974; Poole and Ketner, 1980). However, ongoing recent research focuses on temporally correlating these units based on biogeochronology and regionally persistent angular unconformities within the sequence (Trexler et al., 2003; Villa, 2008; Cashman et al., 2008) to determine whether the AOS actually represents a series of tectonically-induced depositional events (Fig. 3). Their conclusions are

that the deposition occurred within local- to-regional scale, tectonically-created basins.

The AOS rests unconformably over older sedimentary rocks in all locations where the base of the sequence is exposed. In some locations, the basal unit is the Battle Formation, which has been interpreted as a basal lag deposit created by erosion of the Antler Highlands (Roberts et al., 1964). In other locations, upper portions of the AOS sit unconformably atop the Roberts Mountain Allochthon or Antler orogenic belt. The contact between the Battle Formation and the carbonates that overlie it has been described as both unconformable and conformable (e.g., Saller and Dickinson, 1982; Roberts et al., 1964; Hotz and Willden, 1964; Erickson and Marsh, 1974).

The Battle Formation is a poorly sorted and silica cemented pebble to boulder conglomerate, with sub-angular chert and quartzite clasts. It was first named and described by Roberts (1951) after identification of a type section at Battle Mountain, Nevada. In the type section, the matrix is typically red in color and composed of sand- to clay-sized grains. Roberts (1951) divided the formation into three parts at the type locality: upper, middle, and lower. The lower Battle Formation is thickly bedded and solely conglomerate (Roberts, 1951). The middle Battle Formation is interbedded conglomerate, sandstone, shale, and calcareous shale (Roberts, 1951). The upper Battle Formation contains smaller clasts (pebble to granule) and is interbedded with sandstone, limestone, shale, and calcareous shale (Roberts, 1951). However, it should be noted that since being named and recognized, the Battle Formation name has been also been

applied to conglomerates within the overlap sequence that are not basal and that are not necessarily age equivalent or correlative.

In locations where it overlies the Osgood Mountain Quartzite, such as the Osgood Mountains, the quartzite clasts appear to be composed of the same rocks that they overlie (Willden, 1964). In some locations the Battle Formation is up to 600 feet thick (Roberts, 1964) and is absent at the base of the AOS elsewhere (Sweet and Snyder, 2002; Trexler et al., 2003; Villa, 2008). As a consequence of previously defining the AOS as a single continuously deposited succession, the Battle Formation previously was misidentified in some areas as other conglomerates within the AOS, such as the older Iron Point conglomerate at Edna Mountain (Villa, 2008).

The upper units of the AOS are typically in thrust contact with the Golconda Allochthon, thus, a total thickness for this unit is unknown. The observed thicknesses of Pennsylvanian and Permian units in the eastern Great Basin range between 8725 to 20,500 feet or 2659 to 6248 meters (Bissel, 1964). The unconformities present at its base, as well as within the AOS suggest the thickness of the AOS varied laterally during deposition and afterward.

Antler Overlap Sequence in the Dry Hills

The research location was selected based on previous geologic maps (Willden, 1961; Carlisle and Nelson, 1964; Stewart and Carlson, 1977; Jones, 1991) of the Dry Hills that show Pennsylvanian to Permian age limestone, chert, and minor volcanic rocks interpreted as part of the AOS (Fig. 5). The Etchart Formation was identified in the Osgood Mountain area as Pennsylvanian in age

and occurring only in this region (Willden, 1961). These unit ages were based on crosscutting relationships and implied stratigraphic relationships from other dated units (Willden, 1961). These dates have been confirmed by fusulinid dates of Atokan age from the Lower Etchart member on the top of Lone Butte (Fig. 4), in the far southeast of the Osgood Mountains (Verville and Sanderson, 1988).

The geographical location of the Dry Hills allows for correlation of deformation to Edna Mountain (Villa, 2008), Battle Mountain (Verville and Sanderson, 1988), and Carlin Canyon (Trexler et al., 2003) (Fig. 2). The geographical location is also ideal as it is on the easternmost edge of the Golconda Allochthon. This location is also the farthest north location specifically identified for Late Paleozoic deformation.

Previous stratigraphic descriptions of the Etchart Formation within the Dry Hills informally sub-divide the formation into three, two, and no subordinate members (Willden, 1961; Thoreson et al., 2000; Laravie, 2005). The lower member subdivided out of the Etchart Formation is silty chert, carbonate, argillite, and minor sandstone (Thorseson, 1992). The upper unit is grainstone, packstone and wackestone (Saller and Dickinson, 1982; Thorson, 1992).

At Lone Butte, the Etchart Formation was interpreted to be an alluvial deltaic to a shallow marine transgressive sequence (Saller and Dickinson, 1982). The Etchart Formation sediment deposition in this area is thought to be the result of regional subsidence in early Atokan time (Saller and Dickinson, 1982). Sedimentation terminated as relative sea level rise filled the paleovalleys of a deltaic-source paleoriver during the Pennsylvanian, eventually becoming

completely inundated by the sea (Saller and Dickinson, 1982). Inundation initiated the carbonate deposition of the lower AOS in this area, which is represented by the Highway Formation and Lower Etchart limestone (Saller and Dickinson, 1982). The Lower Etchart member carbonates yielded an Atokan fusulinid age implying this inundation was complete by the mid-Pennsylvanian (Verville and Sanderson, 1988), at least for the exposures of the Lower Etchart at Lone Butte.

The Etchart Formation was extensively studied for conodont and depositional lithofacies by Johnson (1987). Johnson (1987) measured six sections of the Etchart Formation in the Dry Hills, collected samples at outcrops and drill cores which were processed for conodonts and used to produce thin sections. Johnson (1987) subdivided the Etchart Formation into three sub-units, upper, middle, and lower, but does not discuss how or where these subdivisions are made. His work recognized 10 separate lithofacies consistent with deposition in a near shore, high energy environment for the Lower and Middle Etchart, and a near storm base or wave base for the Upper Etchart. He also identified six conodont zones that range in age from mid-Missourian to post-early Aktastinian (Artinskian). Johnson (1987) interpreted the sea level change recorded in the Etchart as being a tectonically initiated, shallow water, regressive sequence terminated by an early Permian abrupt transition to transgression and deeper water facies.

Ancestral Rocky Mountains

During Pennsylvanian to Permian time, regional, intra-plate, mid-continent, basement-involved uplift created a series of highlands with associated flexural basins throughout much of Texas, New Mexico, Colorado, and Utah, that are referred to as the Ancestral Rocky Mountains (ARM) (Kluth and Coney, 1981; Geslin, 1998). The coeval timing of uplift and basin creation, as well as similarities in geometry, implies formation in a unified regional event (Ye et al., 1996). The tectonic interactions that created this event are not well understood and remain controversial, largely due to the ARM's distance from plate margins thought to have been tectonically active in the Pennsylvanian and Permian. Multiple theories exist regarding the tectonic driving mechanism for this deformation. Simplified, they theorize that the ARM deformation could be the result of:

- The breakup of Laurentia in response to a continent - continent collision along the Ouachita-Marathon orogenic belt, similar to the modern breakup of Eurasia in response to the collision of India into China (Kluth and Coney, 1981; Kluth, 1986; Kluth et al., 1998).
- Shallow slab subduction off the southwestern edge of North America along the Andean-type margin along east-central Mexico (Ye et al., 1996).
- Reactivation of Proterozoic rift structures in response to compressional stresses from more distant plate margins such as the Ouachita-Marathon orogenic belt (Marshak et al., 2000).

- Stress generated by the sequential subduction of oceanic plates along the Ouachita-Marathon suture (Dickinson and Lawton, 2003).

Uncertainty also remains as to the aerial extent of the ARM deformation. Researchers who favor the theory of Ye et al. (1996) that shallow slab subduction extend the ARM deformation as far west as north-central Nevada. This supports the interpretation that the Roberts Mountain Allochthon was uplifted during the ARM deformation creating flexural subsidence that formed the Paradox Basin (Barbeau, 2003). This interpretation is debated. Researchers that favor theories in which ARM formation is driven by plate interactions along the Ouachita-Marathon belt tend to recognize the region effected by ARM deformation as terminating east of the Roberts Mountain Allochthon and do not recognize ARM deformation within Nevada (e.g., Dickinson and Lawton, 2003).

Recently, Nesse (2008) called for distinction between ARM uplifts to reflect the differences in timing, location, and sedimentation as well as to clearly separate Pennsylvanian-age structures from later uplifts. Nesse (2008) separated the Ancestral Rocky Mountains into three uplifts of different ages. Based on Pennsylvanian isopachs, Nesse (2008) estimated that the western extent of the Pennsylvanian uplift is on the western side of the Paradox basin in Utah.

Humboldt Orogeny

The Humboldt Orogeny was first described by Ketner (1977) as a regional scale, Pennsylvanian-age unconformity at Carlin Canyon, near Carlin, NV. The Humboldt Orogeny remains controversial. As originally conceptualized, the

Humboldt Orogeny is a contractional event that produced north-south shortening and resulted in a foreland wedge of clastic sediments that are contained in the modern day Strathearn Formation of northern Nevada (Ketner, 1977).

The greatest reason for controversy regarding the Humboldt Orogeny was that deformation associated with the tectonic event was only recorded in and near Carlin Canyon. A late Pennsylvanian-age unconformity present within the Strathearn Formation extends into Utah (e.g., Steele, 1960; Snyder, 1984), but is angular only in central Nevada (Jansma and Speed, 1990). Some (Jansma and Speed, 1990) have speculated that the unconformity (at least in the Carlin Canyon area) is not truly angular, but the result of low-angle attenuation faulting during the late Mesozoic contraction that resulted in the Sevier, Eureka/Central Nevada, and Winnemucca thrust belts (Fig. 13).

Debate exists as to what effect the Humboldt Orogeny had on the area, as well as its regional extent. The Humboldt Orogeny is depicted as uneven epeirogenic uplift with associated basins (Snyder et al., 2000; Barbeau, 2003). Such uplifts are similar to the structural style of the Ancestral Rocky Mountains. The similarities in style and age led some authors (e.g., Dickinson, 2001) to assume that the same formation mechanisms are responsible for both events. This interpretation is controversial because the Pennsylvanian paleogeography of Nevada, as well as the rest of the western United States is still poorly understood (Hoy and Ridgway, 2002) and evidence of the Humboldt Orogeny is farther west than the isopach-interpreted edge of the Ancestral Rocky Mountain deformation (Nesse, 2008). As a whole, the Humboldt Orogeny currently

remains so poorly understood that it is commonly overlooked or ignored in tectonic histories of the area, despite evidence for its occurrence.

Unresolved Late Paleozoic Deformation

While many studies of northern Nevada have noted Late Paleozoic deformation at specific locations, this time period is still not widely recognized as tectonically active. Generally speaking, this is largely due to a lack of data to determine the deformation's extent and intensity, and that it is not well enough understood to name it.

This new focus thus far has utilized identification of regionally correlated unconformities created by underlying Pennsylvanian-to-Permian structures (Fig. 3) (Stone and Stevens, 1988a; Snyder et al., 2000; Theodore et al., 2003; Trexler et al., 2003). These structures and angular unconformities are farther west than any temporally equivalent deformation (Fig. 2) and appear to have occurred over a longer period of time. The deformations also occur with different orientations and greater period of time than the Humboldt Orogeny of Ketner (1977).

Sonoma Orogeny

From Permian to Triassic time, collision of the Sonoma volcanic island arc with North America resulted in the Sonoma Orogeny (Speed, 1979; Brueckner and Snyder, 1985; Burchfiel, 1992). This orogeny is characterized by the eastward movement of late Devonian to middle Permian age sandstone, chert, argillite, greenstone, limestone, conglomerate and volcanic rock (Silberling, 1973; Speed, 1979; Babaie and Sleep, 1990; Rilely et al., 2000). These sediments are interpreted to have been deposited in a distant ocean or back arc basin. This

package of rocks was thrust eastward above the western part of the Antler Allochthon and became known as of the Golconda Allochthon (Speed, 1971) (Fig. 11). Saller and Dickinson (1983) suggest that during emplacement underlying strata in the footwall of the Golconda Thrust may have been overturned, but no further research indicates specific orientation or shortening direction to support this hypothesis.

The Golconda Allochthon extends over 350 km along strike in the central and northern Great Basin (e.g., Speed, 1971, 1977, 1979; Silberling 1979) The Golconda Allochthon consists of two general lithographic assemblages: (1) the Shoonover Sequence, and (2) the Havallah Sequence, which consists of the Pumpernickel, Jorry, and Trenton formations (Muller, 1951; Roberts et al., 1958; Willden, 1964). Both sequences are characterized by thick successions of chert-lithic and volcaniclastic sandstone interbedded with chert, argillite, greenstone and mudstone (Fagon, 1962; Miller et al., 1984). The Shoonover Sequence is Devonian to Early Permian in age (Fagon, 1962), whereas the Havallah is given an early Mississippian to Permian age (Willden, 1964).

The Sonoma Orogeny is thought to be similar to the Antler Orogeny in some regards, but did not form a foreland basin that has been recognized (Speed and Sleep, 1982). In response to this problem, Babaie and Sleep (1990) speculated that during its emplacement the Golconda Allochthon tectonically shallowed, shoaled, and was unroofed by erosion, following ramping up on the continental margin. This caused a reduction in the tectonic load. Crafford (2008) theorizes that the Sonoma Orogeny began much earlier, in the late Pennsylvanian to early

Permian, and that the units of the AOS represent the syntectonically depositing “foreland basin” formed by flexural subsidence caused by terrane accretion.

Ketner (2008) proposes that the Golconda thrust may not be responsible for emplacement of the Golconda allochthon, and that the Sonoma Orogeny was not an “orogeny” at all. Ketner (2008) proposed that the Havallah Sequence and Devonian-Permian age Inskip Formation were deposited together in a basin to the west of modern day Nevada. These sediments were folded and faulted in the Pennsylvanian, and then compressed and contracted in the Jurassic creating east-verging thrusts in the eastern portion of the basin, and west-verging thrusts in the western portions of the basin.

Crafford (2008) favors an interpretation where the Havallah Sequence is a series of tectonic terranes accreted onto the western edge of North American along a transpressive plate boundary (Figs. 7 & 8). Crafford cites lithological differences within the Havallah Sequence both vertically and laterally as evidence of this interpretation. Crafford (2008) also contests the idea that the Sonoma Orogeny was actually a compressive orogenic event. Crafford (2008) theorizes that the eastward thrust units traditionally associated with the Sonoma Orogeny were the result of strike-slip movement along the continental/oceanic plate margin. Crafford (2008) theorizes that this strike-slip movement resulted in the accretion of tectonic terranes along the western continental edge.

The Golconda is exposed in the northern Osgood Mountains and the Dry Hills. The Golconda thrust strikes generally north through the western slope of the northern Osgood Mountains (Figs. 5 & 15). In the Dry Hills, the Golconda

thrust strikes generally NE through the center of the Dry Hills (Fig. 15). These exposures are interpreted to be the easternmost extent of the Golconda thrust.

Overprinting Events

It is probable that the rocks in the Dry Hills and Osgood Mountains are far removed from their original location of deposition. Northern Nevada underwent multiple orogenic events in the Mesozoic that have deformed and reoriented many Paleozoic rocks in northern Nevada. The Dry Hills are located ~100 km west of the eastern thrust of the Luning-Fencemaker thrust belt, a thrust belt of the thin-skinned Sevier Orogeny (Fig. 13). The eastward displacement of previously deposited and emplaced rocks in the Dry Hills as well as other areas complicates regional correlations. The magnitude of reorientation and transportation on a regional scale for units of this age is largely unresolved.

Within Nevada the sequence of commonly accepted deformational events from oldest to youngest after the Sonoma orogeny are the orogeny that caused the Luning-Fencemaker emplacement, the Sevier Orogeny, the Laramide Orogeny, and Eocene to Quaternary extension associated with the formation of the Basin and Range province (Burchfiel et al., 1992). These events may obscure older folds, faults, and other earlier structures. Oligocene to Miocene extension was associated with volcanic rocks that overlie Late Paleozoic exposures (Stewart and Carlson, 1987).

Cenozoic Extension

The Cenozoic marked the beginning of multiple periods of extension and volcanism throughout Nevada. Extension has continued intermittently to today

and caused uplift of the mountains which expose Late Paleozoic sections. Cenozoic basaltic volcanism resulted in Late Paleozoic rocks being covered by volcanic rocks. Cenozoic extension also formed a north-northwest trending aeromagnetic anomaly that extends nearly from the Nevada-Oregon border to southeastern Nevada named the Northern Nevada Rift (John et al., 2000). The western edge of the Northern Nevada Rift is thought to be located at the northernmost tip of the Dry Hills (John et al., 2000).

Although located nearby, no alteration or deformation consistent with the Northern Nevada Rift has been located within the Dry Hills. Northern Nevada Rift intrusives are dominantly mafic dikes (John et al., 2000) whereas the Dry Hills contains Miocene basalt and andesite. The Dry Hills lack mafic dikes and appear to have been little affected by the Northern Nevada Rift. Thoreson et al. (2000) noted possible parallelism between the rift and high angle normal faults to the east of the Dry Hills in Paradise Valley (Thoreson et al., 2000). However, the Northern Nevada Rift characteristically does not result in deformation visible in outcrop (John et al., 2000).

CHAPTER 3

METHODS

Geologic Mapping

A portion of the Dry Hills and the northern Osgood Mountains was mapped at 1:4000 scale. Previous mapping of this area has been at 1:250,000 (Carlisle and Nelson, 1964; Crafford, 2007), 1:100,000 (Willden, 1961) and 1:24,000 (Laravie, 2005). The nearby Twin Creeks Mine area was mapped at various scales (Bloomstein et al., 1990; Osterberg, 1990; Osterberg et al., 1990; Thoreson et al., 2000). The area covers 20 square kilometers of the Dry Hills and is centered on the eastern areas. The map does not incorporate areas fenced off or otherwise indicated as under private ownership and extends across the following areas:

- Sections 1, 2, 10-16, and 21-23 of T39N, R42E
- Section 36 of T40N, R42E
- Sections 19, 20, and 28-32 of T40N, R43E1

The map infers bedrock formations in places by minimizing the depiction of Quaternary units covering formations. Quaternary units are differentiated where possible by characteristic changes in Quaternary unit surface expression, such as clast size, clast composition, distribution, and matrix color. In locations where outcrop is scarce, Quaternary sediments with characteristics consistent with soils attributed to one of the previously mentioned formations were differentiated on the map as a proxy for outcrop and as an alternative to simply lumping the Quaternary units as undifferentiated.

Mapping focused on identifying major unconformities and documenting structures associated with them. Bedding, fault, and fold orientations were recorded from the outcrop using a Brunton® compass and measuring board. Nearly 600 bedding measurements were recorded within the area (Table 1) (Plate 1). Unit contacts, unconformities, areas lacking exposure, sample locations, as well as fold, fault, and bedding orientations were recorded as separate layers in Adobe Illustrator® on top of the Dry Hills North and Dry Hills South 7.5 minute United States Geological Survey topographic quadrangles.

Effort was taken to locate strain indicators in the field for thin section analysis. All slickenlines were identified on thin chert layers between beds and were assumed to be the result of flexural slip during folding. They were not sampled or analyzed as this movement sense does not present meaningful data regarding fault motion.

The map was originally created at a 1:4000 scale has been scaled to 1:8000 (Plates 1 and 2) due to its large size. This resulted in the removal of some strike and dip measurement data from the map, but has not resulted in exclusion of any mapped unit or structure. A copy of the original 1:4000 scale map has been retained digitally for data integrity.

Fusulinid Biochronology

Fusulinids are a commonly used method of biostratigraphic age comparison in Middle and Late Paleozoic sedimentary rocks. Fusulinids are a sub-member of the phylum foraminifera. They first appear within the fossil record during the Silurian and disappear by the end of the late Permian. Rapid evolutionary

variation makes fusulinids ideal for high resolution biostratigraphy, and these variations are well documented and well understood (Trexler et al., 2003).

Samples from the three identified Etchart members, Havallah Sequence, Etchart Conglomerates, and sandstone channels were sent to Dr. Vladimir Davydov of Boise State University for identification and to provide age brackets for units (Figs. 16 & 17). Twelve samples yielded fusulinids (Table 2), including units both above and below the P1 unconformity, the Upper Etchart member, the Middle Etchart member, and clasts within the conglomerate within the Upper Etchart member.

Fold and Fault Analysis

Recorded fold orientations were analyzed for number of deformational events and then compared by relative age. This analysis was conducted using both field observations and statistical analyses. Field observations involved fold recognition, description, and geometry measurements. Stereographic analysis was performed with StereoWin® (Allmendinger, 2009) to calculate the current and original fold axis attitude, hinge orientation, and interlimb angles, based on fold geometry data (Figs. 18, 19, 20, & 21). One set of stereograms was generated for each of the three Etchart members that contain fold hinges. Bedding measurements were also taken around folds and then plotted as great circles to determine hinge and orientation along with interlimb angles. Together, these methods were used to determine the overall fold geometries and number of deformational events.

Fault orientations also were analyzed using stereograms. This analysis was used in conjunction with map data to identify fault sets and to attempt removal of rotation from fault blocks. This information was used to aid both the retrodeformation of cross sections and reconstruction of the structural history for the area. The geometries of the faults and folds were compared and analyzed for geometries that implied shared deformational origin.

Cross Sections

Cross sections were selected to cross areas of geologic interest using standard methods. Cross sections with no vertical exaggeration were created overlapping in a grid pattern, to portray a three dimensional distribution of the Etchart Formation and structures in the Dry Hills (Plates 1 and 2). These cross sections are used to aid in visualization, as well as aid in the construction of a structural history.

Step-wise retrodeformation was attempted on the cross sections to reconstruct the tectonic and depositional history of the Dry Hills. It aided in reconstructing the tectonic history, but was limited by the number and orientations of deformations in and out of the section that prevented assumptions of plane strain. Step-wise retrodeformation was undertaken as it quickly and easily conveys the complicated history of the region. The retrodeformed cross sections were used to create conceptualized three-dimensional diagrams of a stepwise retrodeformation for the Dry Hills area (Figs. 22, 23, & 24).

Fold orientation and fault block recognition were used in reconstruction of fault block rotations. An average value was calculated for the hinges of the

youngest fold set. Fault blocks containing these folds were then reoriented such that the folds all were parallel to the average value, in order to calculate the new average orientation of the next oldest fold set. The process was repeated to make estimates of fault-bound blocks' previous orientations, to estimate the magnitude of fault block rotation in the Dry Hills, and to test whether separated fold sets were a single fold set reoriented by faulting. These fault block rotations were used to increase accuracy of the block diagram models, and were used to help reconstruct and visualize the area three-dimensionally.

Quaternary Mapping

This mapping subdivided Quaternary units based on changes in observable surface characteristics that are the result of weathering of the underlying rock and used this information to identify of what rocks underlay the Quaternary units. The Etchart Formation, Havallah Sequence, and unnamed Miocene basalt all erode with distinct characteristics, such as soil color and grain size distribution. This mapping technique has been successful; the Quaternary units differ based on clast counts, sieving, and description (Fig. 25). Mapped Quaternary units were compared to the United States Department of Agriculture Soil Survey of Humboldt County, Nevada to correlate Quaternary units to soil profiles for the Dry Hills. Rather than map all Quaternary units covering underlying rock as a single Quaternary undivided unit, the Quaternary soils were divided based on characteristic visibly defined changes.

Sieving

To provide evidence that the sub-divided Quaternary units were different units, a soil sample was collected from each unit. The sample size was 500 g or larger. Samples were collected with a shovel from at least 4 inches below the surface. Holes that samples were collected from were dug a minimum of 1.5 ft. in diameter to prevent inclusion of surface material. The samples were weighed and sieved after being allowed to dry. The size distribution of samples was calculated by weight percentage of each particle size (Fig. 25). The results were then used to plot the soil types on a standard USGS soil textural ternary plot (Fig. 25).

Thin Sections

Thirteen samples were chosen for thin sectioning based on quality of the cut billet. The thin sections were created by Quality Thin Sections of Tucson, Arizona. The summary of results from these thin sections is presented in Table 3.

These thin sections were created to further characterize newly recognized units and provided evidence for their distinction. Thin sections from within the Etchart members were stained for calcite to distinguish carbonate mineral types, as well as to determine the feasibility of future calcite deformation analysis. Thin sections of conglomerates allow for cement and clast component analysis.

Unconformities

Using a system for naming unconformities, Trexler et al. (2003) and Cashman et al. (2008) recognized and classified six Carboniferous unconformities (C1-C6),

five Permian unconformities (P1-P5), and two Triassic unconformities (T1 and T2) (Fig. 3). These include the unconformity associated with uplift during the classic Antler Orogeny (C1), the surface of the filled Antler foreland basin (C2), and onset of the Sonoma Orogeny (T1). The remaining unconformities are not yet correlated with specific tectonic events. The C5 and P1 appear to be the most regionally significant from previous works (Cashman et al., 2008).

Additional focus during mapping was placed on recognizing and locating angular discordances between bedding surfaces to identify angular unconformities such as those recognized in other IP to P age sections of northern Nevada (Fig. 3) (Cashman et al., 2008). When found, outcrops above and below the contact were searched for samples containing fossils to be relatively age dated using biochronological methods. When these samples were not available, unconformities were constrained using superposition and crosscutting relationships, where available. Deformation beneath angular unconformities was documented. Unconformities located in the Dry Hills were assigned names based on the naming standards outlined by Trexler et al. (2003) (Fig. 3).

CHAPTER 4

DATA

Geologic Map

Mapping of the Dry Hills was completed between June, 2007 and April, 2008. The mapping was conducted at a scale of 1:4000, but has been included in this document at 1:8000. The 1:8000 scale map still contains all the units, contacts, and structures of the 1:4000 map. The map area covers approximately 20 km^2, the largest area of exposed and accessible Etchart Formation in the Dry Hills. The large majority of the eastern edge and a portion of the southern edge of the map area are defined by the fence of privately-owned mine property.

In other directions, the extent of the map area is dictated by unit exposures. The northern border of the map area incorporates the Miocene volcanic rocks but terminates where Miocene volcanic rocks and Quaternary alluvium deposits conceal Etchart Formation exposures. Previous mapping (Willden, 1961; Carlisle and Nelson, 1964; Stewart and Carlson, 1977) shows no Etchart Formation exposures north of the Miocene volcanic rocks in the Dry Hills. To the west, the map area includes a limited amount of the Havallah Sequence that was mapped in order to distinguish the hanging wall of the Golconda thrust. The amount of Havallah Sequence mapped was minimized due to limited exposure and the limited usefulness of the Havallah Sequence in clarifying the late Paleozoic deformation problem.

Stratigraphic Succession

Map and field observations were used to define stratigraphy. These observations utilized the following methods:

1. Lithologic characteristics
2. bedding orientation measurements,
3. fold measurements (Tables 4 & 5),
4. fault orientations.

The map subdivides the Etchart Formation into three members. The beds of all three Etchart members are upright based on ages returned from sampling. Regionally beds tend to strike NE-SW and dip gently towards the northwest. Therefore, most of the stratigraphically highest Etchart member is exposed in the northwest, whereas the stratigraphically lowest Etchart Formation is commonly exposed in the southeast. Faults and folds disrupt this trend at outcrop scale.

These members have distinctive lithologies and are separated by angular unconformities. The Etchart members are overthrust by the Havallah Sequence exposed in the west (Hotz and Willden, 1964; Stewart and Carlson, 1977; Thoreson et al., 2000; Laravie; 2005, this research). In northern locations, the Havallah Sequence and Etchart members are unconformably overlain by unnamed Miocene basalt and andesite (Fig. 26).

The oldest stratigraphic unit exposed in the eastern Dry Hills is the Ordovician age Valmy Formation (Figs. 6 & 9). It is unconformably overlain by the Lower Etchart member. This contact is only exposed in the southernmost part of the map area, Etchart Hill. The contact is an abrupt, unconformable transition from

truncated beds of light gray Valmy Formation argillite to dark black micrite of the Lower Etchart member.

Etchart member thicknesses represented in the stratratigraphic column (Fig. 27) were calculated using standard thickness calculation methods from map data. Multiple faults and folds in the area along with Quaternary alluvial cover reduced the precision of the member thickness estimates. The member thicknesses calculated in this manner are presented as a minimum.

Previous work interpreted the Etchart Formation in the eastern portion of the Dry Hills to be Pennsylvanian to Permian age Antler Overlap Sequence carbonates and conglomerates, e.g. Battle Formation conglomerate and Etchart limestone undifferentiated (Hotz and Willden, 1964; Laravie, 2005). My work identifies four conglomerates stratigraphically within the Pennsylvanian and Permian units of the Dry Hills that each differ in clast type, size, sorting, and matrix properties. The classic definition and interpretation of the Battle Formation is a basal conglomerate to the Antler Overlap Sequence (Hotz and Willden, 1964). It is the lowest overlap sequence unit in all locations that do not contain the Pennsylvanian Inskip Formation (Willden, 1964). Differences in unit characteristics and apparent differences in stratigraphic position imply that the two conglomerates within the Upper Etchart member are not part of the same depositional episode and are the result of different erosion and deposition mechanisms. For these reasons the conglomerates are recorded as separate map units.

Lower Etchart Member

The lower Etchart member is a very thin to thick-bedded, dark gray (N3) silty dolostone, wackestone, and micrite that weathers to dark gray, medium gray, and light gray, with the dominant color being medium gray (N4) (Fig. 28) The fresh surface can also appear speckled white and medium gray, due to extensive secondary calcite and recrystallization. Some grains are peloids and are commonly dolomitized (Fig. 29). The member is generally moderately to poorly bedded, but is massive in areas and locally contains rare trough cross stratification. The lower member is locally interbedded or interfingered with medium-to-thick chert beds (cm to m scale), sandstone channels and lenses, and very thinly bedded siliceous stringers. The sandstone in channels is white, off-white to light tan, fine-grained, well cemented and well sorted with trough cross stratification visible locally. Some sandstone channels contain wackestone-grainstone carbonate channel fill. The member also locally contains alternating dark and light bands of micrite. The lower section transitions conformably to thick (10's of meters scale) massive black micrite. The member generally lacks fossils. The Lower Etchart member is dated as early Atokan in age based on stratigraphic relationships, making it age equivalent to the Upper Ely, Tomera, and Battle formations (Cashman et al., 2008). The age of the Dry Hills Lower Etchart member is possibly constrained by biochronology of previous works that imply the Lower Etchart member is Atokan. However, lack of recognition of angular unconformities and precision of sample locations in previous works leaves these age dates unreliable.

Middle Etchart Member

The Middle Etchart Member is a dark gray (N6) weathering, dark gray (N6), silty packstone to micrite (Fig. 30). Packstone and wackestone grains are peloids in a calcite and dolomite mud matrix (Fig. 31). The unit is generally thick and poorly-bedded. The middle Etchart member contains interbedded chert beds up to 30 cm thick, silt-to-sand sized calcite grains, calcite and dolomite cement, and very rare fossils. The member weathers to smooth edges, and commonly breaks into small fragments or powder when struck, only rarely breaking into larger fragments. Fossils within the member include moderate to small amounts of fusulinids, conodants, crinoids, coral fragments, pellets, and peloids. Several fusulinid samples from the Middle Etchart produced ages. The age of the Middle Etchart member is equivalent to the Wolfcampian Lower Strathearn Formation of Carlin Canyon (V. Davydov, personal communication) based on the sample taken immediately below the P1 unconformity. The Middle Etchart member is temporally correlative to the late Pennsylvanian Lower Strathearn Formation of the Northern Carlin Trend (Trexler et al., 2004), in northern Nevada, as well as the Fergusson Formation (Sweet and Snyder, 2002), and the limestone of the Antler Peak Formation (Villa, 2008). The Middle Etchart member is separated from the Lower Etchart member by an angular unconformity.

Upper Etchart Member

The Upper Etchart Member is a light to medium gray (5b 5/1 – N1), weathering to medium gray, (N6-N7) mixed siliciclastic and carbonate unit

composed of well-bedded packstone/grainstone containing well-sorted, sand-sized, pelletoid and skeletal grains (Fig. 32). The matrix material is crystalline dolomite, calcite, and quartz. The member contains sporadic, very thin (< 1 cm thick) interbedded siliceous and calcareous siltstone/mudstone. The member commonly contains medium to thickly inter-bedded ribbon chert layers and chert nodules. Interbedded, very thin, silty-sandy stingers are common. Upper Etchart Member beds contain local trough cross stratification and locally thicken and thin. Fossils include abundant fusulinids, conodonts, crinoids, brachiopods, and coral fragments within carbonates of the member. Fossil fragment abundance and lack of mud is diagnostic of the unit in outcrop.

Several samples from the Upper Etchart yielded fusulinids for age control (Table 2). At the stratigraphically highest exposures of the Upper Etchart member, the rocks are age equivalent to the Sakmarian to middle-Kungarian age (V. Davydov, personal communication) Pequop Formation of the central Pequop Mountains (Sweet and Snyder, 2002); this is the youngest age of Upper Etchart member samples. The base of the Upper Etchart member is Wolfcampian age making it equivalent in age to the Upper Strathearn Formation (V. Davydov, personal communication) of the Northern Carlin Trend and the Fergusson Mountain Formation of Nine Mile Canyon of the southern Pequop Mountains (Sweet and Snyder, 2002). The Upper and Middle Etchart members are separated by the P1 unconformity (Fig. 3).

Havallah Sequence

The Havallah Sequence in the western Dry Hills is light gray (N7) on a fresh surface and composed of grainstone, packstone, wackestone, and micrite that weather to yellowish gray (5Y 7/2). Carbonates are commonly interbedded with siltstone, silty limestone, chert, argillite, sandstone, and jasperiod (Fig. 33). Bedding thickness varies, but is usually thin to moderately thick, and well bedded. Commonly, the Havallah displays extensive secondary silicic alteration and extreme structural deformation. The Havallah Sequence in the western Dry Hills is referred to as Home Ranch tectonic terrane by Crafford (2008) and is consistent with descriptions of the Mills Canyon or Trenton members of the Havallah Formation by Willden (1964).

Unnamed Miocene Basalt and Andesite

In the Dry Hills, the Havallah Sequence and Etchart members are overlain by black to dark brown vesicular basalt and andesite. The eastern edge of the volcanic rocks is roughly parallel to the interpreted strike of the Golconda thrust in the Dry Hills. The basalt contains abundant plagioclase microlites.

Unconformities

Angular Unconformity within the Lower Etchart Member

Exposed only on the southern side of Etchart Hill is an angular unconformity confined within the Lower Etchart member. At this location, the angular discordance is an abrupt change in bedding angle from 044°; 18°NW in the underlying layer to 315°; 29° NE in the overlying layers. This angular discordance could also be a low-angle fault dipping to the north. Because the

contact is within the Lower Etchart member; stratigraphic offset provides no additional clarity regarding the type of contact. The contact is fully visible in outcrop and is not associated with fault gouge, gash fractures, mineral fill fractures or preferential erosion as there is at other locations associated with faults within the Lower Etchart member. This suggests it is most likely an unconformity. There is no evidence of paleosol or basal conglomerate.

Angular Unconformity between the Lower and Middle Etchart (C5/C6)

An angular unconformity exists between the Lower and Middle Etchart members (Figs. 22, 27, & 34). The angular discordance is an abrupt change in bedding orientation between underlying and overlying layers at all exposed locations. Bedding change varies from 7°-41° in strike and 6°-24° in dip across the unconformity. The contact itself is rarely directly visible due to weathering.

The age of the Lower Etchart member is interpreted as Atokan. This age derived by conodant ages of the Lower Etchart member at Lone Butte by Saller and Dickinson (1982). This age is used to constrain the lowermost age of deformation. The Wolfcampian to Virgilian age of the Middle Etchart member constrains the resumption of deposition within the area. This unconformity leaves a period of unrepresented time that encompasses both the C5 and C6 unconformities of Trexler et al. (2003).

Angular Unconformity between the Upper and Middle Etchart (P1)

The contact between the Middle and Upper Etchart members is angular at all locations where it is exposed (Figs. 34, 35, & 36). At one location, the angular discordance between the members is the result of a southeast-trending,

southeast-plunging fold in the Middle Etchart member that is not recorded in the Upper Etchart member which is gently folded by upright, sub-horizontal, northeast trending folds (Fig. 35).

The angular unconformity between the Middle and Upper Etchart members is constrained temporally by the age of the members that bracket it. These ages were confirmed with samples taken across the contact in the northern portion of the Dry Hills. The Virgilian fusulinid-derived age (V. Davydov, personal communication, 2007) of the Middle Etchart member constrains the oldest age of folding, while the lower Wolfcampian age (V. Davydov, personal communication, 2007) of the Upper Etchart member brackets the reinitiating of deposition within the area. The period of unrepresented time identifies this as the P1 unconformity.

Conglomerates

Lower Etchart Conglomerate 1

At one location, a conglomerate located within the Lower Etchart member is exposed at the top of a ridge within the Dry Hills. The conglomerate is clast supported and consists of pebble-sized chert and quartzite clasts that are sub rounded to well-rounded (Fig. 37). The conglomerate overlies and inter-fingers with fine-grained, gray-colored silty limestone. The conglomerate is very well sorted. Its thickness cannot be calculated due to its fault contact to the north.

Lower Etchart Conglomerate 2

Within the Lower Etchart member, exposed on the southern slope of Etchart Hill (Plate 2) is a clast-supported conglomerate that is made up almost entirely of

carbonate clasts and minor small polycrystalline quartz pebbles lithified in mixed carbonate siliciclastic sand-sized matrix with quartz cement. Petrographic analysis of this conglomerate shows clasts of two carbonate types:

(1) sub-angular to rounded packstone and wackestone, and

(2) micrite rip-up clasts.

This clast composition is not consistent with that of the Battle Formation described by Hotz and Willden (1964), which includes no carbonate clasts in its other locations. The matrix also commonly contains fossil fragments of bryozoans and fusulinids, implying a nearby source area. The stratigraphic position of this carbonate clast conglomerate within the Lower Etchart member as well as the unit thickness and geometry are unknown because the unit is fault bounded.

Upper Etchart Conglomerate 1

The lower of two conglomerates located in the Upper Etchart consists of a mixture of well-sorted, well-rounded, pebble-sized chert and quartzite clasts and pebble- to boulder-sized, subangular carbonate clasts (Fig. 38). The clasts consist of two types of carbonate:

(1) pelloidal and fossil-fragment rich wackestone-packstone, which are locally heavily dolomitized, and

(2) clasts of micrite or finely crystalline carbonate that is highly dolomitized and contains abundant microfractures limited only to this clast type.

The chert clasts are rounded, well-sorted clasts composed of polycrystalline quartz (Fig. 39). Thin sections of this unit also contain siliceous rip-up clasts.

Fossils within the wackestone-packstone clasts are Atokan age (Table 2) (V. Davydov, personal communication). The matrix consists of poorly sorted, sub-angular quartz sand that is red in color at the outcrop scale. The unit is ~10 m thick in the only location where thickness can be measured. The stratigraphic position of this conglomerate unit with respect to the Upper Etchart member is unknown due to faulting.

Interbedded Conglomerates

Uncommonly, in layers of the Upper and Lower Etchart members, thin (10's of centimeters) layers with some pebbles interfinger with the Upper and Lower Etchart lithologies creating thin, quartz clast dominated, pebble layers. Within the other rock types pebble- to cobble-sized clast conglomerate interfinger with carbonate beds and with sandy stringer deposits (Fig. 37). These conglomerates are more common in layers underlying thicker conglomerate deposits (e.g., conglomerates 1 and 2).

Upper Etchart Conglomerate 2

The second mapped conglomerate within the Upper Etchart member consists of a mixture of well-sorted, well-rounded, pebble-sized chert and quartzite clasts (Fig. 40). The clasts are composed of polycrystalline and cryptocrystalline quartz and pebble- to cobble-sized subangular carbonate clasts composed of finely crystalline carbonate and brown secondary dolomite with strain twins (Fig. 41). Matrix is composed of sand-sized mixed quartz and crystalline carbonate grains cemented by quartz. The matrix weathers to a reddish color in outcrops and is gray on a fresh surface. The member is ~10 m thick in the only location where

thickness can be measured and is of unknown position within the Upper Etchart member due to faulting.

Faults

Four fault sets are distinguishable within the Dry Hills. The relative timing of the faults is constrained by cross cutting relationships (Plates 1 & 2). One fault that occurs in the Dry Hills has an orientation that does not easily fit into these fault sets. Due to block rotation, it is difficult to be certain of the correlation of measurements across faults. For this reason, the map of the Dry Hills was used to isolate 23 fault-bounded domains. Orientations of beds, folds, and unconformities were only considered correct with respect each other if both occurred within a single fault-bounded block.

Fault set 1

Fault set 1 is composed of north to north-northeast striking, steeply west- and east-dipping normal faults (Plates 1 and 2, Fig. 42). The faults are cross cut by E-ENE and N-NE striking thrust faults. These faults are observed in the Dry Hills with Upper, Middle, and Lower Etchart members in both their hanging walls and footwalls.

Fault set 2

Fault set 2 is composed of east-northeast striking, moderately to gently south-dipping thrust faults (Fig. 43). These faults cross cut faults associated with fault set 1. The faults are cross cut by NNE-striking thrust faults. These faults are observed in the Dry Hills in Upper, Middle, and Lower Etchart units.

Fault set 3

Fault set 3 is composed of north-northeast striking, moderately to steeply west-dipping thrust faults. These NNE-striking faults are parallel to the Golconda thrust. All set 3 faults have Havallah Sequence in their hanging wall (Figs. 5, 9, 14, 44). Exposed fault surfaces within the Havallah Sequence contain grooves and mullions which support east- or west-movement along fault set 3 faults. Although the direct contacts between NNE-striking faults and other fault sets are commonly obscured, these faults apparently cross-cut faults associated with fault sets 1 and 2 due to the lack of offset of fault set 3 at their intersections throughout the Dry Hills. In the northern Osgood Mountains, the Havallah Sequence is exposed on the western side of the range and is thrust over the Cambrian Comus Formation and Lower Etchart member by a fault of set 3. Within the southern Dry Hills, a fault set 3 curves towards the west. To the north, the exposures of fault set 3, along with rock units, unconformities, and other structures, are obscured by post faulting Miocene-age basalt that overlies the Etchart Formation. Miocene volcanic rocks obscure the fault to the north.

Fault set 4

Fault set 4 is composed of NNW-striking, steeply east-dipping oblique right-lateral normal faults referred to as the Getchell fault zone (Fig. 24). These faults cross-cut and offset faults associated with fault set 3. Fault set 3 fault tips are curved in a right-lateral motion sense where intersecting fault set 4.

A fault set 4 surface is visible from the Dry Hills, but is located on mine property and was not investigated as part of this study. Other researchers have

previously noted right-lateral slickenlines on the fault set 4 surface that overprint dip-slip slickenlines (Cline, 2001).

Unresolved Fault

A single north-south striking fault in the Dry Hills appears to be normal. The fault trace is buried under active channel deposits and is therefore approximately located in its entirety, leaving cross cutting relationships obscured. It is recognizable in the Dry Hills because mapped contacts between units do not align across it. It is included with fault set 1 based on orientations and map relations that are consistent with it being cut by fault set 2 and fault set 3 faults.

Folds

This research documented 82 folds in the Dry Hills area (Fig. 45) (Tables 5). The folds in the Dry Hills are generally upright to slightly inclined, and have open interlimb angles. For 32 of the folds several measurements of bedding were taken across the fold hinge and into the limbs and analyzed with stereographs for fold orientation classification. Folds that had already been classified in this manner multiple times were measured by hinge trend and plunge for plotting on the map (Plates 1 & 2). From these data, at least four fold sets are recognized based on fold hinge orientation. Analysis of the axial surfaces (Fig. 45) from folds in the Upper Etchart member indicates there may actually be two sets of folds with NE-trending hinges, one set that is upright, and one set that is east-vergent. This would be a 5^{th} fold set in the Dry Hills and a 4^{th} fold set within the Etchart Formation Upper member. However, with just these data, it is difficult to distinguish whether these are the result of separate deformational events, the

same singular deformational event, or a deformational event that occurred progressively which deformed previously created folds and created new, upright folds at the same time.

Fold hinges were plotted as points on stereographs by the Etchart member in which they occur, as well as groupings (Fig. 45). This analysis isolated one fold set that was identified only in the lower and middle Etchart members.

The four fold sets recognized in the Dry Hills are:

F1

F1 folds have hinges that trend southeast to south-southeast with gentle to sub-horizontal plunges. The fold geometries are open and upright (Fig. 18). The interlimb angle varies from 140 to 165 degrees and the dip of the axial plane ranges from 90 to 80 degrees to the west. These folds are observed up to outcrop scale. Because these folds are symmetric, no kinematic interpretation can be made beyond general stress field, which indicates northeast-southwest shortening. These folds are located in the Lower and Middle Etchart members, but have not been identified in the Upper Etchart member.

F2

F2 fold hinges trend northwest to north and are sub-horizontal with a plunge of 0 to 10 degrees (Fig. 19). Fold geometries are gentle to open. Fold geometries are gentle with interlimb angles of 130 to 160 degrees. The folds are upright to steeply inclined with axial plane dips that range from 75 to 85 degrees to the west. Fold geometries imply that the maximum principal compressive stress orientation was east-west, and may have been eastward directed,

although the fold vengeance is minor and only present sporadically in F2. F2 folds occur only in the Upper Etchart member.

F3

F3 folds have hinges that plunge gently to moderately to the west-northwest. Hinge plunges range from 05 to 40 degrees. The fold geometry is gentle with interlimb angles ranging from 140 to 170 degrees (Fig. 20). The dips of the axial planes are sub-vertical to steeply inclined with dips ranging from 90 to 70 degrees to the south. The maximum principal stress orientation was north-northeast to south-southwest. These folds have been recognized at the outcrop scale and larger.

F4

F4 folds have hinges that trend north-northeast to northeast with sub-horizontal to moderate plunges. Hinge plunges range from 0 to 40 degrees. The axial planes of folds are upright to moderately inclined with axial plane dips that range from 90 to 60 degrees to the west (Fig. 21). The interlimb angle varies from 165 to 140 degrees indicating that the folds are gentle to open. These folds are observed at outcrop and mountain scales. Weak southeastward vergence of the fold set indicates that the direction of shortening was towards the southeast.

CHAPTER 5

INTERPRETATIONS

Division of the Etchart Formation

The Etchart Formation in the Dry Hills is separated here into three outcrop identifiable informal members that are separated by two angular unconformities, the C6 (or C5) and the P1. In the past, the Etchart Formation has been informally separated into three members (Thoreson et al., 2000; Laravie, 2005). However, their divisions are not consistent with rock types in the Dry Hills. These differences in lithologic and unit characteristics combined with the newly recognized Etchart internal unconformities require that informal Etchart members be recognized as separate depositional units.

Dividing the Etchart Formation into separate formal units and assigning the unit names is advocated by, but not undertaken, in this research. Recognition of separate Etchart informal members was a great benefit to interpretation of the structural history of the area, but data were not collected with the goal of characterizing these members. The sub-units here were separated informally by using unit descriptions, biochronological age, and stratigraphic correlation collected in this research. However, the data collected in this study is insufficient to formally characterizing and renaming the Etchart Formation members problematic. The sub-units require additional data regarding the ranges of unit thicknesses, measured sections, type section descriptions, and more age control, if possible.

The informal Etchart members are temporally equivalent to other units in northern and central Nevada. The Upper Etchart member is temporally equivalent, in part, to both the Upper Strathearn Formation of Carlin Canyon and the Pequop Formation of the Pequop Mountains (cf., Sweet and Snyder, 2002; Trexler et al., 2003). The Middle Etchart member is temporally equivalent, in part, to the Adam Peak Formation of the western Osgood Mountains and Edna Mountain (Saller and Dickinson, 1982; Villa, 2008). The Lower Etchart member is temporally equivalent to the Highway Limestone of Edna Mountain (Villa, 2008). Due to lithologic changes, it remains yet unclear if these informal members of the Etchart Formation are truly stratigraphically continuous with other units throughout Nevada, or just temporally equivalent in the timing of their deposition.

Previous work (Johnson, 1987; Thoreson et al., 2000; Crafford, 2003) did not recognize these separate Etchart Formation units or the angular unconformities that separate them. This presents problems with previous Dry Hills age analysis. Sample locations from previous work are commonly labeled “Etchart Formation” and do not include adequate spatial information regarding the sample collection location. This makes it unclear which Etchart member yielded the ages (e.g., Saller and Dickinson, 1983; Crafford, 2003). Pennsylvanian and Permian uplift and erosion potentially further complicate matters by introducing older reworked sediments into upper portions of the Etchart Formation, such as Atokan age fusulinids (V. Davydov, personal communication) within Upper Etchart member conglomerates.

When conducting previous biochronological age analysis, Jones (1991) and other researchers (Saller and Dickinson, 1982) generally did not sample from the Etchart Formation in the Dry Hills.

Crafford's work (2000, 2002, & 2003) focused on investigating the Havallah Sequence as one of a number of geologic terranes that are interpreted to compose the Golconda Allochthon. She worked extensively in the Golconda Allochthon in the western portion of the Dry Hills and collected numerous samples from the Havallah Sequence. Two samples collected near the Golconda thrust are attributed to the Etchart Formation in the northern portion of the Dry Hills (Crafford, 2003). These yielded an Atokan and an early Permian age. The early Permian age is the recognized age of the Upper Etchart, thus this sample is not troublesome (Crafford, 2008). The location of the Atokan age sample from the northern portion of the Dry Hills lies in an area mapped here as Quaternary Alluvium, but near exposed outcrops of Upper Etchart member and Havallah Sequence. The Upper Etchart is not Atokan age, but the member contains reworked Atokan age sediments, possibly accounting for this result. Alternatively, (1) the Atokan sample represents Havallah Sequence, which was misidentified due to fault proximity, or (2) the sample was poorly located.

The Lower Etchart Formation in the Dry Hills yielded no fusulinid samples for biochronological analysis, but is most likely Atokan in age. The basal AOS unit in the area has been assigned an Atokan age and the tectonostratigraphy of the surrounding area contains no units previously associated with the Antler Foreland Basin. Therefore, assigning an older age to the Lower Etchart member

requires that the unit be temporally correlated to a unit within the Antler Foreland Basin or the Roberts Mountain Allochthon. The presence of the Roberts Mountain Allochthon beneath the Lower Etchart Formation precludes interpretation as a foreland basin deposit. The amount and style of structural deformation within the Lower Etchart member, which is relatively mild, implies that the Lower Etchart member was not a part of the greater deformed Roberts Mountain Allochthon. Also, the C6 (or C5) unconformity between the Lower and Middle Etchart members is not dramatically angular and has no observed basal lag conglomerate, which is typical for the Roberts Mountain Allochthon to AOS transition in other locations.

Thoreson et al. (2000) created a stratigraphic column for the Dry Hills area (Fig. 6) that incorporated the Etchart Formation. It was generated from drill core data and exposures from the Vista Pit in the southern Dry Hills on the Twin Creeks mine property. In this stratigraphic column, Thoreson et al. (2000) informally subdivide the Etchart Formation into three sub-units. However, the upper portions of the Etchart Formation in this exposure do not include the coarse grainstones or conglomerates of the Upper Etchart member in the Dry Hills, implying that this stratigraphic column does not incorporate the upper Etchart Formation observed in the Dry Hills. The Middle Etchart member may be part of this stratigraphic column, but the micrite at the top of Thoreson et al.'s (2000) stratigraphic column is more consistent with base of the Lower Etchart member exposed in the Dry Hills. Faulting between the map area and the drill

hole data used to create Thoreson et al.'s (2000) stratigraphic column likely contributes to this discrepancy.

Depositional Setting

The Etchart Formation as a whole was previously interpreted (Saller and Dickinson, 1982) to represent a transgressive sequence of mixed carbonates and siliciclastic rocks deposited in a deltaic system. These deltas were later flooded during a tectonically-induced sea level transgression that inundated the paleovalleys (Saller and Dickinson, 1982). However, these descriptions were generated from data taken from locations in Lower Etchart member in the mid to southern Osgood Mountains and from exposures at Lone Butte (Saller and Dickinson, 1982). This interpreted depositional setting is still feasible for the Lower member of the Etchart Formation in the Dry Hills, but it is not consistent with rock types in the Middle and Upper Etchart members, nor does it accurately reflect the relative sea level recorded by the Etchart Formation as a whole.

The data collected from the Etchart members in the Dry Hills correlate with Johnson's (1987) lithofacies descriptions and depositional environment interpretations for the Etchart Formation. Facies descriptions and sample locations are consistent with my observations of the Upper and Middle Etchart members' grainstone and packstone. Johnson (1987) notes that most of the facies fall within facies belts 6 to 9 of Wilson's (1975) standard facies belts indicating a relatively high energy platform margin to restricted nearshore environment probably in semi-restricted shallow subtidal to intertidal, open and shallow marine platform, and turbulent shoal water. These interpretations are

consistent with my observations and interpretations of the Upper Etchart member, shallow water depositional settings. Johnson's (1987) evidence of shallow water deposition includes Dascycladacean algae common within beds, which is commonly deposited in water depths less than 15 meters. In addition skeletal grains with micritized rims and meniscus cements within grainstone beds that indicate parts of the Etchart were exposed to vadose cementation. Johnson (1987) also notes that grains from these units are abraded and rounded suggesting derivation from a different environment than that in which what they were deposited. Johnson's (1987) work included some measured sections from the Etchart Formation, but did not recognize the angular unconformities or faulting in the area. Johnson's final depositional interpretations indicated abrupt sea level changes, herein interpreted to be the unrecognized unconformities, which Johnson (1987) believed indicate that deposition of the Etchart members was largely controlled by abrupt tectonically derived uplifts. This research agrees and further defines the nature of tectonism.

Johnson's (1987) exceptions to an interpretation of shallow water deposition were the presence of siltstone and grain-rich wackestone facies. These are interpreted to represent a deeper water transition, similar to the open shelf deposition of facies belt 2 as outlined in Wilson's (1975) standard facies belts. This facies description is consistent with the observed facies of the Lower Etchart member as recognized in this research and is the favored depositional interpretation of the Lower Etchart member. As previously stated, it is possible that Saller and Dickinson's (1982) transgressive sea level interpretation for the

Etchart Formation is still applicable to the Lower Etchart member, the thickest Etchart member within the study area.

Johnson's observations and interpretations of Etchart Formation facies belts are largely consistent with the interpretation of the Upper and Middle Etchart member advocated herein. The depositional environments are (1) possible moderate to deep water for the Lower Etchart member (thick continuous deposition, silt to mud grain sizes, turbidities and channel constrained conglomerates) with multiple tectonically-induced fan channel conglomerates in Late Pennsylvanian time, followed by; (2) sub-tidal to sub-wave base deposition (mixed grain sized and vertical worm borrows) of the Middle Etchart member in latest Pennsylvanian to earliest Permian; to (3) sub-wave base to tidal flat deposition (herringbone stratification) of new and reworked sediments (Atokan-aged conglomerate clasts, integrity of fossil fragments within grainstone) in the Upper Etchart member with multiple tectonically induced conglomerates. The sea level changes are transitions are obscured, not recorded, or removed by formation of the P1 and C6 unconformities.

The Etchart Formation consists of interlayered packstone and micrite with portions showing intermixing of packstone and micrite. The upper portions of the Middle Etchart member contain relatively greater amounts of packstone similar to the Upper Etchart member, but unlike the Lower Etchart member. Farther down within the section, near the base of the Middle Etchart member, are relatively larger amounts of wackestone. The lower portions of the Middle Etchart member contain light and dark gray striping interpreted to be microbial mats similar to

those within the Lower Etchart member. They are interpreted to indicate a below subtidal depositional environment where the microbial mats were able to grow without disruption.

The transition from moderate to deep platform deposits of micrite/wackestone in the basal Lower Etchart member, to shallow wackestone-packstone in the Middle Etchart member, to very shallow-to-exposed packstone-grainstone in the Upper Etchart member implies progressively higher energy and shallower depositional environments. This trend indicates a general shallowing-upward sequence. Due to the unconformities between members, these observations reflect sea level change in Pennsylvanian to Permian time as a whole, and may or may not reflect relative sea level changes recorded within a single Etchart member. The transitions between environments seem to occur within the periods of time accounted for in the unconformities, indicating periods of deposition during relative sea level stability and periods of relatively rapid sea level changes during periods of unconformity creation. This, along with tectonically induced conglomerate deposition, boulder-sized clasts deposited within shallow water depositional settings, and evidence of tectonic activity (e.g., the P1 and C6 unconformities, and deformation constrained between) within the time period, strongly implies that the sea level changes were wholly or partially the result of tectonism.

The reworked sediments in the Upper and Middle Etchart members as well as the angular unconformities imply that Late Paleozoic deformational events in the Dry Hills created or enhanced cycles of deposition, lithification, uplift, and erosion

of recently deposited materials facilitated by the speed in which carbonates lithify. Evidence for this kind of syntectonic deposition is: (1) Atokan age clasts within the Upper Etchart member conglomerates (Table 2) (V. Davydov, personal communication); (2) the large number of distinct conglomerates in the area; (3) clast types within individual conglomerates with distinct rounding, size and sorting attributes; (4) clasts of similar size, composition, and angularity when compared to Etchart conglomerate clasts that are interbedded with turbidite/storm deposits; (5) packages of thinly interlayered conglomerates of similar characteristics within the Etchart members; and (6) correlation of deposition to erosion and vice versa in the Dry Hills to other areas of Nevada (covered later).

Previous paleocurrent direction studies in the Dry Hills have provided flow direction information. Saller and Dickinson (1982) conducted studies at Lone Butte that show the paleocurrent direction in the Lower Etchart member was to the northeast. Paleocurrent measurements taken from the Etchart Formation in the Dry Hills by Saller and Dickinson (1982) show paleocurrent directions are to the south-southeast, which is mostly consistent with Johnson's (1987) paleoflow data. Neither of these studies recognized the Etchart Formation is three separate units. These results do not identify which member the paleocurrent readings were measured in. However, if correct, the apparent changes in paleocurrent direction within the Etchart Formation can be explained one of two ways: (1) the paleocurrent direction changed from the Lower Etchart member to Upper Etchart member. This may be less likely as Saller and Dickinson (1982)

largely worked in Dry Hills areas dominated by Lower Etchart member. Or, (2) the Lower Etchart at Lone Butte and the Dry Hills record deposition from different sources, which is more likely but strongly limits the ability to correlate the two areas.

Johnson (1987) noted that sand content within the Etchart decreased significantly to the southwest; that paleocurrent data indicated a west-southwest transport direction; that the amount and number of conglomerate beds decreased to the southwest; and interpreted a source area to the north-northeast that began releasing increasing amounts of terrigenous material into the Etchart Formation during deposition. This research agrees with this interpretation. Quartzite and chert clasts within Lower Etchart conglomerate 1, the Upper Etchart member conglomerates, the Battle Formation at Lone Butte, the Iron Point conglomerate at Edna Mountain (Villa, 2008), and Highway conglomerate at Edna Mountain (Villa, 2008) appear to all have the same source material. This material is similar in lithology to the Cambrian Osgood Mountain Quartzite in the Osgood Mountains. This source material was apparently exposed to erosion in at least one location throughout most of Late Paleozoic time. If the source location for these conglomerates is to the north-northeast as suggested by Johnson (1987), then the 100 foot (30 m) thick Battle Mountain conglomerate deposit to the south of the Dry Hills at Lone Butte is likely not sourced from the same uplift location as in the Dry Hills, because a similar conglomerate is absent from the Dry Hills at this time. This implies that there was a second area of uplifted and eroding

Osgood Mountain Quartzite, or that later structural block movements altered the lateral position of the two locations.

It remains unclear to what extent the Getchell fault and other structural complexities in the Osgood Mountains and the Dry Hills influence the lateral distribution of the Etchart Formation's facies. This research clearly shows multiple periods of Late Paleozoic age or later deformation. Thus, depositional environment interpretations may be influenced by critical pieces of paleo-geographical information, such as the proximately of temporally equivalent units at deposition or siliclastic sources from more than one location.

Conglomerates

In previous works conglomerate rocks within the Antler Overlap Sequence, including the Etchart Formation, have typically been labeled Battle Formation(Holtz and Willden, 1964). The Battle Formation is defined at its type section as a thick (100's of meters) Atokan-age conglomerate consisting of pebble-cobble sized chert and quartzite clasts at the base of the Antler Overlap Sequence (Hotz and Willden, 1964). The Battle Formation is interpreted as a basal lag conglomerate deposited atop the eroded Antler Allochthon (Willden, 1964). The conglomerate rocks within the Etchart do not strongly correlate to this type section description. This study recognizes these conglomerate rocks as tectonic induced Etchart equivalent deposits.

At the base of the Lone Butte section is clast-supported and consists of angular to sub-angular pebble to cobble quartzite and chert clasts in a reddish sandy matrix that is quartz-cemented. Previous stratigraphic measurements of

this unit indicate it is 100 meters thick (Saller and Dickinson, 1982) The conglomerate underlying the Lower Etchart member at Lone Butte is consistent in clast type, size, distribution and thickness with the type section of the Battle Formation (Hotz and Willden, 1964). The conglomerate transitions into Lower Etchart member at an unconformity at their contact near the top of the section.

This study indicates Etchart conglomerates in the Dry Hills are not the Battle Formation based on their stratigraphic relationships. All exposed conglomerates in the Dry Hills Etchart unit overlie Pennsylvanian or Permian rocks indicating the units are stratigraphically higher than the Battle Formation. The single exposed contact between the Lower Etchart member and the Ordovician Valmy Formation was sharp without a basal conglomerate. The Lower Etchart member is temporally equivalent to the Atokan age Battle Formation at its type section (Hotz and Willden, 1964) allowing for the possibility of a shared provenance for their conglomerate. The early Permian age of the Upper Etchart member is significantly younger than Atokan Battle Formation challenging a shared provenance interpretation. The clast composition and unit thickness of these conglomerate units also are not consistent with regards to clast type, composition, and distribution to descriptions of the type Battle Formation (Hotz and Willden, 1964), or the Battle Formation exposed at the base of Lone Butte (Saller and Dickinson, 1982).

The conglomerate rocks in the Etchart formation can be interpreted to represent cycles of uplift. Upper Etchart conglomerate 1 contains quartzite, chert, and two distinct types of carbonate clasts. One of the carbonate clast

types of Upper Etchart conglomerate 1 contains Atokan-age fossils, indicating erosion and deposition of Atokan age materials during early Permian time. Atokan is the accepted age of the Lower Etchart member at Lone Butte and the interpreted age of the Lower Etchart member within the Dry Hills. This suggests that during Upper Etchart depositional time (early Permian), a source of Atokan carbonate rocks was exposed to erosion. This occurred during a period of the Permian in which sea level is interpreted to be generally rising. The easiest and therefore best interpretation is that the carbonate source was uplifted. This Atokan to early Permian constrained uplift is evidence of tectonic activity during late Paleozoic time. The similar quartzite and chert clasts imply that the same siliceous provenance of the Battle Formation might have been exposed to erosion and depositing sediments southward throughout this time(Saller and Dickinson, 1982; Johnson, 1987). Alternatively, siliciclastic influx may have been the result of recycling, due to cycles of deposition, uplift, and erosion. Thin interbeds of siliclastic pebble conglomerates and thicker deposits containing the same clasts with larger, cobble- to boulder-size carbonate clasts imply that the clasts were eroding elsewhere and periodically washed into the Dry Hills by events in a series of smaller scale events and several larger scale events that carried larger clasts into the thicker conglomerate layers.

The Upper Etchart member is interpreted to represent a nearshore environment. The angular boulder-sized carbonate clasts within the Upper Etchart conglomerate 1 are interpreted to have eroded from relatively close by. Previously, these deposits were interpreted as deep water fan deposits

(Johnson, 1987), but their position within shallow water facies precludes this interpretation. Rather, moderate scale flows are interpreted to have transported the large clasts a relatively short distance from nearby uplifted areas of erosion. This interpretation does not refute a fan deposit interpretation for the Upper Etchart member as advocated by Johnson (1987) and Saller and Dickinson (1988).

The conglomerates in both the Upper and Lower Etchart members are fault-bound, and therefore precise unit thickness, lateral shape, or stratigraphic locations within their members are not known. Etchart conglomerates are likely channel deposits based on outcrop distribution and clast imbrication where locally exposed. The Lower Etchart conglomerates are interpreted to be submarine fan deposits in moderate depth sea level. The conglomerates in the Upper Etchart member are interpreted to be deposited in a shallow, nearshore environment during mass discharge events or sea level retreat in response to tectonism.

Structural Interpretations

Faults

The four fault sets recognized within the Dry Hills map area are organized based on crosscutting relationships from 1 to 4 with 1 being the oldest and 4 being the youngest. The justification for this relative timing is as follows:

(1) Fault set 1 faults are cross cut by fault sets 2 and 3 (Plate 1). The relationship between fault sets 1 and 2 is most easily observed in the field at ridge tops where outcrops are best exposed. The relationship between fault set

1 and 3 is best observed near the edge of the easternmost thrust associated with set 3. There a set 1 fault terminates without offset of a set 3 fault or its hanging wall unit, the Havallah Sequence.

(2) Faults of set 2 are cross-cut by the easternmost thrust associated with fault set 3. This relationship is observable in the northern and central Dry Hills where fault set 2 intersects fault set 3, which occurs in the northern and north-central areas of fault set 3 exposures.

(3) Fault set 3 (Golconda Thrust) is cross cut by faults of set 4. This occurs in the southern portion of the Dry Hills, outside of the map area (Plates 1 and 2).

Consideration was given to whether or not fault set 2 and fault set 3 are the product of different deformations, or the result of the same deformation, such as synchronous deformation of the lower plate Etchart Formation during the thrust emplacement of the Golconda Allochthon during the Sonoma Orogeny and/or back thrusting. The reason these alternate theories initially may seem favorable is due to observations that a) both fault set 2 and 3 are thrust faults and b) the strikes are similar in orientation (fault set 2 strikes roughly WSW-ENE, fault set 3 strikes NE-SW). These interpretations are not preferred in the Dry Hills for the following reasons:

1. The strike of faults from fault set 2 and 3, although roughly similar, still differ by no less than 20 degrees measuring between the two locations they are closest to parallel, and differ by as much as 60 degrees at the areas where they are most dissimilar. The dips are also in opposite directions. Fault set 3 thrusts dip northwest based on unit offset

relationships, while fault set 2 thrusts dip southeast based on kinematic indicators and unit offsets. This is considered too significant a difference for a synchronous deformation as a result of a single thrusting deformation, even with changes in deformation that may be expected by different rock types in the lower and upper plates.

2. The dip of fault set 3 is relatively shallow in the Dry Hills, ranging from 20-30 degrees northwest, while set 2 fault dips are steeper (45-55 degrees south). These differences in fault plane dip do not support a conjugate fault interpretation.
3. Fault sets 2 and 3 are interpreted to be parts of fold and fault pairs. If fault sets 2 and 3 truly were the result of a single thrusting deformation and the favored interpretation was changed to reflect this, it would not reduce the number of deformations that occur in the Dry Hills area unless F3 and F4 occurred synchronously as well. For that to occur, the upper and lower plates of the thrust would have to deform in separate manners resulting in two fold-and-fault sets of differing orientations as a result of a single deformation. This may be possible, in theory, with the correct combination of principal stresses, emplacement mechanics, and rock types. However, recognition of two separate events is simpler and therefore is more convincing.

In the northern Osgood Mountains vertical offset and block tilting resulted in erosion of the Upper and Middle Etchart Formations members, exposing a stratigraphically lower Golconda Allochthon atop Ordovician Valmy Formation.

Fault set 3, the Late Permian to Triassic age Golconda thrust on the western slopes of the northern Osgood Mountains display thrust sheets of the Havallah Sequence atop Lower Etchart member. The unusual relationship of a younger unit (Mississippian Havallah Sequence) thrust over an older unit (Cambrian to Ordivitan Formations) is interpreted to be the result of much thicker successions of units within the thrust plate, erosion and unroofing of younger units in the footwall prior to thrusting, or both.

The Dry Hills fault sets are more easily recognizable and systematic in the northern portion of the Dry Hills than in the south. In the southern portion of the map area, fault exposures are poor and fault orientations are less systematic and appear to have been modified. Therefore, the faults are more difficult to group into their respective fault sets. This is interpreted to be due to proximity to the Getchell fault zone.

Previous mapping has not attempted to quantify the offset of the Golconda Allochthon by the Getchell fault. More regional scale maps (Hotz and Willden, 1964; Stewart and Carlson, 1978;) incorporate the Getchell fault into the Golconda thrust as a bend in the fault trace. Previously published research at a more localized scale focused simply on the Getchell fault, as it relates to local ore deposits and not its crosscutting relationships (Cline et al., 2000).

Recognizing offset of the Lower Etchart and the Golconda thrust allows attempts to better quantify offset along the Getchell Fault utilizing previous geologic maps (Fig. 5), field observations, and geometric relationships. The Getchell Fault previously was considered an oblique-slip fault that is largely

normal with minor right-lateral offset. These efforts indicate the Getchell fault is likely dominated by right lateral displacement with lessor normal offset.

An estimate of the vertical offset of the Getchall fault can be generated utilizing the Etchart Formation. At the northern tip in the Osgood Mountains, the Golconda thrust puts Havallah Sequence atop Lower Etchart Formation south of where it is cross-cut by the Getchell Fault. In the southern portion of the Dry Hills, the Golconda thrust puts Havallah Sequence atop the Upper Etchart member.

Assuming equal thickness of stratigraphy on both sides of the Getchell fault prior to its initiation, a minimum estimate of the Getchell fault's maximum vertical offset can be calculated based on the total thickness of the Etchart Formation. The maximum thickness of the Etchart Formation observed reported anywhere is 2000 feet or 0.6 km (Thoreson et al., 2000). As, the "true" thickness of the Etchart could be actually be greater than anywhere previously observed, this provides a minimum estimate of the maximum vertical displacement of the Getchell Fault in the Dry Hills area. It is no more than 0.6 km. This estimate is likely greater than the true displacement, as the Etchart Formation near the Getchell fault zone appears to be much thinner than the maximum thickness recorded by Thoreson et al. (2000).

Right-lateral offset is more difficult to precisely estimate. Field observations and mapping indicate that the right-lateral offset of the Getchell Fault may bend the Golconda thrust. Fault-bound blocks containing the Golconda thrust are present in the Getchell fault zone, creating the question of whether the

northernmost block containing the Golconda thrust records the orientation of the Golconda thrust prior to being cut and offset (Fig. 5). If the block is not rotated by Getchell fault movement, then the apparent right-lateral offset is measured from that intersection to the Dry Hills. If the block is rotated, then a more north-south orientation of the Golconda thrust along the western edge of the Osgood Mountains records the correct orientation. This would require projection to an intersection with the Getchell fault to measure apparent offset. The distance from the intersection of the northernmost block containing the Golconda thrust to the Golconda thrust in the Dry Hills records 3.5 km of apparent offset; projecting the trace of the thrust from the edge of the Osgood Mountains records approximately 9 km of apparent right-lateral offset.

This relationship can be illustrated mathematically (Fig. 46). Simplistically, the amount of apparent horizontal offset of a planar feature within a lowered block that is then leveled off is $F(x)=Vo / \tan(Fa*\pi/180)$, where Vo is the vertical offset and Fa is the dip angle of the vertically offset planar feature. The resulting values were subtracted from the measured apparent offset in order to make estimates of right-lateral offset. Using the estimates from the field data, where the vertical offset of the Getchell fault is 0.6 km (based on Etchart Formation thickness), and the dip of the Golconda thrust is on average 30 degrees in the Dry Hills, then the apparent right-lateral offset caused by vertical displacement is 1.04 km. When subtracted from the measured apparent right-lateral offset in the area, this leaves 2.5 or 8 km of apparent horizontal offset, indicating the Getchell fault is dominantly right-lateral by a factor of 2.5 or 8 times more right-lateral

offset than vertical offset. According to these calculations, in order for the more conservative 3.5 km estimate of apparent offset to be the result of dominant vertical offset, the dip of the Golconda thrust would have to been 10 degrees (1/3 the observed dip) at 0.6 km vertical offset, or 25 degrees (still less than the observed dip) and the true vertical offset 1.2 km (twice the thickness of the Etchart than has ever previously been recorded). These calculations, along with standard geometric projections of right-lateral offset that were undertaken, lack precise estimates of right lateral offset. However, the results of all estimates undertaken, regardless of method, show the Getchell fault has been dominantly right-lateral since the emplacement of the Golconda Allochthon. The results have all been greatly within reasonable error margins. This results also are supported by recognition of right-lateral slickenlines superimposed atop normal sense slickenlines on Getchell fault surfaces (Cline, 2001).

Acceptance of the Getchell fault as an oblique right-lateral fault has several repercussions. The assumption that the stratigraphy was roughly equivalent in both the hangingwall and footwall of the Getchell fault is reasonable as the dip of the Getchell fault is near vertical, ranging from 65-80 degrees, averaging 75 degrees east (Thoreson et al., 2000). With 0.6 km vertical offset, the northward horizontal displacement accounts for only 0.29 to 0.12 km, with an average of 0.17 km of northward apparent displacement due to normal movement along the Getchell fault. These small amounts of apparent displacement minimize the possibility that the stratigraphy, specifically the thickness of the Etchart Formation used to estimate of the vertical offset, is radically different across the fault.

However, the more dominantly right-lateral the Getchell fault is, the farther the Etchart in the footwall may have traveled. This decreases its precision as an estimate the vertical offset of the Getchell fault. Interestingly, this argument requires recognition that the Getchell fault is dominantly right-lateral in order to move distant stratigraphy into the current hangingwall.

Right lateral movement on the Getchell Fault appears to have bent the northern tip of the Golconda Thrust fault in the Osgood Mountains to the east and bent the southern tip of the Golconda Thrust fault to the west in the Dry Hills. Describing the faults as bent is not intended to imply bending must have been the result of drag. The bending of the fault tips may also have been the result of fault propagation folding. As shown in previous maps (Willden, 1964; Crafford, 1999), several blocks exposing the Havallah Sequence thrust over the Etchart Formation are present along the eastern edge of the Getchell Fault system in the Dry Hills, implying this offset was not a case of simple planar fault offset within the Golconda fault zone. This is interpreted to be caused by thrusts near a restraining bend in the Getchell fault in the northern Osgood Mountains, near the Twin Creeks mine (Fig. 5).

Folds

This research recognizes four fold sets in the Dry Hills as shown in the data section. The ages of members the folds deform, and refolding exposed in outcrop are used to interpret the relative timing of folding.

(1) F1 is constrained to the lower and middle Etchart members. F1 folds are open, upright, and have a wavelength on the order of at least several 10's of

meters. F1 folds indicate a shortening direction of SW-NE in their current orientation, although subsequent faulting probably reoriented these folds. Folds of this geometry constitute 3 of 12 folds identified in the Lower Etchart member and 1 of 9 folds recorded in the Middle Etchart. Also, a F1 anticline is observed directly beneath the P1 unconformity, where a F2 syncline directly overlies the P1 unconformity that separates the folds (Fig. 35).

2) The F2 fold hinges are parallel to sub-parallel to fault set 1, both are temporally constrained to the Upper Etchart member. Based on this observation, F2 and fault set 1 are interpreted to be the result of the same deformation. Fault set 1 is interpreted to be the oldest fault set occurring above the P1 unconformity based on crosscutting relationships and F2 is the oldest folding event above the P1 unconformity. F2 folds are observed refolded by F3 and F4 folds. Folds are cylindrical and symmetrical, indicating a general east-west shortening direction relative to their current orientation. F2 folds appear to be regional in scale, with parasitic folds commonly visible in outcrop. Younger folding events refold F2 folds, which is best observed on F2 fold limbs. When refolding occurred across F2 fold hinges, the hinges are interpreted to be tightened.

3) The F3 hinges are parallel to sub-parallel to fault set 2 strikes and both fault set 2 and F3 folds are temporally constrained to the Upper Etchart member or younger (Plate 1). F3 folds are observed refolding F2 folds and are refolded by F4 folds (Fig. 47). Fault set 2 cross cuts fault set 1 and is cross cut by fault set 3. Based on this observation, both F2 faults and F3 folds are interpreted to be the result of the same deformation based on parallelism.

4) The F4 fold hinges are parallel to sub-parallel to fault set 3 strikes and both are temporally constrained to the Upper Etchart member above the P1 unconformity. F4 folds are observed refolding all other folds above the P1 unconformity, and set 3 faults cut fault sets 1 and 2 (Fig. 48). F4 folds indicate eastward directed shortening, and faults associated with fault set three have an eastward thrust motion sense. Based on these observations, fault set 3 and F4 folds are interpreted to be the result of a single deformation event.

Generally, the folds recorded in the Dry Hills are upright and symmetric, which provides little kinematic information beyond general shortening direction. The exceptions are the F4 folds, which have axial plane dips that range from 90 to 65, indicating they are slightly eastward verging. In some rare cases, F3 folds are observed that are close to northward verging (75 degrees), although their axial planes still fall within a range classified as upright.

Deformational Sequence

Based on the structural data and interpretations presented in this thesis, the following structural history is interpreted for the Dry Hills area.

D1, Tilting of the Lower Etchart member

D1 deformation is evident from the angular discordance across the C5/C6 unconformity between the Middle and Lower Etchart members. The timing is constrained by fusulinids in the lower Middle Etchart member to post-Atokan to prior to mid-Missourian. The unconformity was subsequently deformed, but attempts to remove the deformation seem to imply the tilting was roughly ~50

degrees to the NW. If the deformation resulted in large scale folding, the tilting may change geospatially.

D2, F1

D2 deformation is recorded in the Lower and Middle Etchart members and not observed in the Upper Etchart member. Timing of D2 is bracketed between the mid-Missourian by the initiation of deposition of the Middle Etchart member and early Wolfcampian by the deposition of the Upper Etchart member. The maximum principal shortening direction appears to be NE-SW, although subsequent rotation of the fault blocks in which this deformation is recorded in may have altered the orientation. This deformation resulted in upright, cylindrical regional-scale folds and is interpreted to be the cause of the P1 angular unconformity.

D3, Fold-and-fault set 1 composed of F2 and fault set 1

D3 structures are exposed in all three Etchart members. Timing of D3 is bracketed between early Wolfcampian and the Triassic prior to D4 due to cross cutting relationships. Deformation is extensional.

D4, Fold-and-fault set 2 composed of F3 folds and fault set 2

D4 deformation is exposed in all three Etchart members. Timing of D4 deformation is bracketed between early Wolfcampian following D3 faulting and Triassic prior to D5 deformation due to cross cutting relationships. The folds are interpreted to be fault-propagation folds. Assuming minimal rotation of the Dry Hills block, D4 indicates north-south shortening with northward thrusting that may

be somewhat similar in style to the older aged Humboldt Orogeny of Ketner (1977).

D5, Fold-and-fault set 3 composed of F4 and fault set 3

D5 is exposed in all three Etchart members. Timing of D5 is bracketed between Late Leonardian by the youngest age of the footwall Etchart Formation to the Miocene by unnamed basalts that overlie it in the Dry Hills and prior to the most recent movement of the D6 fault. D5 is contractional with an ESE shortening direction that resulted in ESE directed thrusting and slightly vergent folds that indicate thrusting was directed towards the east-southeast. D5 is interpreted to be the emplacement of the Havallah Sequence along the Golconda thrust. This interpretation implies that the timing of D5 is no younger than Triassic in age.

D6, Fault set 4

D6 deformation is recorded south of the Dry Hills and north of the Osgood Mountains. The D6 Getchell fault cuts all non-Quaternary units it crosses and timing of deformation is confined between the Leonardian (youngest Etchart age) and Quaternary (modern alluvium) and following D5 deformation.

Possible Additional Deformation, Low-Angle Faulting

Previous workers (Theodore, 2000) noted that the contact at the base of the Lower Etchart in the southern Dry Hills appears sheared in some drill cores. If true, low-angle thrusts beneath the Etchart Formation would be constrained only to post Atokan by the age of the Lower Etchart member in the hanging wall. As it is observed only in drill core samples, its crosscutting relationships, and

geospatial position are unknown. The fault, if present, would be inferred to be a very low-angle fault, and this orientation is unlike other faults present in the Dry Hills. This implies that the low-angle faults may be a separate deformation. Alternately, it may be faulting associated with D1 or D5. The contact below the Lower Etchart member is present at Etchart Hill in the southern portion of the map area. The contact there is interpreted to be an unconformable contact between the Lower Etchart and Ordovician Valmy Formation that underlies it and does not display evidence of shearing, or other motion sense indicators. Although it may be Late Paleozoic in age, this thrust could also be the result of later contractional deformation. Further research and evidence is required to characterize this thrust and conclusively determine if is present at all. It is mentioned here for completeness.

Correlation to Other Areas

Correlation to Lone Butte

The stratigraphy of Lone Butte was measured by Saller and Dickinson (1982) and consists of a basal unit of Osgood Quartzite followed by 100 m of Battle Mountain conglomerate and 85 m of the Lower Etchart member conformably deposited over the Osgood Quartzite. Saller and Dickinson (1982) collected multiple conodont samples that were assigned an Atokan age at Lone Butte. Investigations of Lone Butte during this research failed to locate fusulinids to confirm this age.

The thick succession of the Battle Formation at Lone Butte is unlike the base of the Lower Etchart member in the Dry Hills. At Etchart Hill, the base of the

Lower Etchart member is an unconformable contact between argillite in the upper Valmy Formation and Lower Etchart member micrite and silty wackestone, with no conglomerate present. Conglomerates within the Dry Hills are stratigraphically contained within younger rocks. Also, the Lower Etchart member in the Dry Hills map area yielded no datable fossils, whereas Saller and Dickinson (1982) were able to find several in a relatively small exposure. These data suggest that the Lower Etchart member at Lone Butte may not be entirely equivalent in age or depositional environment to the Lower Etchart member of the Dry Hills.

With a thick basal conglomerate transitioning into Atokan-age fusulinid bearing carbonates, the stratigraphy of Lone Butte is more correlative with the Iron Point Conglomerate and Highway Limestone on the east side of Edna Mountain measured by Villa (2008). The stratigraphically lowest AOS limestones at both these locations are Atokan age based on multiple samples. In its current location, Lone Butte is over 30 km south of the Dry Hills, with numerous faults between locations, including the Getchell Fault.

Correlation to Edna Mountain, Carlin Canyon and the Central Pequop Mountains

Edna Mountain is approximately 45 km to the south of the Dry Hills (Fig. 2), and has been structurally investigated for Late Paleozoic deformation by Villa (2008) (Figs. 49 & 50). The correlation of the tectonostratigraphic history of Edna Mountain and the Dry Hills is as follows:

Atokan time to Missourian

- In Edna Mountain, the Antler Peak Formation was deposited and then deformed in a series of tight to close, asymmetric, moderate to steeply inclined and locally overturned to the west-southwest folds (Fig.50) (Villa, 2008). Following folding, the Iron Point low-angle normal fault activated. This deformation is followed by a period of erosion that created the C5-C6 unconformity (Fig. 49) (Villa, 2008; Cashman et al., 2010).
- In the central Pequop Mountains (Fig. 2), the Ely Limestone is deposited and deformed by minor thrusts and fault propagation folds indicated NW directed shortening (Sweet and Snyder, 2002). The C5 unconformity is the upper boundary. Desmoinesian Hogan Formation overlies the C5 unconformity, terminated at the top by the P2 unconformity (Sweet and Snyder, 2002). The Hogan Formation is also deformed, but timing of the deformation is constrained from Desmoinesian to Leonardian to Sakmarian-middle Kungarian (Sweet and Snyder, 2002).
- At Carlin Canyon (Fig. 2), the Atokan age Tomera Formation is deposited and deformed by imbricate thrusts and northwest verging, overturned folds (Fig. 50) (Trexler et al., 2004). This deformation is interpreted to allow creation of the C5 +/- C6 unconformity, which trims the thrusts at the top of the Tomera Formation (Trexler et al., 2004).
- In the Dry Hills, the Lower Etchart member is deposited and undergoes a structural tilting event. No evidence of a low-angle fault was documented in the Dry Hills to correlate to the Iron Point Fault of Edna Mountain; however the Dry Hills do record high angle normal faulting in the early Permian. No similarly

oriented folds to those at Edna Mountain, Carlin Canyon, or the Pequop Mountains were located in the Dry Hills. The Lower Etchart member contains an angular unconformity within it, identified at Etchart Hill. It is interpreted to probably be the C5 unconformity (Fig. 12), which is also exposed in the Pequop Mountains. The C6 angular unconformity, as in Carlin Canyon, is present in the Dry Hills, interpreted to have been formed as a result of the tilting event.

Missourian to early Wolfcampian time

- At Edna Mountain (Fig. 2) following the formation of the C6 unconformity, the Antler Peak Limestone was deposited (Villa, 2008). The Antler Peak Limestone is terminated at its top by the P4 angular unconformity where it is dated as Missourian (Fig. 12) (Villa, 2008). The rocks between these unconformities do not record any deformation constrained to this time period (Fig. 49) (Villa, 2008).
- In the central Pequop Mountains (Fig. 2), this time period is unrepresented due to an unconformity (Sweet and Snyder, 2002).
- At Carlin Canyon, the Lower Strathearn Formation is deposited and deformed by open, upright, NE-trending and plunging folds (Trexler et al., 2004). This deformation is interpreted to have caused the formation of the P1 angular unconformity (Trexler et al., 2004) (Fig. 12).
- In the Dry Hills, above the C6 unconformity, the lower Wolfcampian age Middle Etchart member was deposited. The Middle Etchart member deposition continued until the early Wolfcampian. Following deposition of the Middle Etchart member, the rocks were folded by SW-trending and plunging, open,

gentle, symmetric folds. This deformation is interpreted to have caused formation of the P1 unconformity, which serves as the base of the Middle Etchart. This depositional and erosion cycle closely resembles the history of Carlin Canyon during this time.

Wolfcampian to Leonardian time

- At Edna Mountain this time period is unrepresented due to the P4 unconformity (Fig. 12) (Villa, 2008).
- In the central Pequop Mountains the early portion of this time is unrepresented due to an unconformity that spans of this time period (Sweet and Snyder, 2002). During this time, specifically the Sakmarian-middle Kungarian, the Pequop Formation was deposited. No structures have been recognized as constrained to this time (Sweet and Snyder, 2002).
- At Carlin Canyon, the Upper Strathearn Formation is deposited in the Wolfcampian and deformed prior to formation of the P2 unconformity (Figs. 12 & 50) (Trexler et al., 2004). Following the formation of the P2 unconformity, the Leonardian age Buckskin Mountain Formation was deposited (Trexler et al., 2004). These units are deformed by open, upright, NNE-trending and plunging folds. The timing of these folds is not well constrained and may be of Leonardian age or younger (Trexler et al., 2004).
- In the Dry Hills the Upper Etchart member is deposited throughout this time period. Multiple deformations are interpreted to occur during this time period, starting with W-E extension resulting in a fault propagation fold-and-normal fault

set (D2). This deformation is followed by N-S shortening resulting in a fold-and-thrust fault set (D3).

Late Cisuralian to Guadalupian time

- At Edna Mountain, the Edna Mountain Formation is deposited atop the P4 unconformity (Figs. 12 & 50) (Villa, 2008). The upper contact of the Edna Mountain Formation is the thrust emplaced Golconda Allochthon of the Sonoma Orogeny (Villa, 2008). No structural deformation is constrained to this time period in this location (Villa, 2008).
- Carlin Canyon and the central Pequop Mountains do not contain units of the Cisuralian to Guadalupian age to record deformation.
- At the Dry Hills this period of time is unaccounted for due to thrust emplacement of the Golconda Allochthon.

Correlation Summaries

In summary, the depositional histories of Edna Mountain and the Dry Hills are similar from the Atokan to Missourian. From that point forward, the two locations appear to record different depositional histories. From the Missourian to the Leonardian, the Dry Hills record deposition that is unrepresented at Edna Mountain due to an unconformity. From the late Cisuralian to the Guadalupian Edna Mountain recorded deposition that is unaccounted for in the Dry Hills due to a fault contact.

The structural histories of the Dry Hills and Edna Mountain locations do not appear to be similar prior to emplacement of the Golconda Allochthon. Edna Mountain's only late Paleozoic deformation occurs prior to the C6 unconformity,

whereas the Dry Hills record progressively increasing deformation that culminates in the Wolfcampian to Leonardian.

The depositional history of the Dry Hills and central Pequop Mountains are similar below the C5 unconformity and similar during the late Wolfcampian and Leonardian above the P2 unconformity. The Dry Hills record deposition during a period not accounted for in the central Pequop Mountains.

The structural histories of the Dry Hills and the central Pequop Mountains differ greatly. Deformation in the central Pequop Mountains is largely confined to the Atokan, and is relatively minor. Deformation in the Dry Hills is much more frequent, and constrained to younger periods of time.

The depositional histories of the Dry Hills and Carlin Canyon are very similar. The timing of unit deposition at Carlin Canyon is synchronous with the timing of deposition of the Etchart members. Uplift or subsidence to form the angular unconformities appears to have occurred in both locations at the same time. However, lithologic differences in units leave their paleogeographical relationship throughout Late Paleozoic time unclear.

The structural history of the Dry Hills and Carlin Canyon are somewhat similar, with regard to late Pennsylvanian and early Permian open, gentle folds. However, the orientations of these folds greatly differ, implying differences in shortening direction. This implies that the locations may not have shared the same paleogeographical distribution in the Late Paleozoic.

Like the age-equivalent Upper and Lower Strathearn Formation of the Carlin Canyon, the Upper and Middle Etchart member are separated by the P1

unconformity (Fig. 12). The Upper Etchart member and Upper Strathearn Formation both contain conglomerates. The conglomerate type and characteristics dramatically differ between the Upper Etchart and Upper Strathearn Formations. Specifically, the conglomerate within the Upper Etchart member contains ~25-45% pebble-to-boulder limestone clasts some of which contain Atokan age fusulinids (V. Davydov, personal communication), whereas the conglomerate within the Upper Strathearn consists of chert and siliceous clasts. The Lower Strathearn inferred depositional setting of mid-to-deep shelf (Trexler et al., 2003) also differs from the higher energy environment required for deposition of the Upper Etchart packstone to grainstone. The Upper Etchart member also displays cross stratification and possible herringbone stratification (UTM 11T 0481644 4566293) implying deposition closer to a nearshore environment than the Strathearn Formation. Due to this, the two units are interpreted as not being correlative beyond age.

Regional Late Paleozoic Analysis

The amount of research regarding Pennsylvanian to Permian deformation in northern Nevada is sufficient enough to begin regional reconstructions of the regional deformation in Nevada. The deformational sequence from Atokan to Triassic has been compiled (Figs. 51-57) with other locations in Nevada (Larson and Riva, 1963; Saller and Dickinson, 1982; Sweet and Snyder, 2002; Trexler et al., 2003, 2004; Villa, 2008; Cashman et al., 2008, Cashman et al., 2010). The regional compilation separates Atokan to Triassic time, and utilizes angular unconformities C5-P4, the areas of deposition between angular unconformities,

and notes deformation. The following incorporates interpretations based on the regional compilation, in time slices.

Deformation in the Atokan (Fig. 51) is observed at Edna Mountain, the Pequop Mountains, and Nine Mile Canyon, indicating a northwest-southeast principal stress that is interpreted to be overall shortening. Contraction was focused in the north central to east central portion of the state. Deformation at Edna Mountain during the Atokan is extensional, which is possibly backarc extension or gravitational collapse. This assumes a single tectonic terrane being interacted upon by plate margin interactions along the western edge of the United States, currently the most commonly accepted hypothesis. Alternatively, extension and contraction within the Atokan also supports may support the hypothesis of multiple tectonic terranes. In this scenario, Atokan deformation occurs in separate paleogeographical locations before being later emplaced in their current location by later deformation (Crafford, 2008). In this case, the sub-parallel alignment of contraction at Nine Mile Canyon and the Pequop Mountains implies that these locations were a part of one tectonic domain to the east, while the extension occurred in at least one other tectonic domain to the west.

Sedimentary deposition in the Atokan consists of carbonates, siliclastic, conglomerate deposits, and mixed conglomerate and carbonate units. Deposition of conglomerates is focused in the northcentral portion of northern Nevada, with thick successions of conglomerate more central in the western Osgood Mountains and Battle Mountain, before thinning and intermixing more to the north-northwest in the western Osgood Mountains and Dry Hills. To the east, at

Nine Mile Canyon, Three Mile Canyon, and the Pequop Mountains, deposition is carbonate, as is deposition at Edna Mountain. This implies that carbonate deposition and open water is southward. Deposition is interpreted to be the result of uplifts from a north-northeastern to north-northwestern direction. Paleocurrent directions from the Osgood Mountains taken from the Atokan age deposits by Saller and Dickinson (1982) indicate northeast and southwest directions, although the sample number (n=8) lessens precision.

The regional extent of the C5 unconformity (Fig. 51) is not entirely known. The lateral distribution of the C5 unconformity is interpreted to have occurred in at least the northeastern corner of northern Nevada. However, the distribution of the C5 unconformity is not constrained in the central and north-central areas because units that would have constrained it may have been eroded by later (younger) unconformities in the area. The C5 unconformity is interpreted to be the result of Atokan-age northern uplifts from a western plate boundary. The edge of the C5 unconformity is not well defined by studies of late Paleozoic rocks. Therefore, it is not possible to interpret the C5 unconformity's shape or aerial extent. Any rocks that further constrain the C5 unconformity are not accounted for in a band from the northwest to the southeast from the Osgood Mountains to Carlin Canyon due to the C6 unconformity. The C5 to the south and southeast at Three Mile Canyon and Secret Canyon is removed by Permian age unconformities (P1 and P3).

Deformation during Desmoinesian time (Fig. 52) is interpreted to be the result of shortening in a south-southeast to north-northwest direction as

interpreted from folds in the Dry Hills and Carlin Canyon. Folds constrained to Desmoinesian at Carlin Canyon are overturned and northwest verging. Desmoinesian age faults at Carlin Canyon also support this interpretation. Folding at Edna Mountain indicates a more west-southwest verging strain field. This discrepancy in shortening direction is interpreted to perhaps be the result of changes in the stress field orientation across a non-linear plate margin or changes in stress field orientation across pre-existing paleo-topography. This shortening is interpreted to be the cause of uplifts that led to the C6 unconformity. This discrepancy in structural parallelism between Dry Hills and Carlin Canyon and the structures of Edna Mountain also is consistent with Crafford's (2008) interpretation of separate paleogeographic areas, or later reorientation. In that case, deformation in the Dry Hills and Carlin Canyon would have occurred in a tectonic terrane during Desmoinesian time that was emplaced at a later time.

Sedimentary deposition in the Desmoinesian consisted of conglomerate deposition at Edna Mountain, carbonate deposition at Nine Mile Canyon and the Pequop Mountains, and possibly mixed carbonate and conglomerate deposition in the Dry Hills, although deposition of Desmoinesian age is not conclusively proven at that location. Rocks of this age are not present at the other locations have either not been deposited or removed by erosion. It may be that the lack of Desmoinesian deposits and the lack of exposures of the C5 unconformity indicate that deposition was thin and/or sporadic and large scale deposition did not initiate, or was short lived. It may also indicate that Desmoinesian

deformation was relatively minor, and did not lead to large scale or numerous basins, although this interpretation is questionable due to the C6 regional unconformity above sediments of this age. It is most likely that the most of the sediments of this age were removed below the C4 unconformity.

The C6 angular unconformity (Fig. 52) is exposed through most of central to north-central Nevada. At Secret Canyon in the center of Nevada, the C6 is not accounted for due to the P1 unconformity. In eastern Nevada at Nine Mile Canyon and the Pequop Mountains, the C6 unconformity is unaccounted for because of deep erosion below the P2 unconformity. This leaves the extent of the C6 unconformity unknown.

Deformation constrained to between Missourian and early Wolfcampian time (Fig. 53) has been identified at several locations in north-central to northern Nevada. These structures change in orientation from northeast to southwest at Carlin Canyon, north-south at Edna Mountain, and northwest to southeast in the Dry Hills. These structures are interpreted to result from deformation with a southeast to northwest maximum principal stress orientation. No faults have been constrained to this time period to determine shortening or extension, although shortening is preferred based on the folds and on the prior tectonic interpretation of the region in the Atokan and Desmoinesian. Changes in structural orientation are interpreted to be a rotation of the stress field due to disruption of the deformation across a non-linear plate margin or contraction into a paleotopographic high. The three non-parallel structures also support the idea of deformation in separate tectonic domains as proposed by Crafford (2008). In

this interpretation the Dry Hills, Edna Mountain, and Carlin Canyon would be separate tectonic terranes that are not emplaced until the Jurassic. However, in the Desmoinesian the structures of the Dry Hills have a parallelism to structures in other areas of Nevada, suggesting they were part of the same tectonic terrane. Missourian to early Wolfcampian, structures in the Dry Hills and Carlin Canyon are not parallel, implying they may not have been a part of the same tectonic domain.

Deposition resumed in the Missourian to early Wolfcampian throughout northcentral to eastern Nevada and consisted of mostly carbonates. Deposition is interpreted to be syntectonic and is identified in the Osgood Mountain, the Dry Hills, Battle Mountain, Carlin Canyon, and the Pequop Mountains. Deposition was at least sufficient to preserve the C6 angular unconformity in most locations as it is not removed by subsequent unconformities throughout most of north-central and central Nevada. Rocks of this age are not present in Nine Mile Canyon, Three Mile Canyon, and Secret Canyon probably due erosion below younger unconformities or deeper erosion southward. This may imply thickening of units northward, but this cannot be confirmed due to the distribution of the younger unconformities.

The P1 unconformity (Fig. 53) is present in the Dry Hills, western Osgood Mountains, Carlin Canyon, and Secret Canyon. The P1 unconformity appears to largely be preserved only to the west. To the east, the P1 unconformity is unaccounted for due to the P2, P3, and P4. The extent of the unconformity is

regional. The distribution cannot be ascertained as it is unknown if it was present in all locations.

Wolfcampian deformation (Fig. 54) at Dry Hills and Secret Canyon contains structures with north-south strikes, indicating an east-west maximum principal stress direction. Deformation at Beaver Peak (which may be older) or Carlin Canyon (which may be younger) is sub-parallel to that deformation. Deformation is extensional in the Dry Hills and contractional at Secret Canyon. If the deformation at Carlin Canyon and Beaver Peak occurred during this time, then the overall tectonic setting is contractional. A contractional plate margin setting in the Wolfcampian also fits into previous interpretations for northern Nevada during Late Paleozoic time. In this setting, the extension experienced in the Dry Hills may represent local gravitational collapse, localized extension as the result of oblique faulting, or back arc extension.

The sedimentary record during the Wolfcampian consists of carbonate deposition recorded at Secret Canyon, Carlin Canyon, and the Dry Hills. The deposition of sediments is obscured at the P2, P3, and P4 unconformities elsewhere in the region. Depositional environment interpretations imply that uplift to the north, with shallow Wolfcampian sediments in the Dry Hills and mid shelf carbonates deposited at Secret Canyon and Carlin Canyon. This location of uplifts is similar to interpreted uplifts in Desmoinesian time, indicating that the driving tectonic mechanism or at least the resulting uplifts may have been similar in location and/or orientation.

The P2 unconformity (Fig. 54) is only conclusively recorded in the rocks of Nine Mile Canyon (Sweet and Snyder, 2002); although there are locations in the Dry Hills that may contain an angular unconformity constrained to a similar time period. In most other locations, the P2 unconformity is removed from the stratigraphic section by younger unconformities or the section of proper age to host the P2 is unaccounted for. For these reasons, the P2 unconformity is interpreted to be the result of a localized uplift. Although it may also be that units deposited atop of the P2 were less thick, or that younger unconformities eroded deeper removing larger amounts of stratigraphy at some locations.

Leonardian deformation (Fig. 55) is definitively located at Secret Canyon (Fig. 12) (Sweet and Snyder, 2002). Carlin Canyon and Beaver Peak both host deformation that may be Leonardian age or older. Deformation at all four locations is contractional (Figs. 12 & 55), indicating a shortening event, although parallelism of structural strikes leaves the shortening direction unclear.

Sedimentary deposition in the Leonardian is accounted for in the Dry Hills, Pequop Mountains, Nine Mile Canyon, Three Mile Canyon, and Secret Canyon (Fig. 12). This is one of the largest distributions for Late Pennsylvanian to early Permian rocks, along with the Missourian and Atokan. This may indicate relatively longer periods of tectonic stability, increased rate of subsidence, or both. The interpreted depositional setting continues to be very shallow in the Dry Hills, with deeper sediments to the south and east, indicating shore edges were northward of the mapped locations. Increasing sea level fall recorded through this time indicate continued sea level regression or tectonic uplift.

Deposition prior to the P4 unconformity (Fig. 55) is rarely preserved, and the P3 unconformity that underlies it is only recorded in the Pequop Mountains (Sweet and Snyder, 2002). This time period is not associated with deformation. For these reasons, time slices from this period are not included.

The P4 unconformity is identified at Edna Mountain, Battle Mountain, and Carlin Canyon (Figs. 12 & 55). These three locations are the only locations that contain rock units stratigraphically young enough to exhibit this unconformity. It is difficult to make interpretations about the P4 unconformity based on the limited amount of data. But, it appears that the P4 angular unconformity was a major unconformity that is simply little preserved. This is based on the high percentage of locations it has been located where rocks of the correct age are available. As rocks below the P4 have been rarely located and contain no deformation constrained between P3 & P4, it is difficult to interpret what event caused its formation.

At the three locations (Fig. 56) with Leonardian to Triassic age rocks above the P4 angular unconformity, the deformation of the rocks is relatively minimal and is not constrained to this time. Although, deformation associated with the emplacement of the Golconda Allochthon is recorded in these rocks at Edna Mountain and Carlin Canyon (Trexler et al., 2003; Villa, 2008). Due to this time slice reconstruction and observations of clastic influx at the Dry Hills, the Golconda Allochthon is interpreted to already be encroaching from the west by this time. The basins or single large basin that sediments of this age were shed

into are interpreted to be the result of eastward flexural subsidence from the westward thrusting Golconda Allochthon.

Deformation related to the Golconda thrust sheet (Fig. 56) emplacement is recorded at Edna Mountain, the Dry Hills, and Carlin Canyon (Trexler et al., 2003; Villa, 2008). In all three locations, fold orientations indicate a southeast-directed thrust direction, rather than strictly eastward thrusting. Thrusting from this direction is somewhat consistent with older Pennsylvanian and Permian shortening directions, indicating that the tectonic settings that are responsible for the structures may be related.

Crafford (2008) suggested that perhaps the entire AOS is actually the "foreland" basin to a slowly eastward emplacing Golconda Allochthon. This regional late Paleozoic reconstruction does not require that tectonic mechanism, although it allows for the possibility that this is correct. Increasing influx of clastic materials and clasts from Atokan to Leonardian, along with a shallowing upward sequence, and increased tectonism during this time in the Dry Hills supports a slow southeastward emplacement of the Golconda allochthon.

This regional time slice reconstruction of deformation in northern Nevada can also be analyzed to clarify two competing ideas which have been described more robustly previously, for late Paleozoic and Permian deformation. These are: (a) thrusting originating from a subduction zone along the western US continental margin (Trexler et al., 2003) or (b) accretion of tectonic terranes along a strike-slip plate boundary along the western US that have been deformed in other paleogeographical locations (Crafford, 2008). This reconstruction provides

evidence at times that supports both interpretations. However, this reconstruction also implies the true explanation is likely more complicated than either of these scenarios can easily explain.

This time slice reconstruction does not discredit the idea that the Late Paleozoic plate setting was transform or that rock records exposed are the result of deposition in separate basins later emplaced in their current locations by piggybacking on later tectonic structures. This idea would easily explain the variation in structural orientation and patterns in sedimentation by separating the study locations into small areas where the structures appear parallel to each other. The Pequop Mountains and Nine Mile Canyon appear to have had very similar depositional and deformational histories, although these histories seem very different from the history of Carlin Canyon, or even Secret Canyon. However, correlation within the time slices and to each other appears to show times and places where a tectonic domain interpretation does not work. For example, the Dry Hills and Carlin Canyon expose structures that are roughly parallel in the Atokan indicating they may be part of the same tectonic domain, but have folds at nearly 90 degrees to each other in the Missourian to Wolfcampian indicating the locations maybe from separate tectonic domains. The two locations again have structures that are somewhat similar in the Wolfcampian, very dissimilar in the Leonardian, and have nearly identically oriented structures associated with the Golconda Allochthon emplacement. While it is possible these rocks may have been deposited in separate locations, it is difficult to believe the locations were emplaced by chance such that half of

their Pennsylvanian and Permian structures are now parallel to sub-parallel through time.

This time slice reconstruction indicates that if eastward or southeastward thrusting from a subduction plate margin is the tectonic setting responsible for Late Paleozoic deformation, than the resulting stress fields were changing orientations, type, and intensity throughout space and time. This can be explained by thrusts across various paleogeography and paleorelief, but to do so suggests that pre-existing conditions had a large effect on thrusts and contraction, while the resulting uplifts were still sufficient to result in localized gravitational collapse and/or back arc extension, or both near the beginning (Atokan, Edna Mountain) and near the culmination (Wolfcampian, Dry Hills) of deformation. These situations are invoked to explain the variations in deformation throughout the area at each time. However, while a western subducting plate margin is more strongly favored, supporting evidence regarding the arc location, subducting plate direction and angle, uplift locations, uplift magnitude, and plate margin location is still unaccounted for rather than the interpretation that is truly likely to be correct.

Although not previously proposed, it is worth noting that both theories could in fact be correct at the same time if subduction along a western plate margin was oblique. This setting would produce large scale, regional eastward and southeastward contractions and associated deformations, a wide range of localized variations in stress field and localized deformation type, and could even lead to accretion of separate tectonic terranes within the Golconda Allochthon as

supported by Crafford (2008). This interpretation would utilize the strengths of both contractional and transform plate margin interpretations.

Plate Margin/Tectonic Setting

During the Late Paleozoic the area of the Dry Hills appears to have been undergoing episodic cycles of uplift, erosion, and redeposition within local basins driven by pulses of tectonic deformation that occur throughout the Late Pennsylvanian (Lower Etchart member conglomerates) to early-mid Permian (thrust faults, angular unconformities, and conglomerate deposits). The frequency of these events in the Dry Hills appears to have increased throughout this time, transitioning from relatively long periods of relatively continuous, uninterrupted deposition during the Late Pennsylvanian (e.g., the Lower Etchart member's rare and small conglomerate deposits, sandstone channels and no deformation isolated to the unit) to deposition frequently interrupted by deformation by the early-mid Permian (e.g., larger, more common conglomerate deposits with large clasts, and multiple deformations within the Upper Etchart member). The conglomerate deposition in the Dry Hills indicates an eroding silciclastic source that began shedding increased amounts of siliciclastic material, including Osgood Quartzite, southward into the Dry Hills from Pennsylvanian to Permian time. In the Permian, multiple carbonate clast sources, one of which was Atokan age, were uplifted or unroofed and began shedding boulder-sized clasts into the area, indicating the Dry Hills was proximal to this uplift.

The deformation and deposition in the Dry Hills differs from current ARM deformation models, which describe single, large uplifts, driven by basement

uplifts (Kluth, 1986; Ye et al., 1996; Marshak et al., 2000; Barbeau, 2003). This is unlike the Dry Hills Pennsylvanian to Permian deformation which appears to record deformations that occur in pulses. The Dry Hills exist in close proximity to both the edge of incompletely understood ARM associated uplifts and Late Paleozoic deformation of northern Nevada. Therefore, it is not possible to rule out an ARM influence on the deformational history of the Dry Hills. However, the ARM influence is interpreted to be minimal, if present, because of the presence of multiple contractions and differences in structural orientation.

The tectonic driving force for the Pennsylvanian and Permian tectonism has initially been interpreted as eastward-directed contraction driven by subduction along the plate margin of the western United States (Trexler et al., 2004). Alternatively, Crafford (2008) proposed that the deformation is the result of tectonic terrane accretion along a western United States strike-slip plate boundary. The tectonic history recorded in the Dry Hills supports Pennsylvanian to Permian tectonic deformation, but does not provide evidence that supports or refutes either interpretation.

Crafford (2008) suggests that Late Paleozoic tectonism represents an earlier initiation of the Sonoma Orogeny, and that the AOS represents the “foreland basin” of a slowly emplaced Golconda Allochthon. The interpreted late Paleozoic tectonic history of the Dry Hills supports this theory. An earlier, slow, and multiepisodic southeastward emplacement of the Golconda Allochthon would explain the increasing southeastward directed influx of siliceous sediments, episodic basin formation, and increasing frequency of tectonic events of the Early

Permian Dry Hills. This interpretation also removes the lack of a foreland basin deposit for the Golconda Allochthon, as the Etchart Formation would represent basin deposits caused by subsidence from the approaching Golconda Allochthon.

Recognition of Late Paleozoic deformation strongly implies that the western United States continued to have a plate margin along the continental edge following the Antler Orogeny. This interpretation simplifies models of the western United States from the Paleozoic to Triassic. Models of the Antler Orogeny would no longer require the absence of a plate margin for passive margin sedimentation (miogeoclinal), only to resume subduction on plate margin in roughly the same location for the Sonoma Orogeny. The current amount of Late Paleozoic structural data prevents certainty as to the nature of this plate boundary: contractional (Trexler et al., 2004), strike-slip (Crafford, 2008), or a combination of both.

CHAPTER 6

CONCLUSIONS

Summary of Results

The Dry Hills are located north of the Osgood Mountains in eastern Humboldt County, Nevada (Fig. 2). Stratigraphically, the Dry Hills contain Cambrian to Ordovician sedimentary rocks of the Roberts Mountain Allochthon with overlying mixed siliciclastic and carbonate rocks from the Antler Overlap Sequence named the Etchart Formation. The Golconda Allochthon is thrust over the Etchart Formation in the western Dry Hills. In the northwestern to northern Dry Hills, Cenozoic basalt and andesite rest atop all non-Quaternary units. The Etchart Formation is divided into three sub-units by the P1 and C5/C6 angular unconformities.

Structural and stratigraphic analysis in the Dry Hills provides new evidence for late Paleozoic deformation, with at least three deformational events that can be constrained to prior to the Sonoma Orogeny. Angular unconformities between the informal Upper, Middle, and Lower Etchart members provide evidence for sub-division of the Etchart Formation into three distinct carbonate formations separated by angular unconformities. Fusulinid biogeochronology suggest correlation of the Etchart Formation to carbonates from the Antler Overlap Sequence. Stratigraphic constraints and clast analysis have identified conglomerates within the Upper Etchart member that are not the Battle Formation. Atokan age clasts provide further evidence of erosion within the late Pennsylvanian to Early Permian.

The Etchart Formation in the Dry Hills has undergone six outcrop identifiable deformations. D1 consists of tilting. D2 consists of gently southeast plunging open folds. D3 consists of north striking high angle normal faults and gently north plunging open folds. D4 consists of northeast striking, south dipping reverse faults and northeast plunging open folds. D5 consists of northwest striking, west dipping reverse faults and northwest trending, gently northwest plunging, gently east inclined folds. D5 faults have been interpreted to be related to the emplacement of the Golconda Allochthon. D6 consists of an oblique right-lateral normal fault zone known as the Getchell fault.

Spatial analysis of Late Paleozoic deformation research conducted previously and herein indicates two regionally significant deformations in northern Nevada. The first regional deformation occurs during the Desmoinesian. Structures associated with regional deformation display multiple orientations throughout the state, but the general shortening direction appears to be southwest to northeast. This regional deformation resulted in the creation of the C6 angular unconformity. The second regionally significant deformation occurred during the Missourian to early Wolfcampian time. Structures associated with this deformation occur in multiple orientations throughout northern Nevada. This is interpreted to be the result of compression along non-linear paleogeography or due to structural reorienting of blocks. This deformation is responsible for the formation of the P1 angular unconformity.

REFERENCES CITED

Allmendinger, R.W., 2009, Stereonet v 1.2.0 for windows. http://www.geo.cornell.edu/geology/faculty/RWA/programs.html

Babaie, H. A. and Sleep, R. C., 1990, Origin of kink bands in the Golconda Allochthon, Toiyabe Range, Nevada, Geological Society of America Bulletin, v. 102, p.315-321.

Barbeau, D.L., 2003, A flexural model for the Paradox basin: implications for the tectonics of the Ancestral Rocky Mountains: Basin Research, v. 15, p. 97–115.

Berger, B.R., 1975, Trace element variations associated with disseminated gold mineralization at the Getchell Mine, Humboldt County, Nevada: Economic Geology and the Bulletin of the Society of Economic Geologists, v. 70, p. 1318.

Bissell, H.J., 1964, Patterns of sedimentation in Pennsylvanian and Permian Strata of part of the eastern Great Basin, *in* D.F. Merriam, Ed., Symposium on Cyclic Sedimentation: Kansas Geological Survey, Bulletin 169, p. 43-56.

Bloomstein, E.I., Massingill, G.L., Parratt, R.L., Peltonen, D.R., and Cuffney, B., 1990, Discovery, geology, and mineralization of the Rabbit Creek gold deposit, Humboldt County, Nevada; Geology and ore deposits of the Great Basin; program with abstracts, *in* Geology and ore deposits of the Great Basin, Reno, NV, Geological Society of Nevada, Reno, NV, United States (USA) p. 821-843.

Boskie, R.M. and Schweickert, R.A., 2001, Structure and stratigraphy of lower Paleozoic rocks of the Getchell Trend, Osgood Mountains, Humboldt County, Nevada: *in* Shaddrick, D.R., Zbinden, E, Mathewson, D.C., Prenn, C., ed., Regional tectonics and structural control of ore; the major gold trends of northern Nevada; proceedings and field trip guide [modified], Special Publication - Geological Society of Nevada, v. 33, p. 263-293.

Brueckner, H. K., and Snyder, W. S., 1985, Structure of the Havallah sequence, Golconda allochthon, Nevada: Geological Society of America Bulletin, v. 96, p. 1113-1130.

Burchfiel, B.C., Cowan, D.S., and Davis, G.A., 1992, Tectonic overview of the western United States, The Geology Society of America, V. G-3, The Cordilleran Orogen: Conterminous U.S., p. 407-479.

Burchfiel, B.C., and Davis, G.A., 1972, Structural framework and evolution of the southern part of the Cordilleran orogen, western United States: American Journal of Science, v. 272, p. 97–118.

Burchfiel, B.C., and Royden, L.H., 1991, Antler orogeny: A Mediterranean-type orogeny: Geology, v. 19, p. 66–69, doi: 10.1130/0091-7613(1991)019<0066:AOAMTO>2.3.CO;2.

Carlisle, D. and Nelson, C.A., 1964, Geologic map of the Humboldt County, Nevada: United States Geological Survey, Map 97, scale 1:250 000, 1 sheet.

Carpenter, J. A., Carpenter, D.S., and Dobbs, S.W., 1993, Structural analysis of the Pine Valley area , Nevada *in* Gillispie C.W., ed, Structural and

Stratigraphic relationships of Devonian reservoir rocks, East-Central Nevada: Nevada Petroleum Society 1993 Field Conference Guidebook, p. 9-49.
Cashman, P. H., Villa,D.E., Taylor, W.J., Davydov, V.I., and Trexler, J.H., 2010, Late Palerozoic contractional and extentional deformation at Edna Mountain, Nevada: Geological Society of America Bulletin. Doi: 10.1130/B30247.1
Cashman, P., Trexler, J., Snyder, W., Davydov, V., and Taylor, W., 2008, Late Paleozoic deformation in central and southern Nevada; Field guide to plutons, volcanoes, faults, reefs, dinosaurs, and possible glaciation in selected areas of Arizona, California, and Nevada: Geological Society of America Field Guide, v. 11, p. 21-42, doi: 10.1130/2008.fld011(02).
Cline, J.S., 2001, Timing of gold and arsenic sulfide mineral deposition at the Getchell carlin-type gold deposit, north-central Nevada: Economic Geology and the Bulletin of the Society of Economic Geologists, v. 96, p. 75-89
Crafford, A.E.J., 2008, Paleozoic tectonic domains of Nevada; an interpretive discussion to accompany the geologic map of Nevada: Geosphere, v. 4, p. 260-291, doi: 10.1130/GES00108.1.
Crafford, A.E.J., 2007, Geologic map of Nevada: U.S. Geological Survey Data Series 249, scale 1:250,000, 1 CD-ROM, 46 p., 1 plate, URL: http://pubs.usgs.gov/ ds/2007/249/.
Crafford, E.J., 2000, The Osgood block: A structurally unique Paleozoic terrane in northern Nevada: Geological Society of America Abstracts with Programs, v. 32, no. 7, p. A-383.
Davis, G.A., Monger, J.W.H., and Burchfiel, B.C., 1978, Mesozoic construction of Cordilleran "collage," central British Columbia to central California: Bulletin of the American Association of Petroleum Geologists, v. 62, p. 2352-2353.
Dickinson, W.R., and Lawton, T.F., 2003, Sequential intercontinental suturing as the ultimate control for Pennsylvanian Ancestral Rocky Mountains deformation: Geology, v. 31, p. 609-612.
Dickinson, W.R., and Gehrels, G.E., 2000, Sandstone petrofacies of detrital zircon samples from Paleozoic and Triassic strata in suspect terranes of northern Nevada and California, *in* Soreghan, M.J., and Gehrels, G.E., eds., Paleozoic and Triassic paleogeography and tectonics of western Nevada and northern California: Boulder, Colorado, Geological Society of America Special Paper 347, p. 151–171.
Dickinson, W.R., Harbaugh, D.W., Saller, A.H., Heller, P.L., and Snyder, W.S., 1983, Detrital modes of Upper Paleozoic sandstones derived from Antler orogen in Nevada: Implications for nature of Antler Orogeny: American Journal of Science, v. 283, p. 481-509.
Dott, R.H. Jr., 1955, Pennsylvanian stratigraphy of Elko and northern Diamond Ranges, northeastern Nevada: Bulletin of the American Association of Petroleum Geologists, v. 39, p. 2211–2305.
Erickson, R.L., and Marsh, 1974, S.P., U.S. Geological Survey Geologic Quadrangle Map GQ-1175, scale 1:24,000.
Fagan, J.J., 1962, Carboniferous cherts, turbidites, and volcanic rocks in northern Independence Range, Nevada: Geological Society of America Bulletin, v. 73, p. 595–612.

Gehrels, G.E., and Smith, M.T., 1987, “Antler” allochthon in the Kootenay arc?: Geology, v. 1, p. 769-770.
Gehrels, G.E., and Dickinsen, W.R., 2000, Detrital zircon geochronology of the Antler overlap and foreland basin assemblages, Nevada; Paleozoic and Triassic paleogeography and tectonics of western Nevada and Northern California: Special Paper - Geological Society of America, v. 347, p. 57-63.
Geslin, J.K., 1998, Distal ancestral Rocky Mountains tectonism; evolution of the Pennsylvanian-Permian Oquirrh-Wood River basin, southern Idaho: Geological Society of America Bulletin, v. 110, p. 644-663, doi: 10.1130/0016-7606(1998)110<0644:DARMTE>2.3.CO;2.
Holtz, P. E., and Willden, R., 1964, Geology and mineral deposits of the Osgood Mountains quadrangle, Humboldt County, Nevada: US Geological Survey Professional Paper 431, 128p.
Holtz, P.E., and Willden, C.R., 1961, Preliminary geologic map and sections of the Osgood Mountains Quadrangle, Humboldt County, Nevada: U. S. Geological Survey, Reston, VA, United States (USA), Report MF-0161.
Hoy, R.G., and Ridgway, K.D., 2002, Syndepositional thrust-related deformation and sedimentation in an ancestral Rocky Mountains basin, Central Colorado Trough, Colorado, USA: Geological Society of America Bulletin, v. 114, p. 804-828, doi: 10.1130/0016-7606(2002)114<0804:STRDAS>2.0.CO;2.
Jansma, P.E., and Speed, R.C., 1990, Omissional faulting during Mesozoic regional contraction at Carlin Canyon, Nevada: Geological Society of America, v. 102, p. 417-427.
Jansma, P. E., and Speed, R.C., 1995, Kinematics of underthrusting in the Paleozoic Antler foreland basin: Journal of Geology, v. 103, p. 559-575.
Jansma, P.E., and Speed, R.C., 1993, Deformation, dewatering, and decollement development in the Antler foreland basin during the Antler Orogeny: Geology (Boulder), v. 21, p. 1035-1038, doi: 10.1130/0091-7613(1993)021<1035:DDADDI>2.3.CO;2.
John, D.A., Wallace, A.R., Ponce, D.A., Fleck, R.B., and Conrad, J.E., 2000, New perspectives on the geology and origin of the northern Nevada Rift, *in* Cluer, J.K., et al., eds., Geology and ore deposits 2000: The Great Basin and beyond: Geological Society of Nevada, 2001 Symposium Proceedings, p. 127–154.
Jones, A.E., 1990, Geology and tectonic significance of terranes near Quinn River Crossing, Nevada, in Harwood, D.S., and Miller, M.M., eds., Paleozoic and early Mesozoic paleogeographic relations; Sierra Nevada, Klamath Mountains, and related terranes: Boulder, Colorado, Geological Society of America Special Paper 255, p. 239–253.
Jones, A.E., 1991, Tectonic significance of Paleozoic and Early Mesozoic terranes accretion in northern Nevada [Ph.D. thesis]: Berkeley, University of California, 256 pp.
Jones, A.E., 1993, Northwest vergent folding in the Harmony Formation, north-central Nevada—Lower Paleozoic tectonics revised: Geological Society of America Abstracts with Programs, Cordilleran Section meeting, v. 25, no. 5. p. 59.

Kerr, W., 1962, Paleozoic sequences and thrust slices of the Seetoya Mountains, Independence Range, Elko County, Nevada: Geological Society of America Bulletin, v. 73, p. 439–460

Ketner, K.B., 1977, Deposition and deformation of lower Paleozoic western facies rocks, northern Nevada, *in* Stewart, J.H., Stevens, C.H., and Fritsche A. E., ed., Paleozoic Paleogeography of the Western United States: Pacific Coast Paleogeography; Society Economic Paleontologists and Mineralogists., Pacific Section, Symposium v. 1, p. 251–258.

Kluth, C.F., Ye, H., Royden, L.H., Burchfiel, C., and Schuepbach, M., 1998, Late Paleozoic deformation of interior North America; the greater ancestral Rocky Mountains; discussion and reply: American Association of Petroleum Geologists Bulletin, v. 82, p. 2272-2279.

Kluth, C.F., and Coney, P.J., 1981, Plate tectonics of the ancestral Rocky Mountains: Geology, v. 9, p. 10-15.

Kluth, C.F., 1986, Plate tectonics of the Ancestral Rocky Mountains, *in* Peterson, J.A., ed., Paleotectonics and sedimentation in the Rocky Mountain region, United States: American Association of Petroleum Geologists Memoir 41, p. 353–369.

Laravie, J.A., 2005, Geologic map of the Kelly Creek area, Humboldt, Elko, and Lander Counties, Nevada: Nevada Bureau of Mines and Geology Open-File Report 05-1, scale 1:24,000.

Larson, E.R., and Riva, J.F., 1963, Preliminary geologic map of the Diamond Springs quadrangle, Nevada: Nevada Bureau of Mines Map 20, scale 1:62,500.

Little, T.A., 1987, Stratigraphy and structure of metamorphosed Upper Paleozoic rocks near Mountain City, Nevada: Geological Society of America Bulletin, v. 98, p. 1-17.

Marshak, S., Karlstrom, K., and Timmons, J.M., 2000, Inversion of Proterozoic extensional faults: An exploration for the pattern of Laramide and Ancestral Rockies interaction deformation, United States: Geology, v. 28, p. 735-738.

Merriam, C.W., and Anderson, C.A., 1942, Reconnaissance survey of the Roberts Mountains, Nevada: Bulletin of the Geological Society of America, v. 53, p. 1675–1726.

Miller, E. L., Holdsworth, B. K., Whiteford, W. B., and Rodgers, D., 1984, Stratigraphy and structure of the Schoonover sequence, northeastern Nevada: Implications for Paleozoic plate-margin tectonics: Geological Society of America Bulletin, v. 95, p, 1063-1076.

Nesse, W.D., 2008, Separating “Geomythology” from the Reality of the Late Paleozoic Uplifts in Colorado, Utah, Wyoming, New Mexico, and Adjacent areas; abstracts with programs, *in* Geological Society of America: Cordilleran/Rocky Mountain Section meeting, v. 40, p. 38.

Osterberg, M.W., Guilbert, J.M., and Cuffney, B., 1991, Wall-rock alteration of the Chimney Creek sediment-hosted gold deposit, Humboldt County, Nevada; Geology and ore deposits of the Great Basin; Program with Abstracts, *in* Geology and ore deposits of the Great Basin, Reno, NV, United States:

United States (USA), Geological Society of Nevada, Reno, NV, United States (USA), p. 805-819.
Osterberg, M.W., 1990, Geology and geochemistry of the Chimney Creek gold deposit, Humboldt County, Nevada [Ph.D. thesis]: United States (USA), University of Arizona, Tucson, AZ, United States (USA), p. 173 .
Poole, F.G., 1974, Flysch deposits of the Antler foreland basin, western United States, in Dickinson, W.R., ed., Tectonics and Sedimentation; Society of Economic Paleontologists and Mineralogists, Special Publication 22, p. 58-82.
Poole, F. G., and Sandberg, C. A., 1977, Mississippian paleogeography and tectonics of the western United States, *in* Stewart, J. H, Stevens, C. H., and Fritsche A. E., eds., Paleozoic Paleogeography of the Western United States, Society of Economic Paleontologists and Mineralogists, Pacific Section, p. 67-89.
Poole, F.G., and Ketner, K.B., 1980, Lower Paleozoic rock fragments in Antler flysch, northern Nevada: U. S. Geological Survey, Reston, VA, United States (USA), Report P 1175, 88 p.
Poole, F.G., and Sandberg, C.A., 1991, Mississippian paleogeography and conodont biostratigraphy of the western United States, *in* Cooper, J.D., and Stevens, C.H., eds., Paleozoic paleogeography of the western United States II:Pacific Section, Society of Economic Paleontologists and Mineralogists, Field Trip Guidebook, v. 67**,** p. 107-136.
Poole, F.G., Stewart, J.H., Palmer, A.R., Sandberg, C.A., Madrid, R.A., Ross, R.J., Hintze, L.F., Miller, M.M., and Wrucke, C.T., 1992, Latest Precambrian to latest Devonian time: Development of a continental margin: *in* Burchfiel, B.C., Lipman, P.W., and Zoback, M.L., eds., The Cordilleran orogen: Conterminous U.S.: Boulder, Colorado, Geological Society of America, Geology of North America. G-3, p. 9-56.
Rilely, B.C.D., Snyder, W.S., and Gehrels, G.E., 2000, U-Pb detrital zircon geochronology of the Golconda allochthon, Nevada: Geological Society of America, Special Paper 347, p. 65-75.
Racheboef, P.R., Moore, T.E., and Blodgett, R.B., 2004, A new species of Dyoros (Brachiopoda; Chonetoidea) from Nevada (United States) and stratigraphic implications for the Pennsylvanian and Permian Antler Overlap assemblage Une nouvelle espece de (Brachiopoda; Chonetoidea) du Nevada (Etats-Unis) et implications stratigraphiques pour le Complexe chevauchant d' Antler (Pennsylvanien et Periem): Geobios, v. 37, p. 382-394.
Roberts, R.J., 1951, Geology of the Antler Peak quadrangle, Nevada: U.S. Geological Survey Geologic Quadrangle Map GQ-10, scale 1:62,500.
Roberts, R.J., 1964, Stratigraphy and structure of the Antler Peak quadrangle, Humboldt and Lander Counties, Nevada: U.S. Geological Survey Professional Paper 459-A, 93 p.
Roberts, R.J., Hotz, P.E., Gilluly, J., and Ferguson, H.G., 1958, Paleozoic rocks of north-central Nevada: Bulletin of the American Association of Petroleum Geologists, v. 42, no. 12, p. 2813-2857.
Stewart J.H. and Carlson, J.E., 1977, One million scale set geologic map of Nevada: Nevada Bureau of Mines and Geology, scale 1:1 000 000, 1 sheet.

Saller, A.H., and Dickinson, W.R., 1982, Alluvial to marine facies transition in the Antler overlap sequence, Pennsylvanian and Permian of north-central Nevada: Journal of Sedimentary Research, v. 52, p. 925-940.
Saucier, A.E., 1997, The Antler Thrust System in Northern Nevada. The Roberts Mountain Thrust Elko and Eureka Counties, Nevada; Nevada Petroleum Society Field Trip Guidebook, p. 1-16.
Schweikert, R. A., and Snyder, W. S., 1981, Paleozoic plate tectonics of the Sierra Nevada and adjacent regions, *in* Ernst, W. G., ed., The geotectonic development of California: Englewood Cliffs, New Jersey, Prentice-Hall, p. 183-201.
Silberling, N.J., 1973, Geologic events during Permian-Triassic time along the Pacific margin of the United States, *in* Logan, A., and Hills, L.V., eds., The Permian and Triassic Systems and their Mutual Boundary: Calgary, Alberta, Canadian Society of Petroleum Geologists Memoir 2, p. 345–362.
Smith, J.F. Jr., and Ketner, K.B., 1968, Devonian and Mississippian rocks and the date of the Roberts Mountains thrust in the Carlin-Piñon Range area, Nevada: U.S. Geological Survey Bulletin 1251-I, 18 p.
Smith, J.F. Jr., and Ketner, K.B., 1977, Tectonic events since early Paleozoic in the Carlin-Piñon Range area, Nevada: U.S. Geological Survey Professional Paper 867-C, 18 p.
Speed, R.C., 1977, Island arc and other paleogeographic terranes of late Paleozoic age in the western Great Basin, in Stewart, J.H., Stevens, C.H., and Fritsche, A.E., eds., Paleozoic Paleogeography of the Western United States: Los Angeles, California, Society of Economic Paleontologists and Mineralogists, Pacific Section Pacific Coast Paleogeography Symposium 1, p. 349–362.
Speed, R.C., 1979, Collided Paleozoic microplate in the western United States: Journal of Geology, v. 87, p. 279–292.
Speed, R.C., and Sleep, N.C., 1982, Antler orogeny and foreland basin – a model: Geological Society of America Bulletin, v. 93, p. 815-828.
Stewart, J.H., and Carlson, J.E., 1977, Million-scale geologic map of Nevada: Nevada Bureau of Mines and Geology, Reno, NV, United States (USA), Report 57.
Stewart, J. H., and Palmer, A. R., 1967, Callaghan Window-a newly discovered part of the Roberts Thrust, Toiyabe Range, Lander County, Nevada: U.S. Geological Survey Professional Paper 575D, p. 56-63.
Steele, G., 1960, Pennsylvanian-Permian stratigraphy of east-central Nevada and adjacent Utah: Geology of east central Nevada, p. 91-113.
Stevens, C.H., Yancey, T.E., and Hanger, R.A., 1990, Significance of the provincial signature of Early Permian faunas of the eastern Klamath terrane, California, *in* Harwood, D.S., and Miller, M.M., eds., Paleozoic and Early Mesozoic Paleogeographic Relations; Sierra Nevada, Klamath Mountains, and Related Terranes: Boulder, Colorado, Geological Society of America Special Paper 255, p. 201–218.

Stevens, C.H., Stone, P., and Kistler, R.W., 1992, A speculative reconstruction of the middle Paleozoic continental margin of southwestern North America: Tectonics, v. 11, p. 405-419, doi: 10.1029/91TC02884.

Stone, P., and Stevens, C.H., 1988a, An angular unconformity in the Permian section of east-central California: Geological Society of America Bulletin, v. 100, p. 547-551.

Sweet, D., and Snyder, W.S., 2002, Middle Pennsylvanian through Early Permian tectonically controlled basins: Evidence from the central Pequop Mountains, northeast Nevada: Late Paleozoic tectonics and hydrocarbon systems of western North America—The greater Ancestral Rocky Mountains: Tulsa, AAPG Hedberg Research Conference, p. 74–77.

Theodore, T.G., Moring, B.C., Harris, A.G., Armstrong, A.K., and Finney, S.C., 2003, Geologic map of the Beaver Peak quadrangle, Elko and Eureka Counties, Nevada: Nevada Bureau of Mines and Geology Map 143, scale 1:24,000.

Theodore, T.G., Armstrong, A.K., Harris, A.G., Stevens, C.H., and Tosdal, R.M., 1998, Geology of the northern terminus of the Carlin trend, Nevada: Links between crustal shortening during the Late Paleozoic Humboldt Orogeny and northeast-striking faults, *in* Tosdal, R.M., ed., Contributions to the gold metallogeny of northern Nevada: U.S. Geological Survey Open-File Report 98-338, p. 69–105.

Thoreson, R.F., Jones, M.E., Breit, F.J. Jr., Doyle-Kunkel, M.A., and Clarke, L.J., 2000, The geology and gold mineralization of the Twin Creeks gold deposits, Humboldt County, Nevada, *in* Crafford, A.E.J., ed., Geology and ore deposits of the Getchell region, Humboldt County, Nevada: Reno, Nevada, Geological Society of Nevada Symposium 2000 Field Trip Guidebook 9, p. 85–111.

Trexler, J. H., Cashman, P.H., Snyder, and W.S., Davydov, V.I., 2004, Late Paleozoic tectonism in Nevada: Timing, kinematics, and tectonic significance Geological Society of America Bulletin, v. 116, p. 525-538.

Trexler, J. H., Cashman, P.H., Cole, J.C., Snyder, W.S., Tosdol, R.M., and Davydov, V.I., 2003, Widespread effects of middle Mississippian deformation in the Great Basin of western North America: Geological Society of America Bulletin, v. 115, p. 1278-1288.

Verville, G.J., and Sanderson, G.A, 1988, Early Atokan fusulinids from the lower Antler Overlap Sequence, Lander and Humboldt County, Nevada: Journal of Paleontology, v. 62, p. 520-529.

Villa, D.E., 2008, Timing and Kinematics of the Iron Point Thrust at Edna Mountain, Humboldt County, Nevada [MS thesis]: University of Nevada, Reno, 109 p.

Willden, R., 1961, 1:200 000 scale, Preliminary Geologic Map of Humboldt County, Nevada: United States Geological Survey, Miscellaneous Field Studies Map MF-236.

Willden, R., and R. C. Speed, 1974, Geology and Mineral Deposits of Churchill County, Nevada., Bulletin 83, Mackey School of Mines, University of Nevada, Reno, 95 p.

Wernicke, B., 1992, Cenozoic extensional tectonics of the U.S. Cordillera. The Geologic Society of America, v. G-3, The Cordilleran Orogen: Conterminous U.S., p. 553-581.
Wyld, S.J., Rogers, J.W., and Wright, J.E., 2001, Structural evolution within the Luning-Fencemaker fold-thrust belt: progression from back-arc basin closer to intra-arc shortening: Journal of Structural Geology, v. 23, p. 1971-1995.
Ye, H., Royden, L., Burchfiel, C., and Schuepbach, M., 1996, Late Paleozoic deformation of interior North America: The greater Ancestral Rocky Mountains: American Association of Petroleum Geologists Bulletin, v. 80, p. 1397-1432.

APPENDIX 1

FIGURES

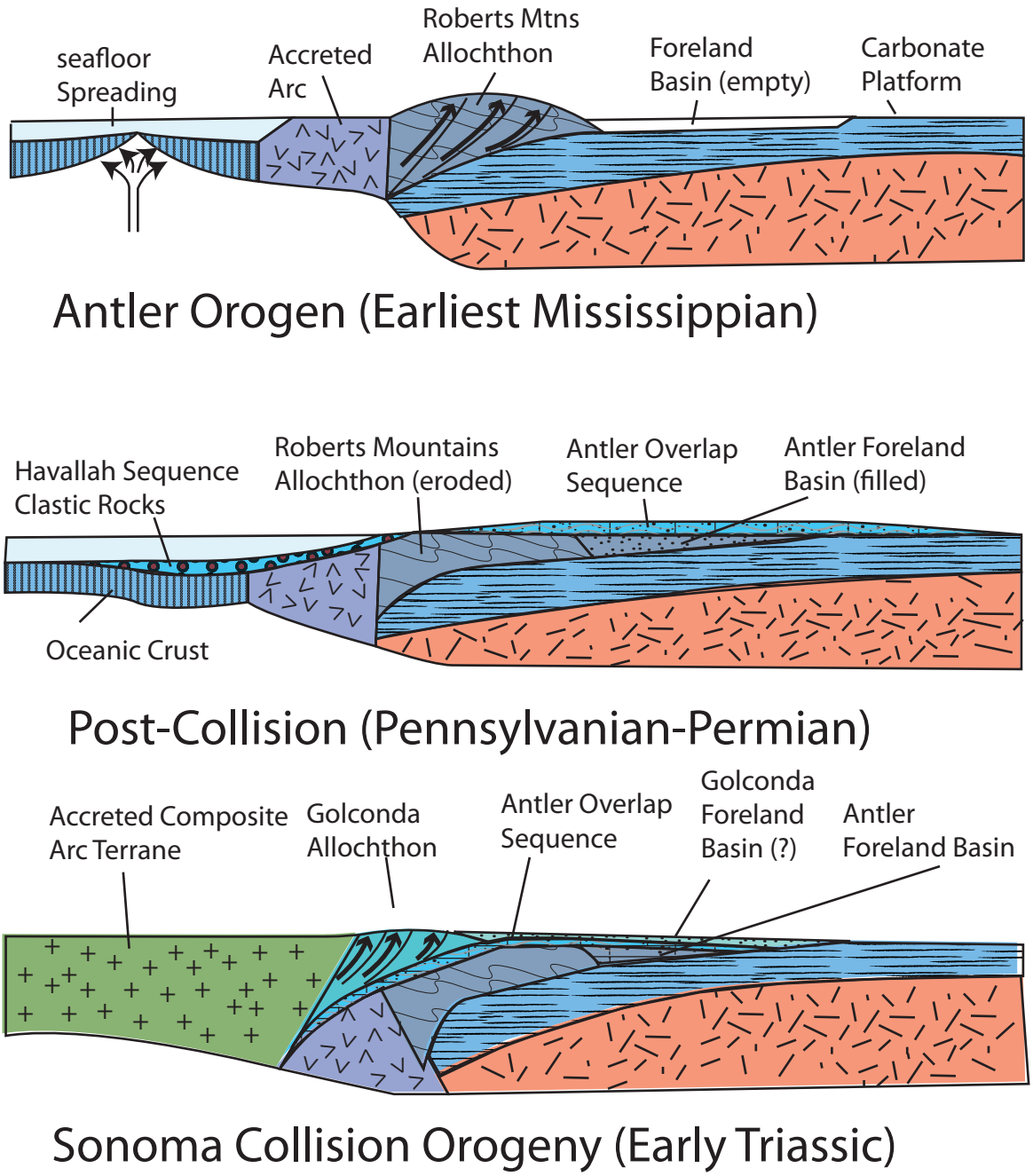

Figure 1. Model of the tectonic overview of the western United States from Mississippian to Triassic time (modified from Burchfiel et al., 1992). In this model, the Antler Overlap Sequence is deposited in a period of quiescence between the Antler and Sonoma orogenies.

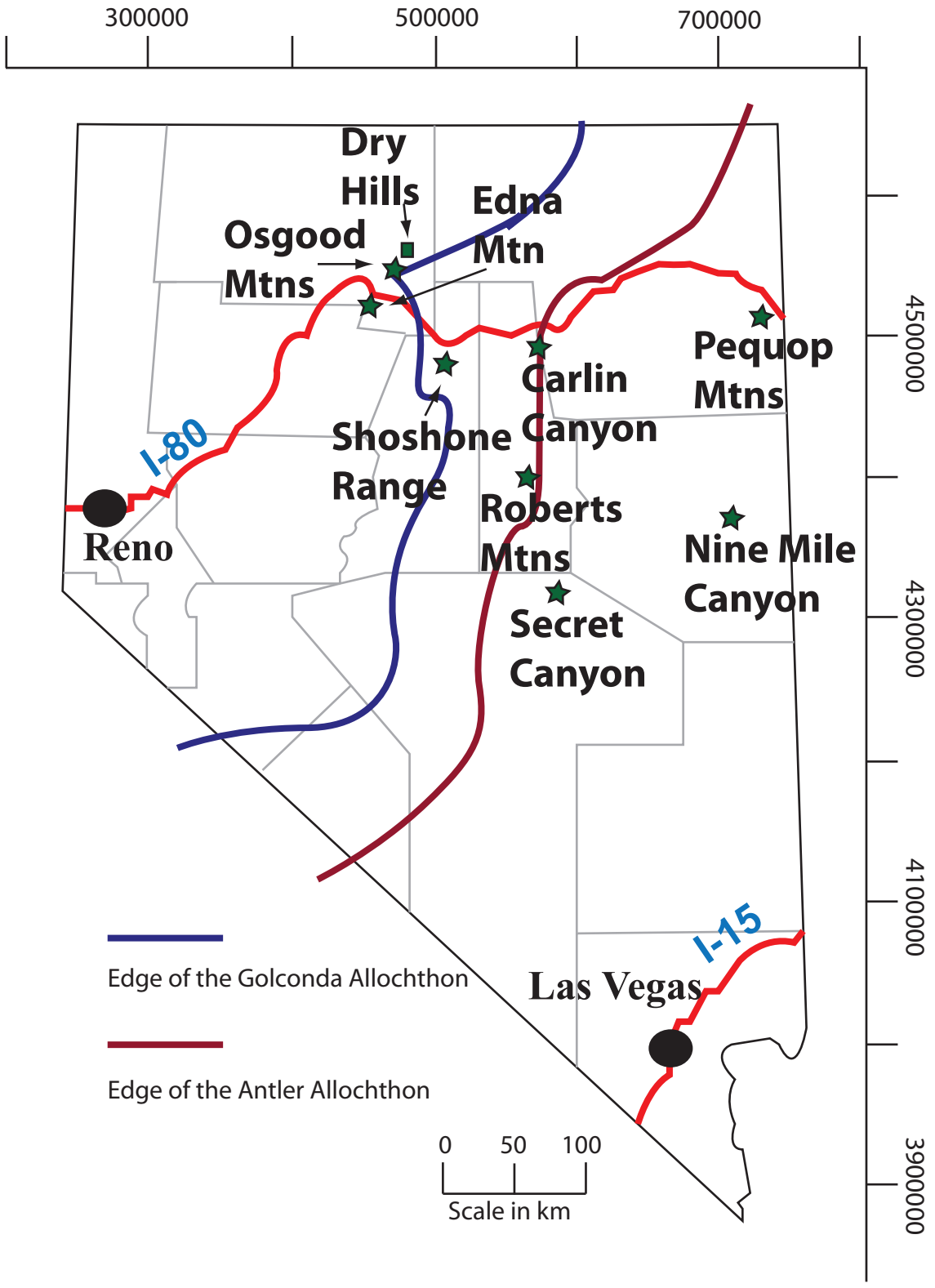

Figure 2. Location map showing areas containing Late Paleozoic deformation (Modified from Villa, 2008).

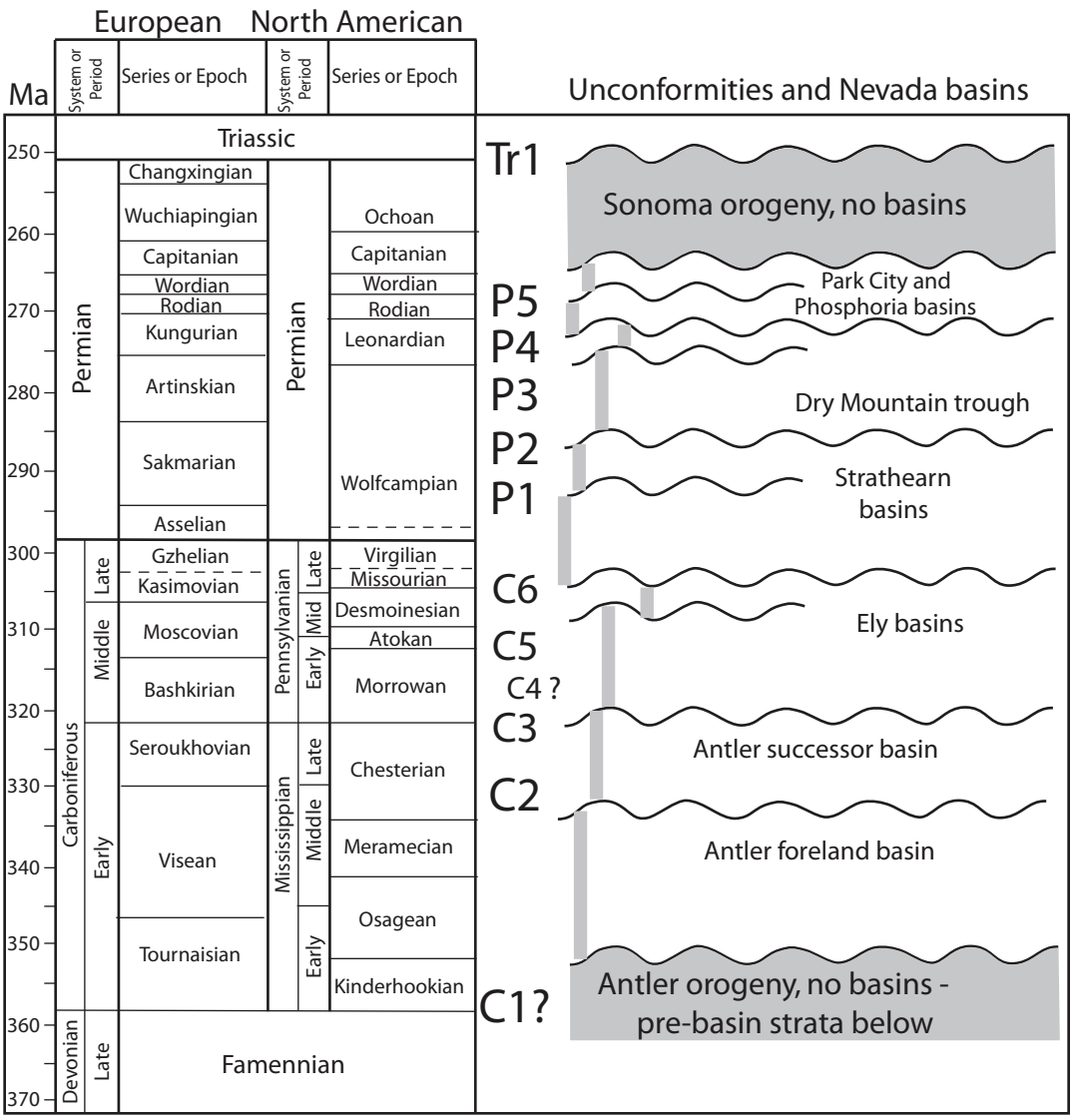

Figure 3. Trexler et al. (2003), Snyder et al. (2002) and other researchers adopted a system for documenting late Paleozoic angular unconformities within the western United States. This system assigns each age-defined unconformity within a region a name consisting of a letter and a number. The letter represents the age period, (i.e., P for Permian, or C for Carboniferous). The number following the letter represents the relative age of the unconformity within the age period, with 1 signifying the oldest and subsequent numbers for progressively younger unconformities, e.g., P2 is the second oldest unconformity within Permian time. From Cashman et al. (2010).

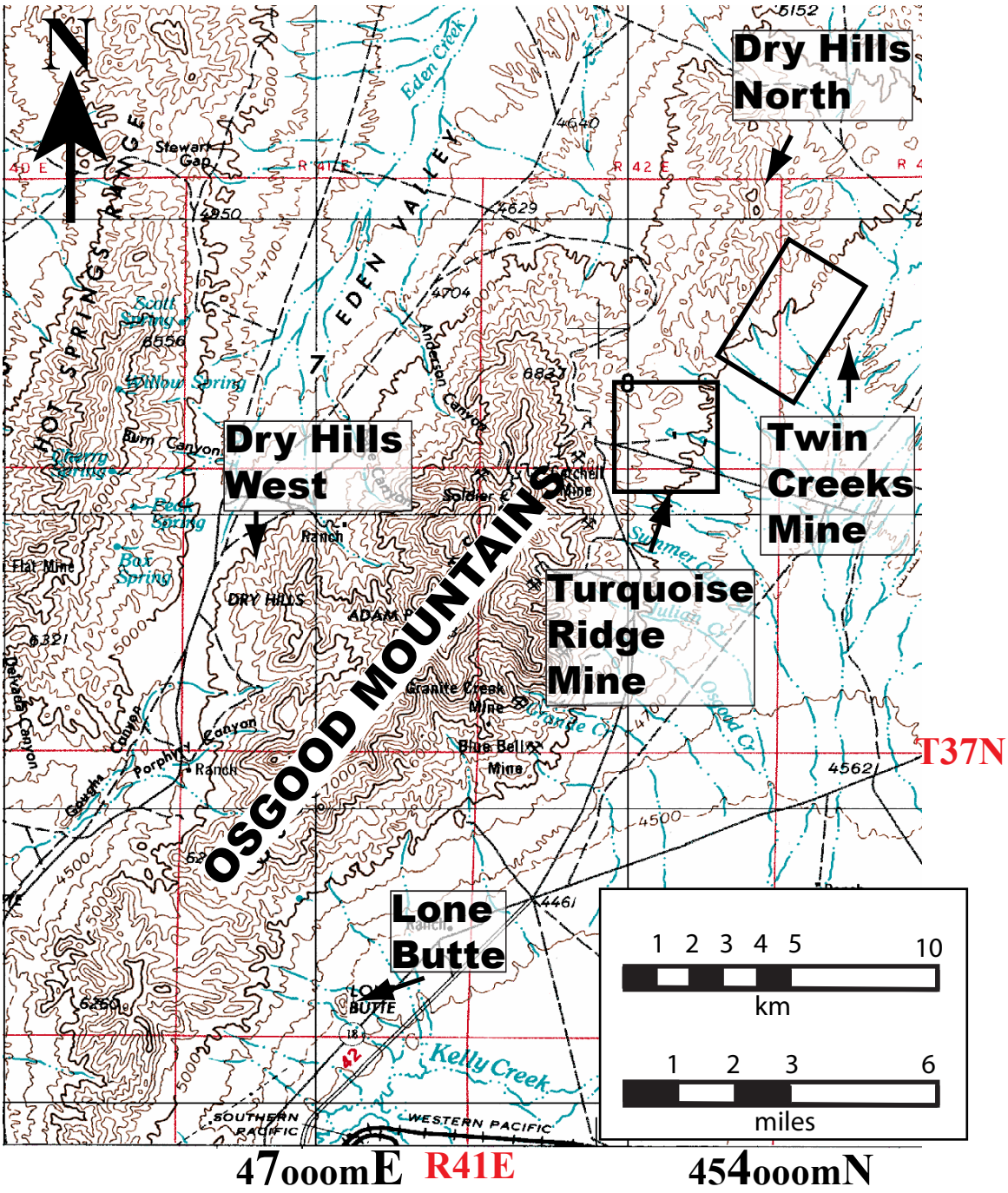

Figure 4. This 1:100 000 topographic map shows the location of the Osgood Mountains, the Dry Hills and Lone Butte (Modified from USGS, topographic map of Humboldt County).

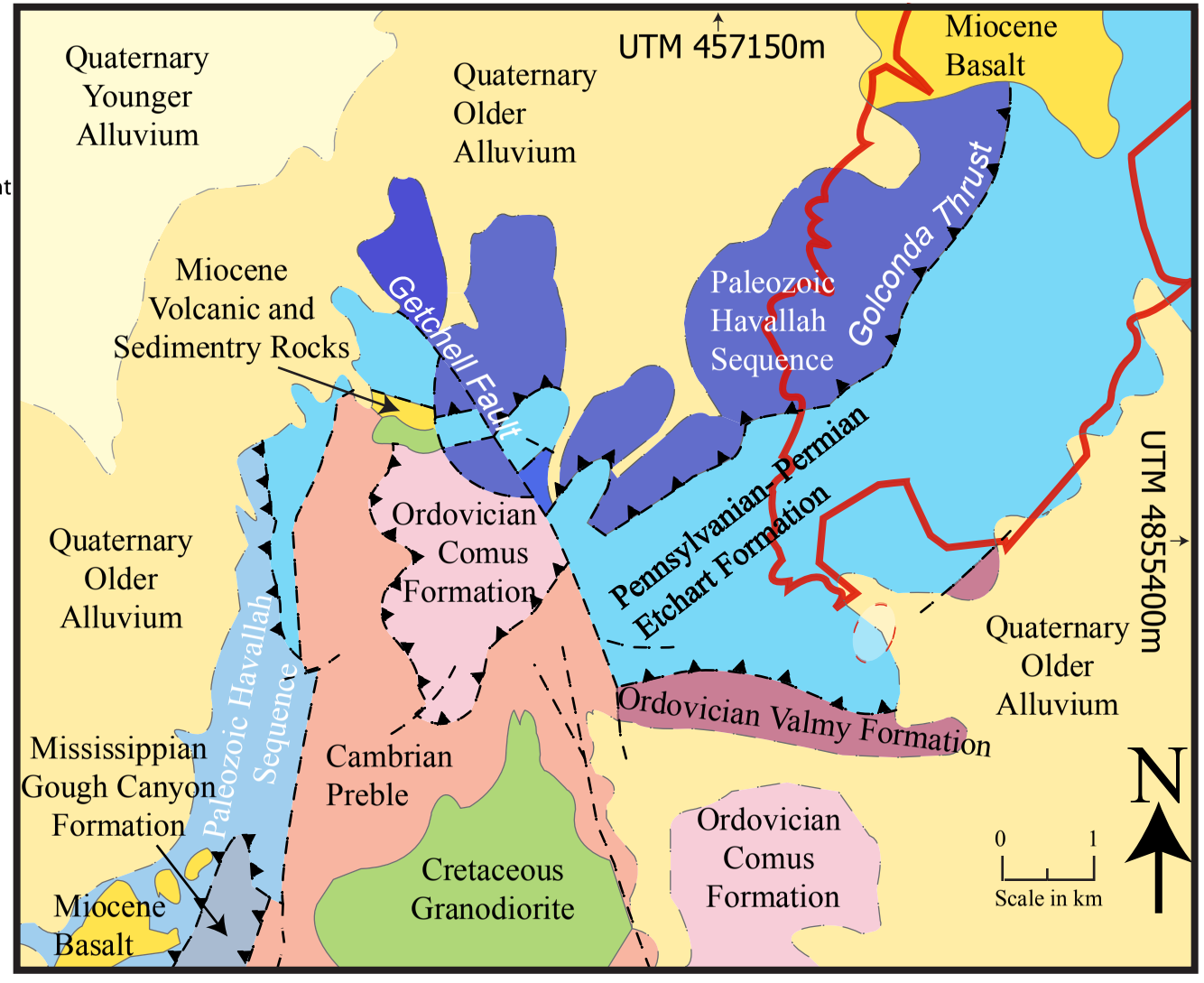

Figure 4. This is a 1:65,000 scale geologic map of the Dry Hills area. The Etchart Formation is overthrust by the Golconda Allochthon. The allochthon is cut by the Getchell Fault, with apparent right-lateral offset. Dry Hills map area outlined in red (Modified from Crafford, 2007).

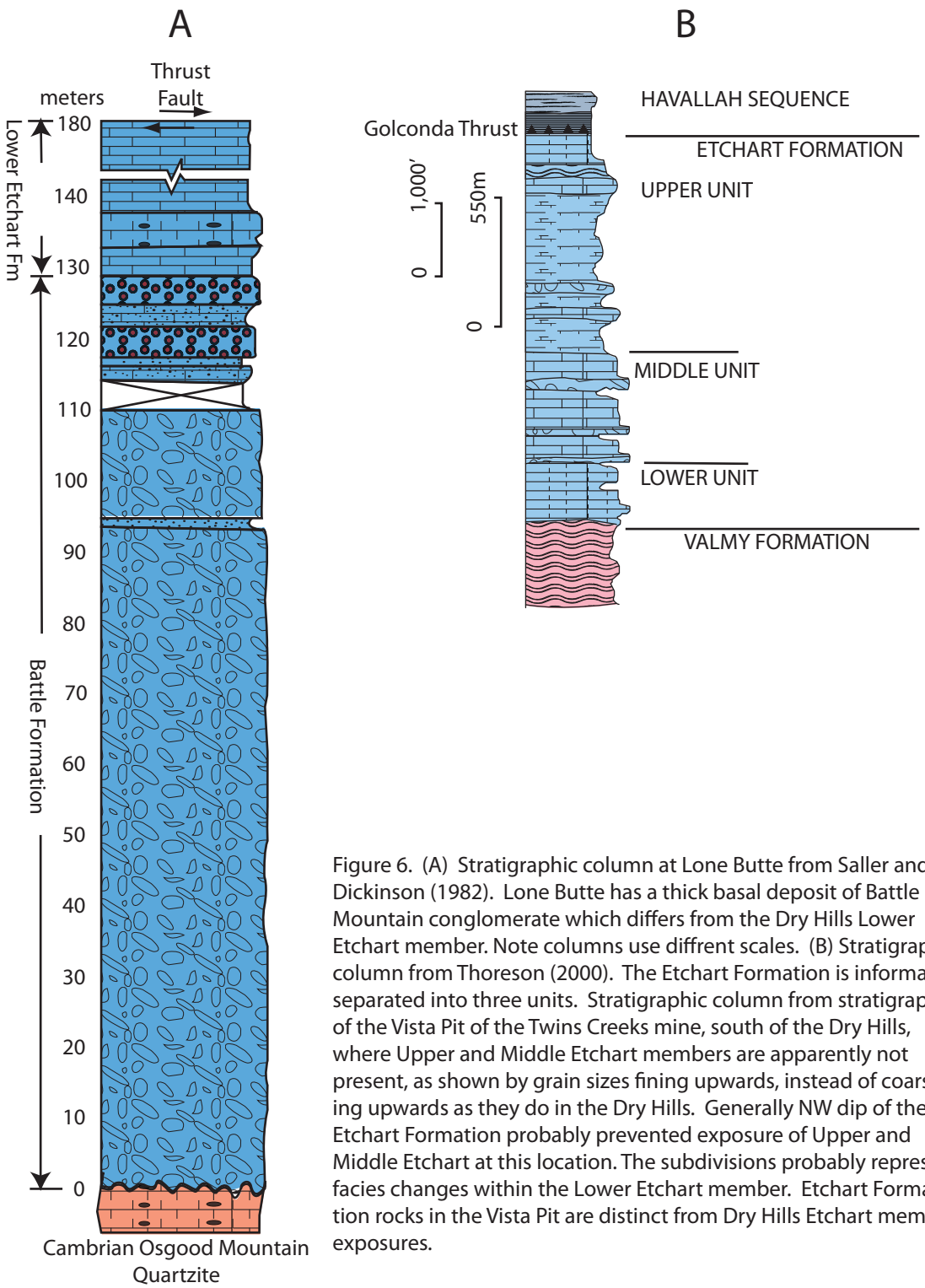

Figure 6. (A) Stratigraphic column at Lone Butte from Saller and Dickinson (1982). Lone Butte has a thick basal deposit of Battle Mountain conglomerate which differs from the Dry Hills Lower Etchart member. Note columns use diffrent scales. (B) Stratigraphic column from Thoreson (2000). The Etchart Formation is informally separated into three units. Stratigraphic column from stratigraphy of the Vista Pit of the Twins Creeks mine, south of the Dry Hills, where Upper and Middle Etchart members are apparently not present, as shown by grain sizes fining upwards, instead of coarsening upwards as they do in the Dry Hills. Generally NW dip of the Etchart Formation probably prevented exposure of Upper and Middle Etchart at this location. The subdivisions probably represent facies changes within the Lower Etchart member. Etchart Formation rocks in the Vista Pit are distinct from Dry Hills Etchart member exposures.

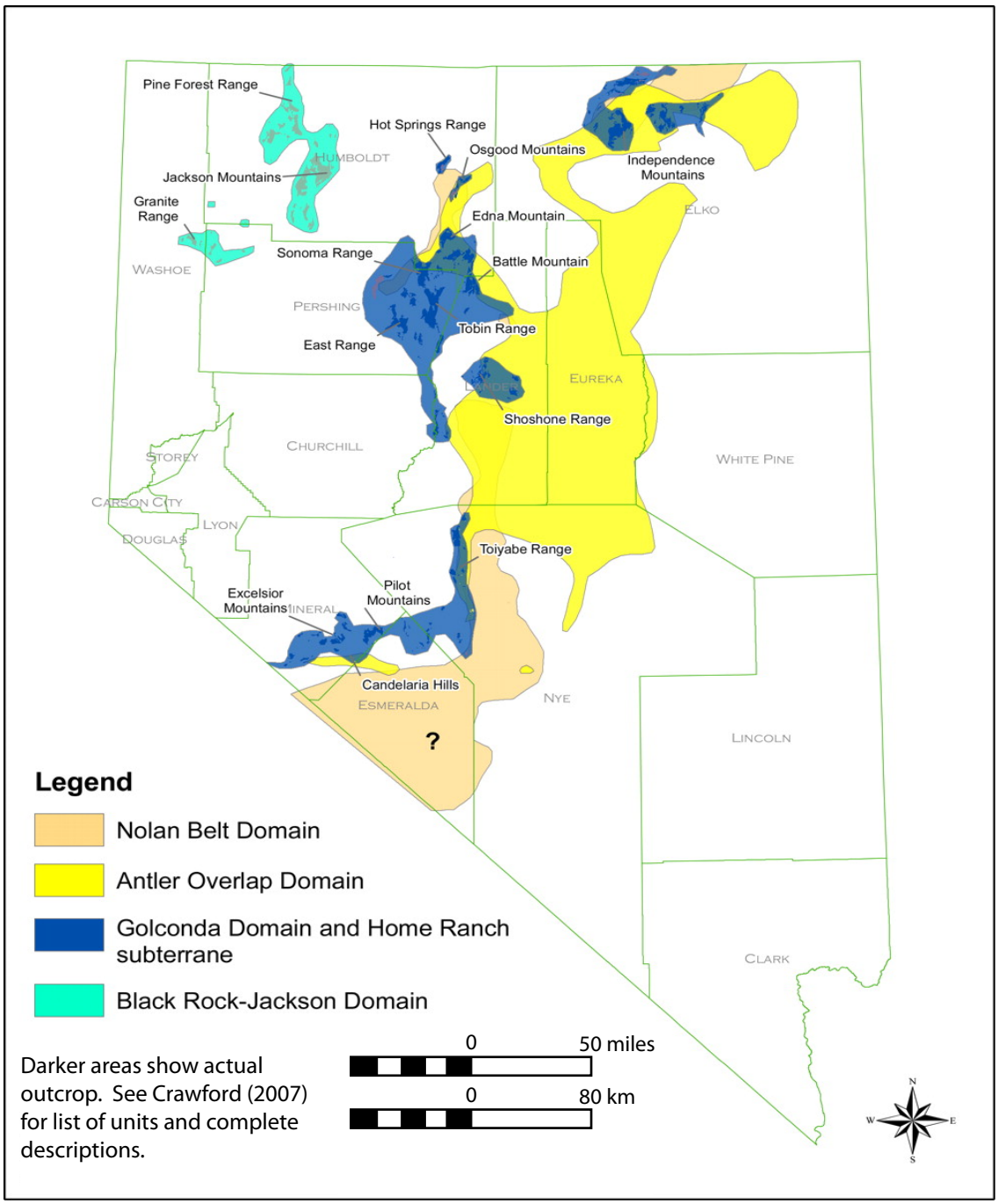

Figure 7. Figure from Crafford (2008) displaying the distribution of Antler Overlap and Golconda tectonic domains in Nevada.

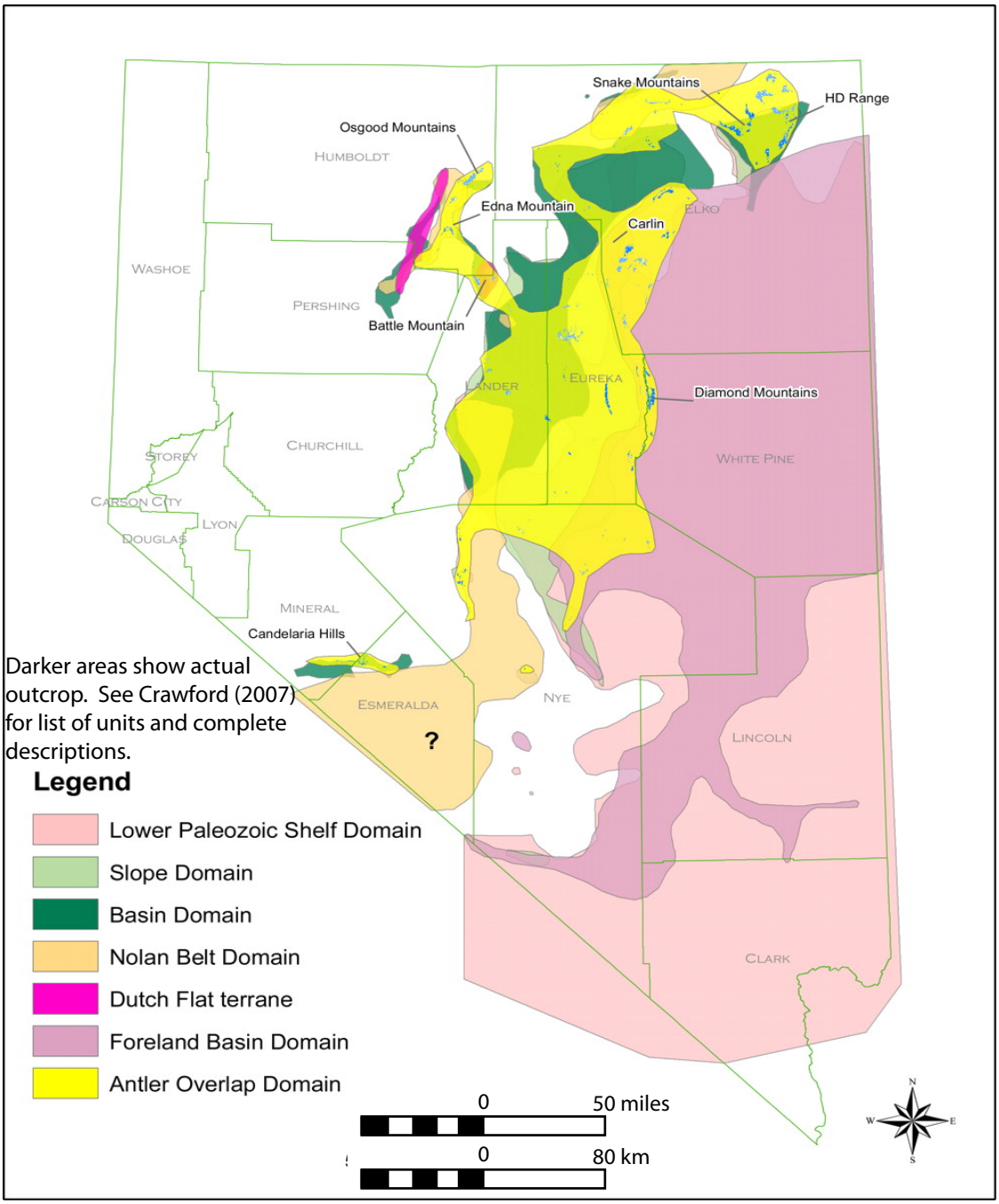

Figure 8. Figure modified from Crafford (2008) displaying the distribution of tectonic domains associated with the Antler Orogeny, which consists of the Lower Paleozoic shelf, slope, basin, and foreland basin domains.

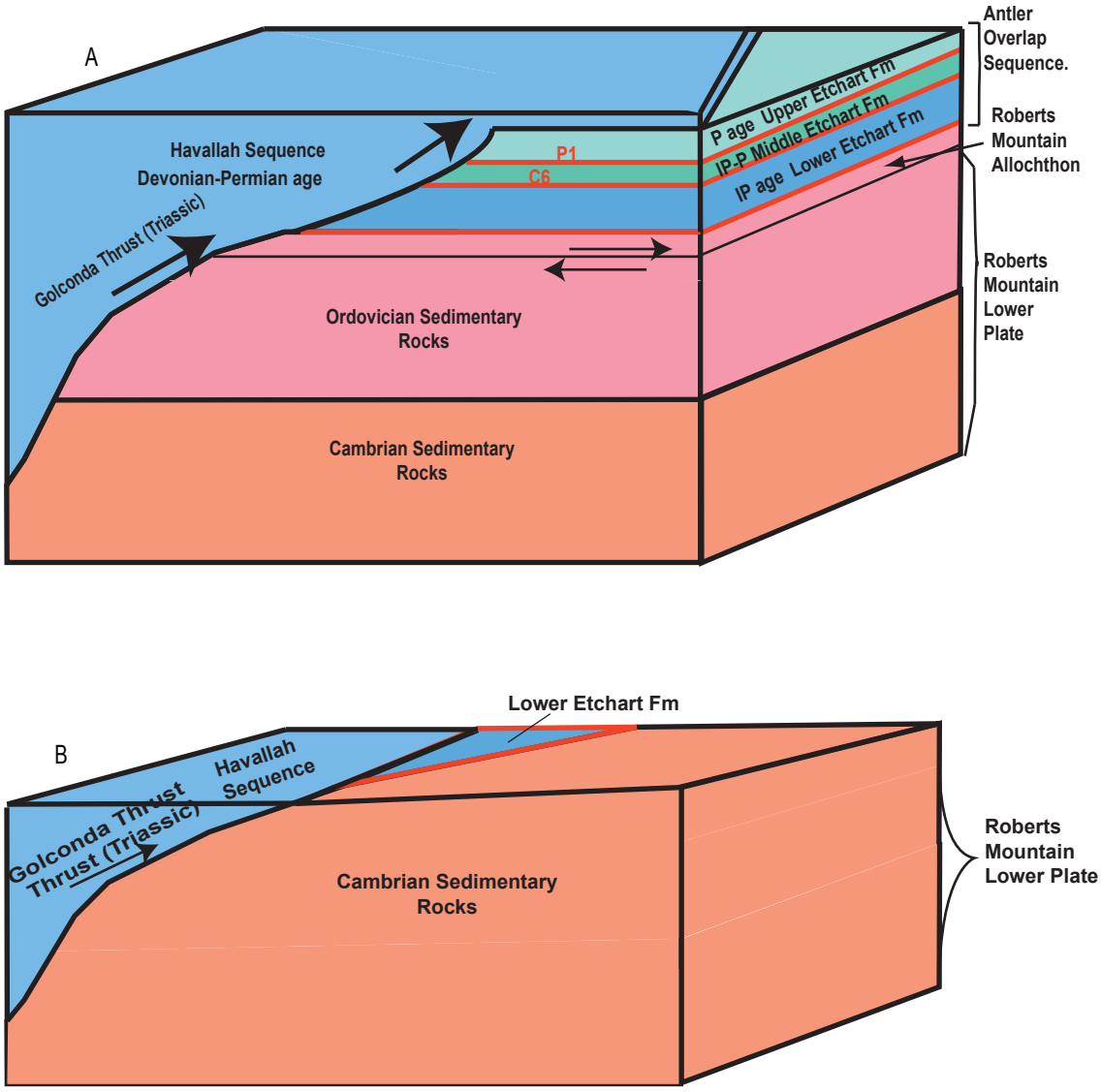

Figure 9. Idealized tectonostratigraphy of the (A) Dry Hills and (B) northern Osgood Mountains. Red lines and lettering represent unconformities surfaces and names, as given in Fig. 3.

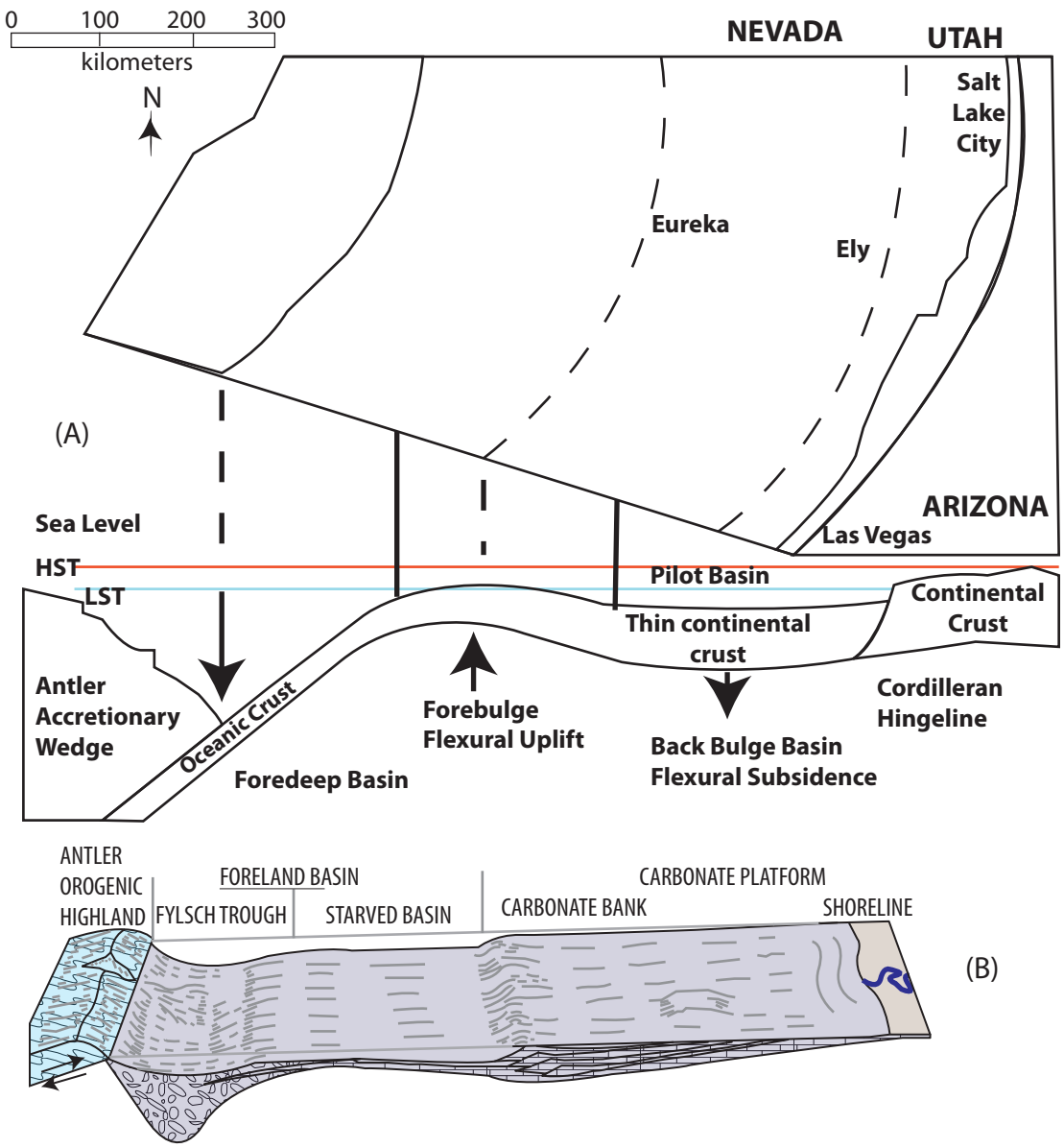

Figure 10. (A) A model for the Antler Orogeny in which subduction occurs to the west, off the edge of the figure. The sea level high stand (HST) and low stand (LST) are depicted in the figure (Modified from Racheboef et al., 2004). (B) Cross section displaying geometry of the Antler Foreland Basin as proposed by Poole and Sandberg (1977). The carbonate bank and flysch trough were separated by the forebulge, which created a topographic high that separated sediment influxes within the Antler Foreland Basin (Modified from Poole and Sandberg, 1977).

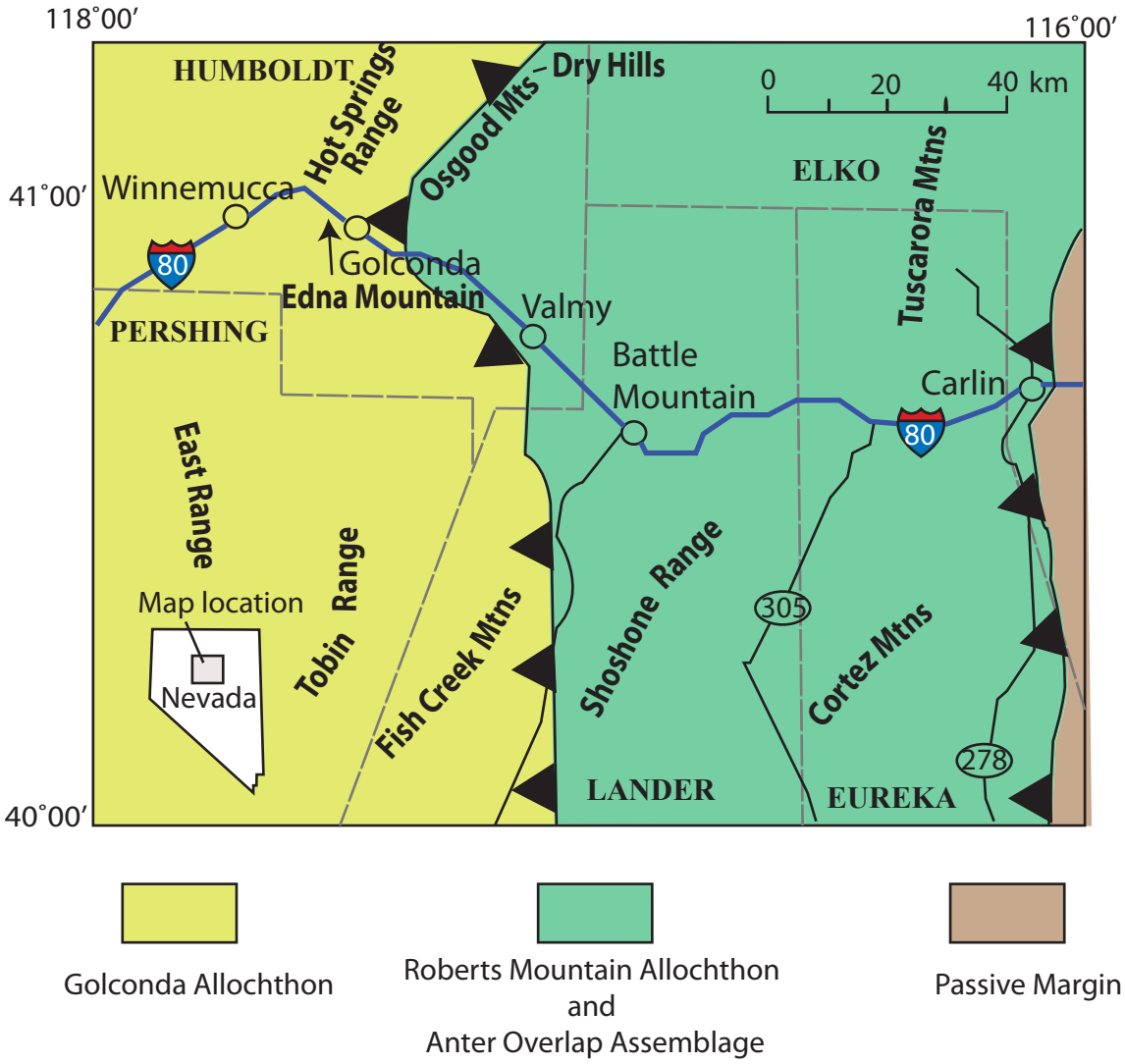

Figure 11. This figure displays the distribution of the Roberts Mountain Allochthon, Antler Overlap Sequence, Golconda Allochthon, and the edge of the passive margin east of the foreland basins. Also, within the figure is the location of the Osgood Mountains and Dry Hills in Nevada (Modified from Rocheboef, 2002).

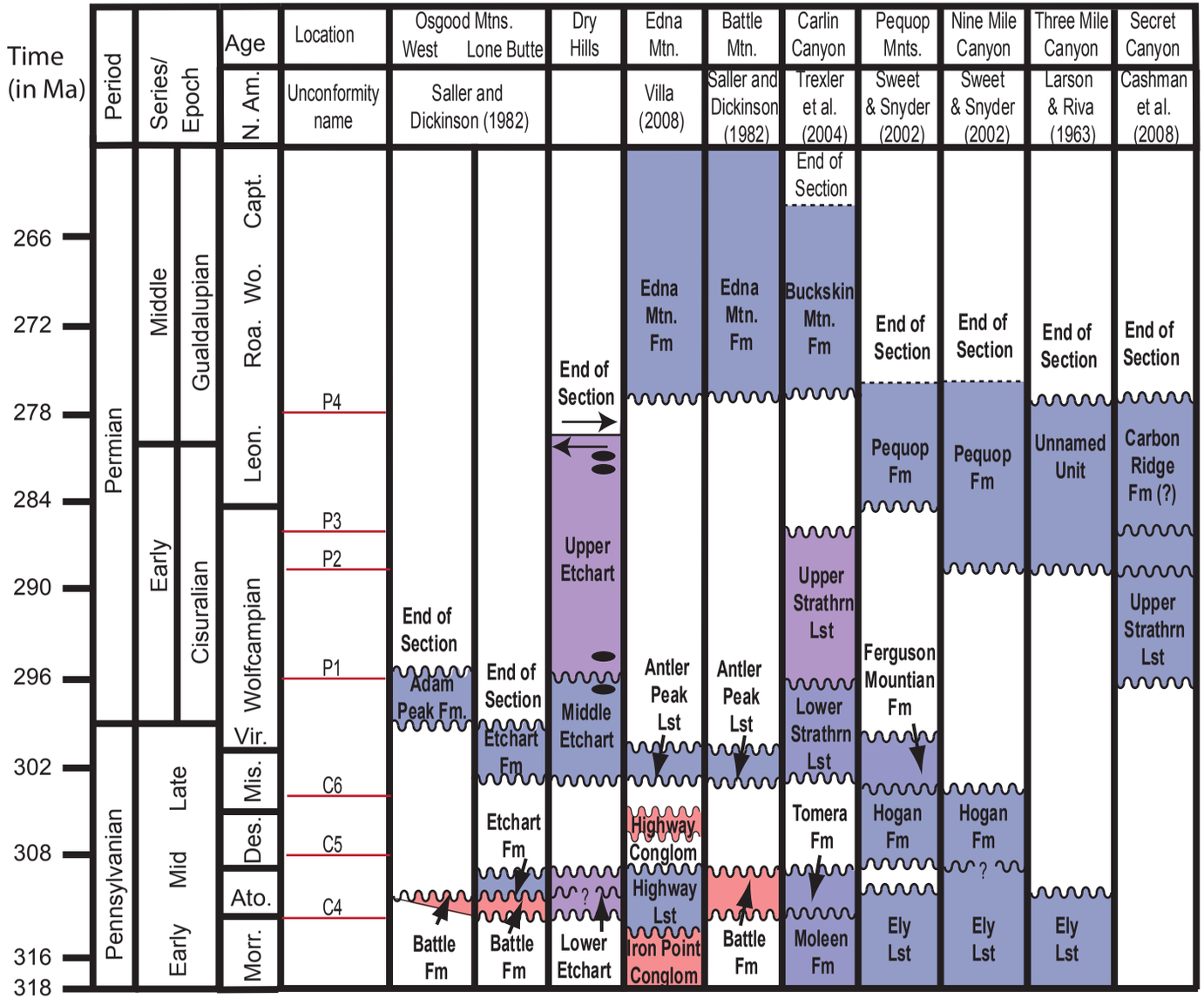

Fig 12. Stratigraphic correlation of Etchart equivalent units throughout Nevada, as well as the sources for the stratigraphic columns. Note the scattered occurrence of the basal Battle Mountain conglomerate, and the regional persistence of the P1 and C5 angular unconformities. Black ovals in the Dry Hills column represent fusulind based ages returned from this research. Age name abbreviations: Morr.=Morrowan; Ato.=Atokan; Des.=Desmoinesian; Mis.=Missourian; Vir.=Virgilian; Leon.=Leonardian; Roa.=rodian; Wo.=Wordian; Capt.=Capitanian; N. Am.= North American

Unit name abrievations: Strathrn=Strathearn

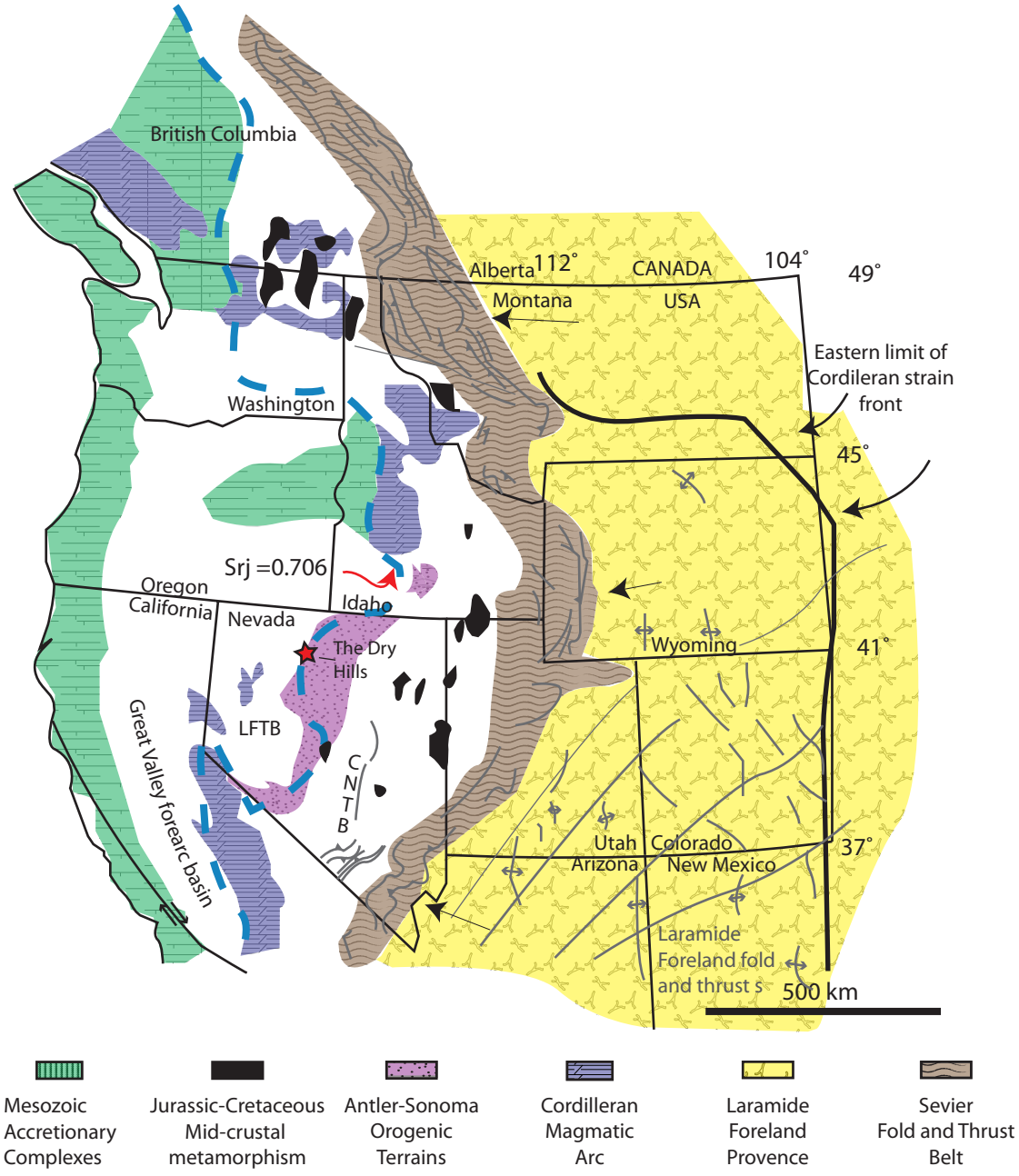

Figure 13. Map of Mesozoic deformation in the western United States and the Sr 0.706 line (teal). Note the similarities of the location of the Sr 0.706 line and the interpreted location of the Golconda thrust. The Central Nevada Thrust Belt (CNTB) and Luning Fencemaker Thrust Belt (LFTB) are located on the figure (Modified from Willden, 2002).

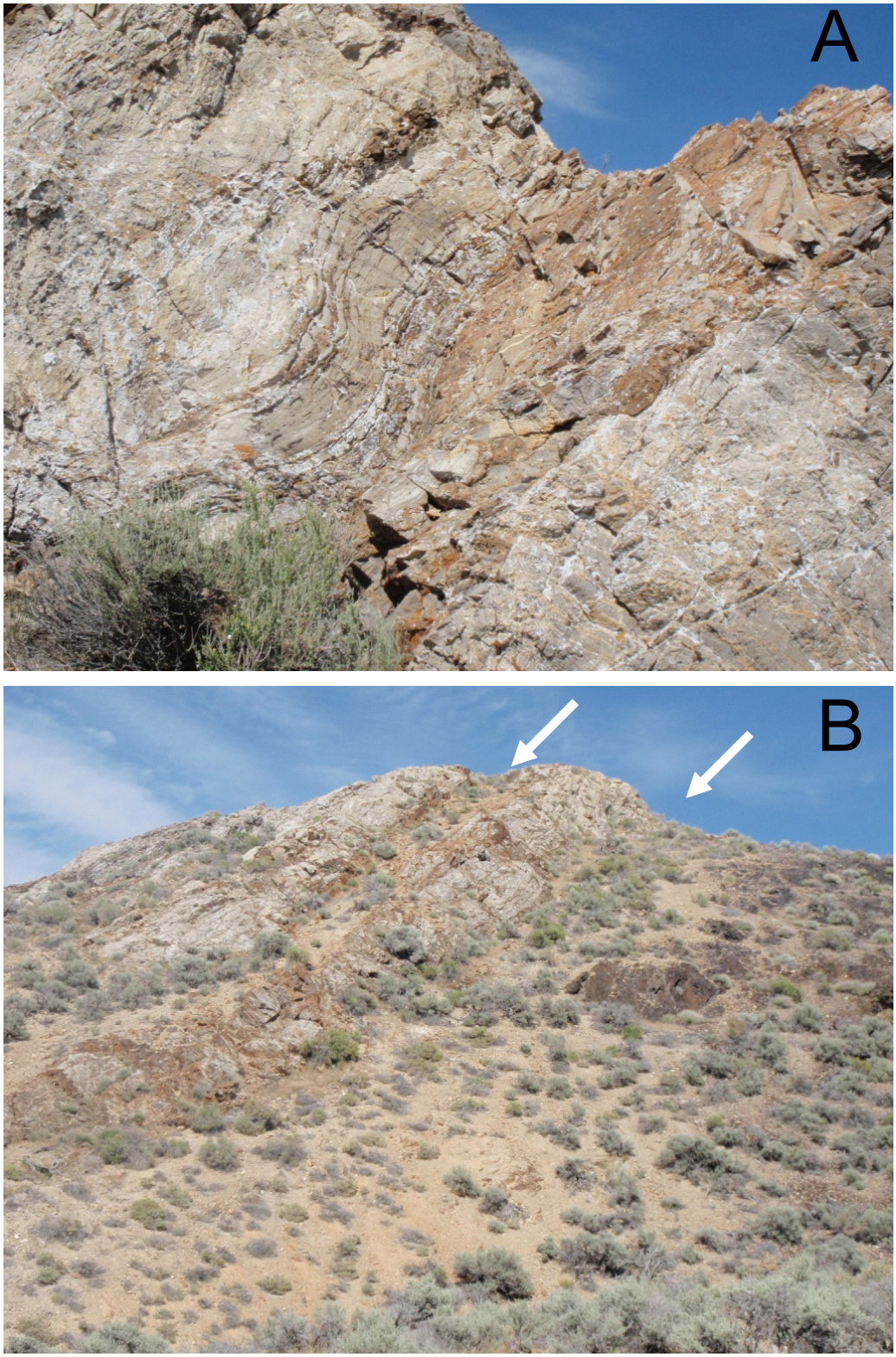

Figure 14. Photograph of thrust sheets (faults marked by arrows) within the Lower Etchart member taken from the western edge of the northern Osgood Mountains, facing north. (A) close up photograph of thrust sheet with internal folding. (B) Wider angle photo of thrust sheet.

Figure 15. Photograph of the Golconda thrust fault (marked by white arrow, and trace denoted by dotted line) in the Dry Hills. Photo taken facing north.

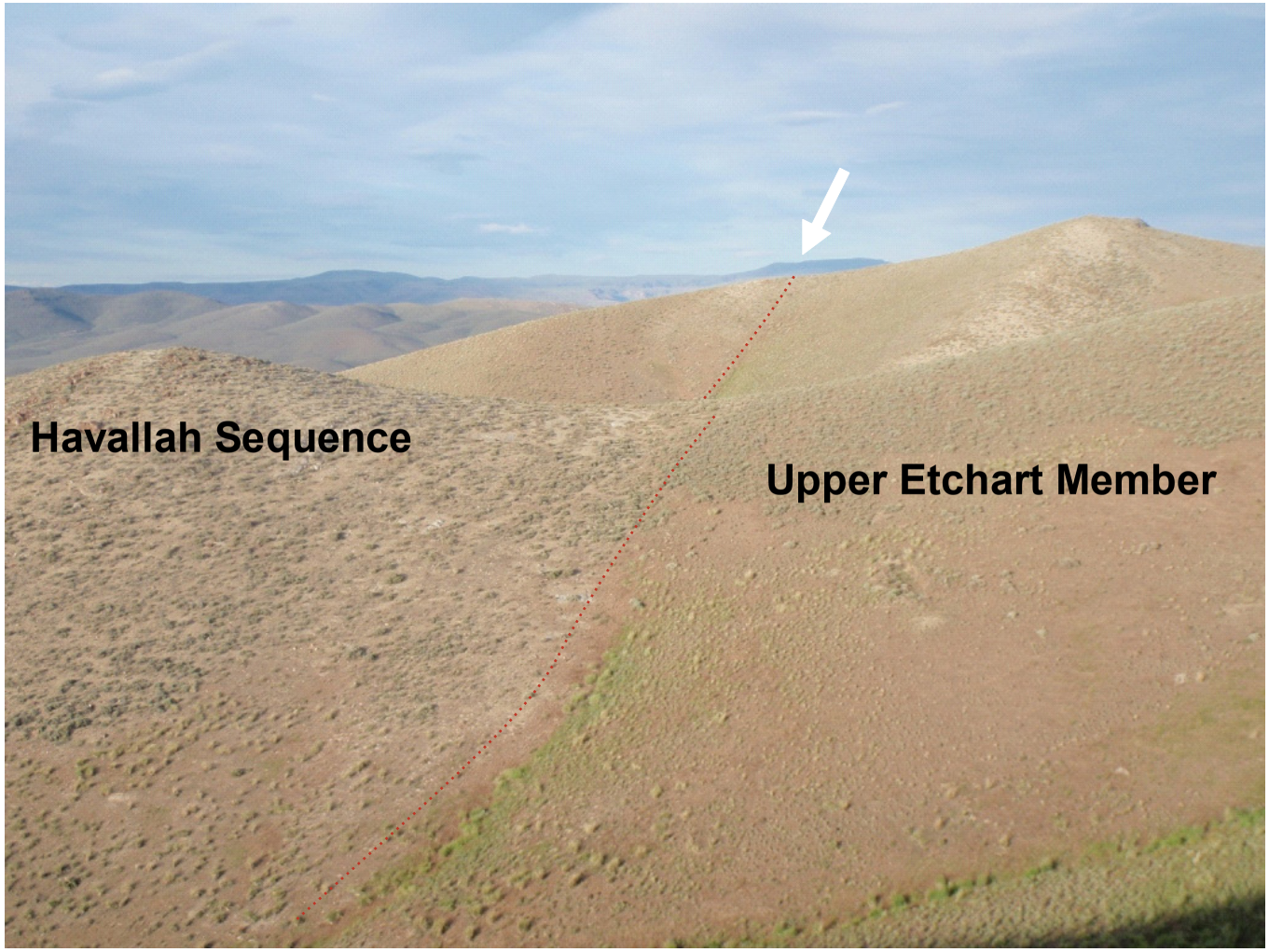

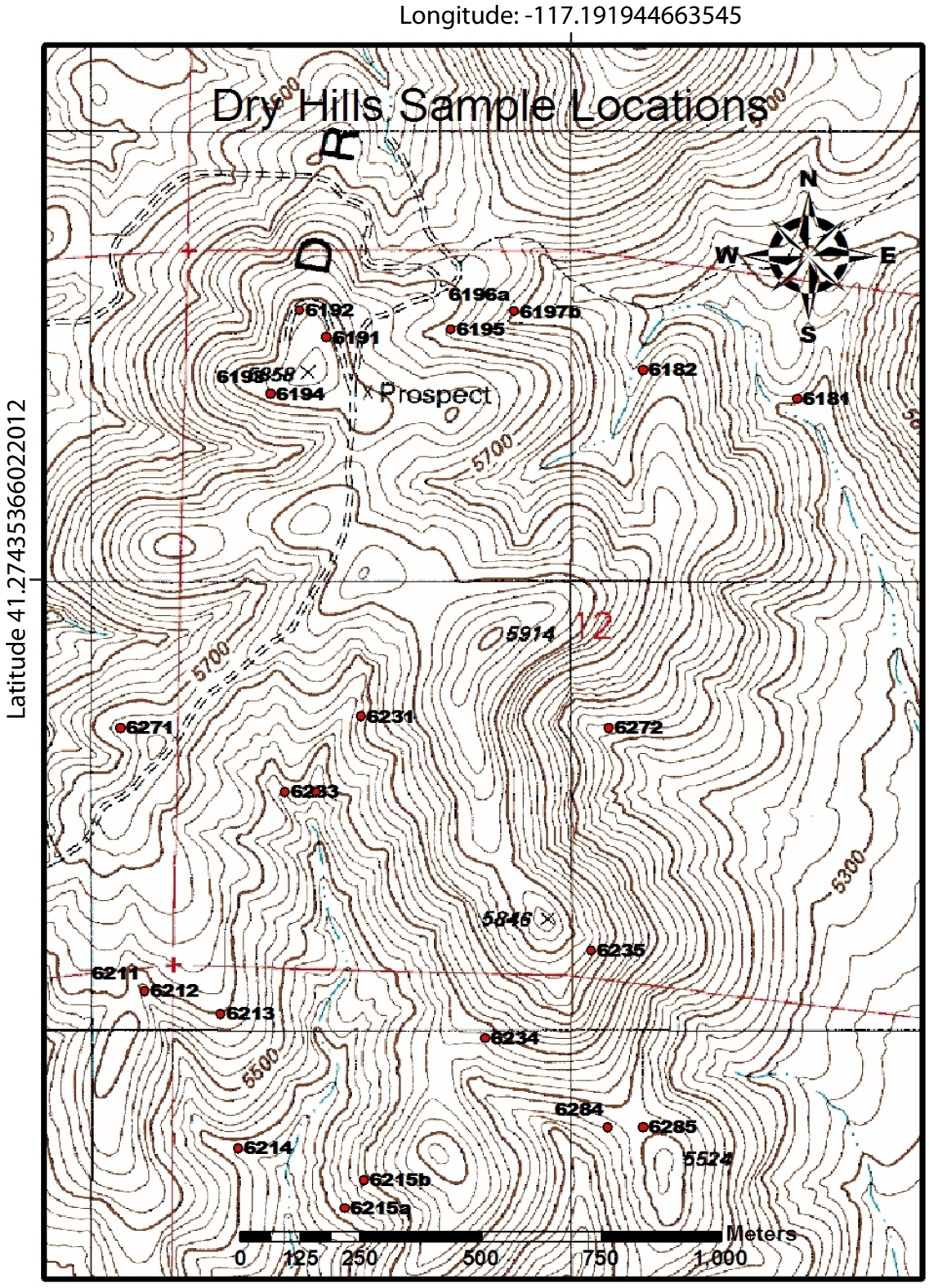

Figure 16. Map of locations sampled for fusulinid dating in the Dry Hills.

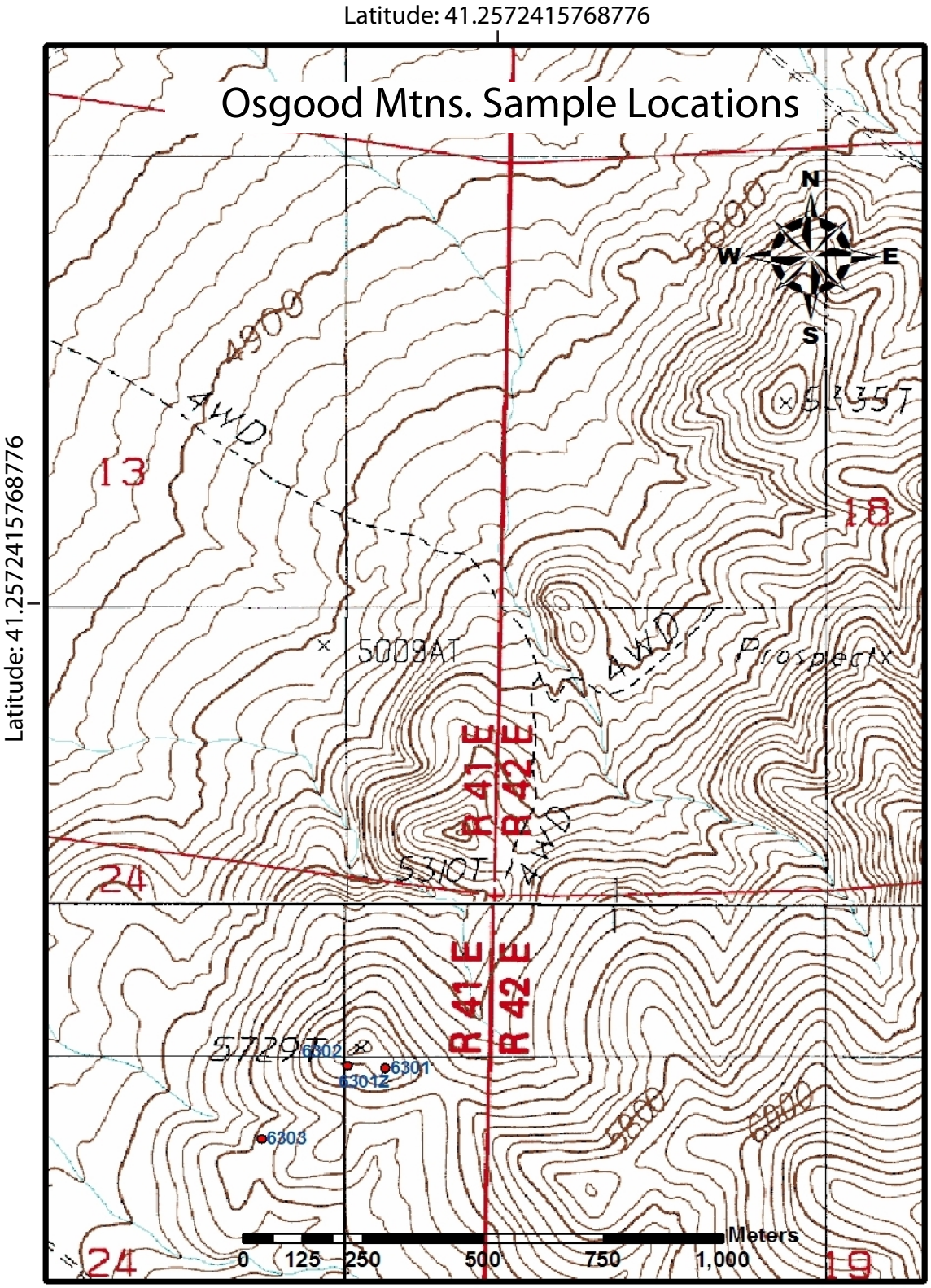

Figure 17. Location map of samples taken for fusulinid aging in the northern Osgood Mountains

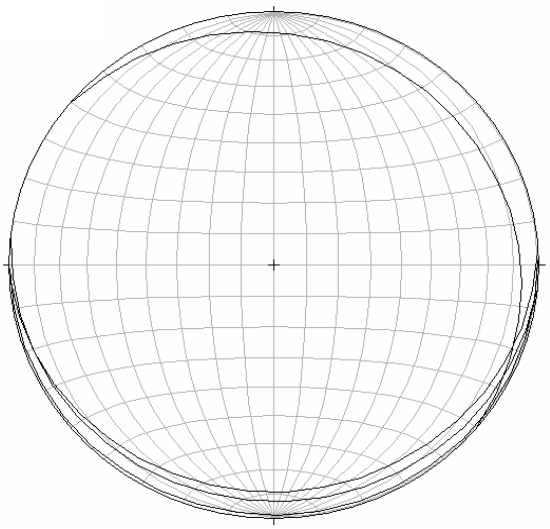

Figure 18. Stereographic analysis of fold limbs from taken from the lower Etchart member (UTM 0482579 4565199). Fold set 1 consists of open, upright folds plunging to the SE. N=4.

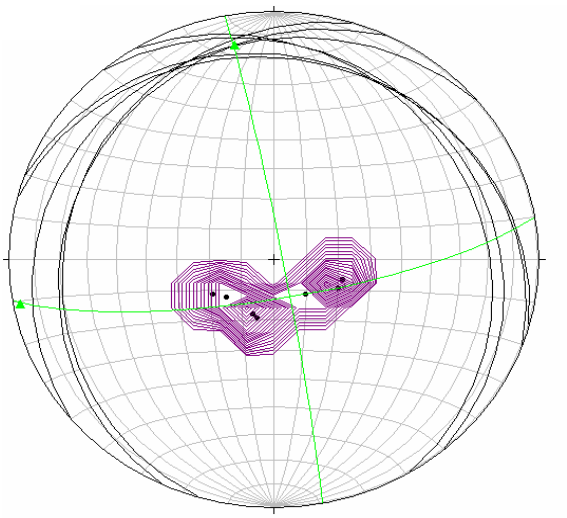

Fig. 19 Stereograph depicting changes in bedding orientation across a F2 fold from the Upper Etchart member. Hinge is oriennted 13; 350. Axial Plane 259; 87E. This fold is classified as a gentle, gently-plunging, upright fold. N=7.

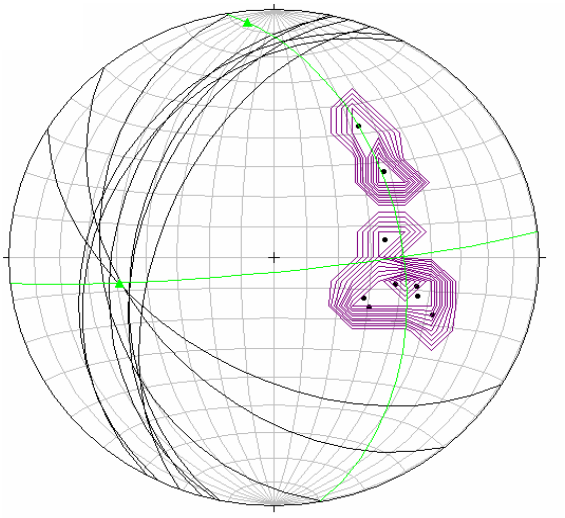

Fig. 20 Stereograph depicting changes in bedding orientation across a F3 fold in the Upper Etchart member. The hinge is 40; 260. The axial plane is 084; 85S. Interlimb angle is 118°. N=19.

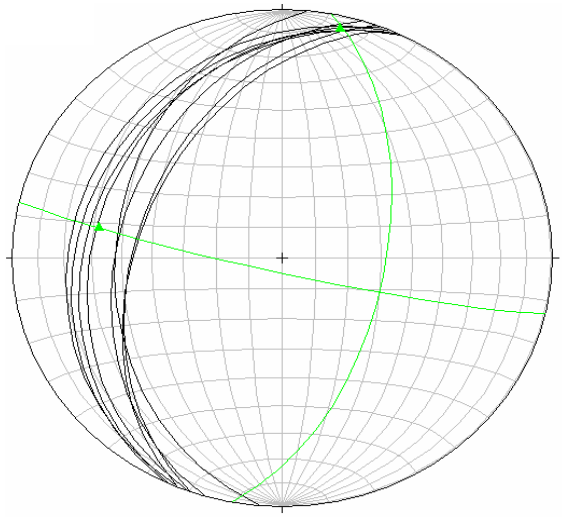

Fig. 21 Stereograph depicting a F4 fold from UTM 043770 4569094 +/- 6m. The hinge is 05; 013. The axial plane is 011; 59SE. The interlimb angle is 158 degrees. This fold is classified as a gentle, sub-horizontal, east inclined fold. N=8.

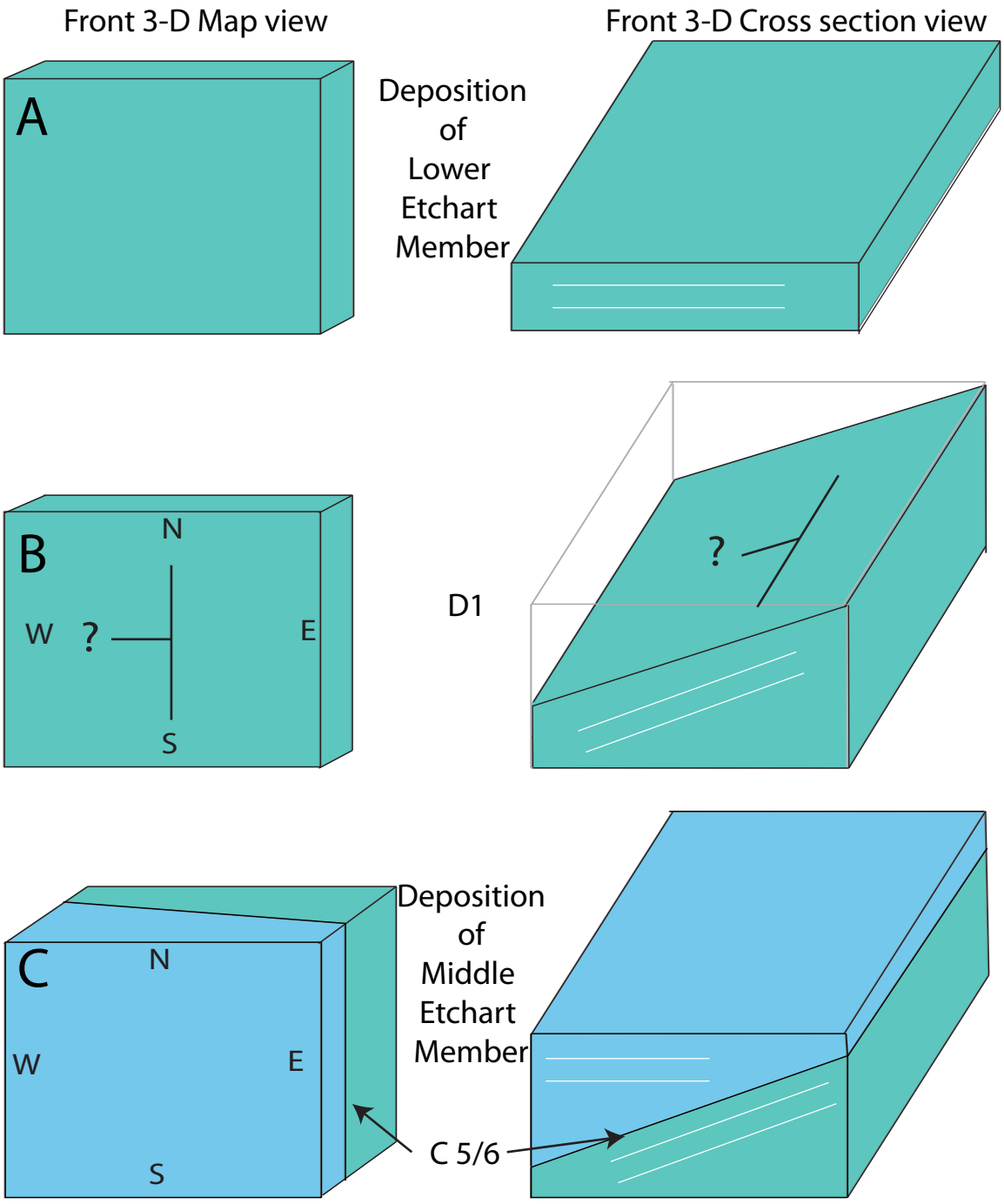

Figure 22. First of three consecutive figures showing a cartoon, idealized retrodeformation of the Dry Hills, following the structural history interpreted from this research. The uppermost two blocks depict (A) the Lower Etchart member deposition. The middle two blocks represent (B) the tilting event that creates the C5/6 angular unconformity. The lowest two blocks depict (C) the deposition of the Middle Etchart member.

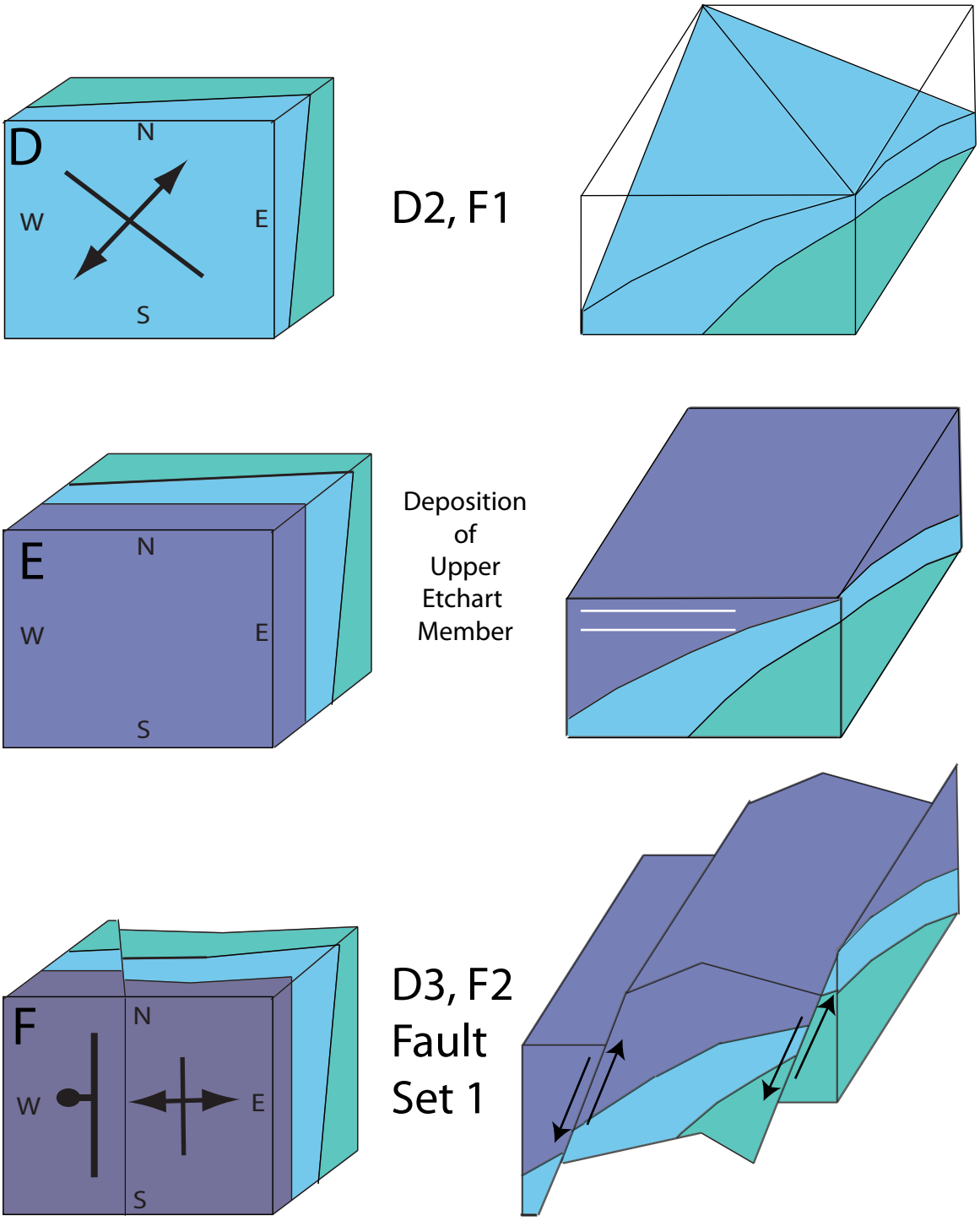

Figure 23. A cartoon, idealized retrodeformation of the Dry Hills, following the structural history interpreted from this research. The uppermost two blocks (D) depict F1 folding, D2. The middle two blocks (E) represent the deposition of the Upper Etchart member. The lowest two blocks (F) depict the first fold-and-fault set, composed of F2 folds and fault set 1. The map view block (on left) is simplified with a single fault, while the cross section block (on right) depicts a more accurate fault set.

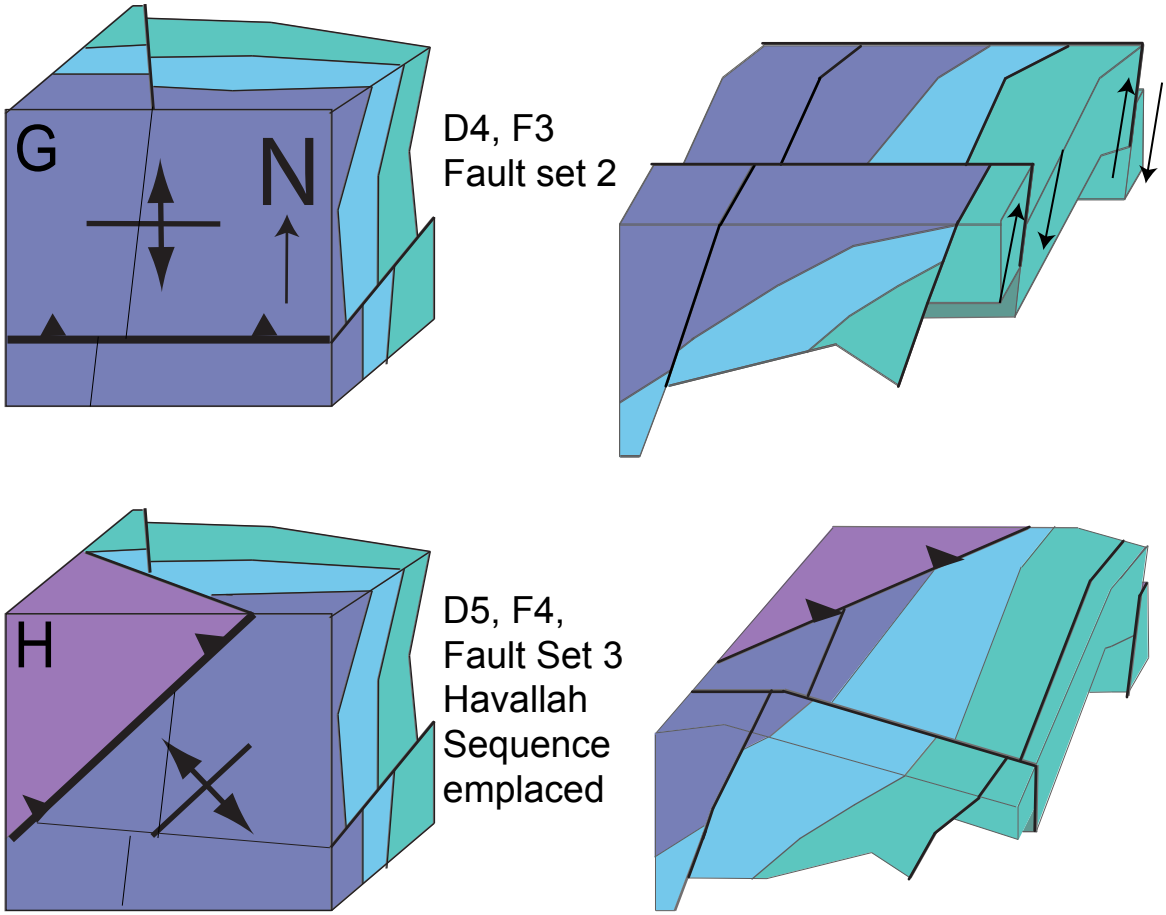

Figure24. A cartoon, idealized retrodeformation of the Dry Hills, following the structural history interpreted from this research. In the uppermost two blocks (G) the second fold-and-fault set, composed of F3 folds, and fault set 2 are shown. The lowest two blocks (H) depict the third fold and fault set, composed of F4 folds and fault set 3, interpreted as the Golconda thrust.

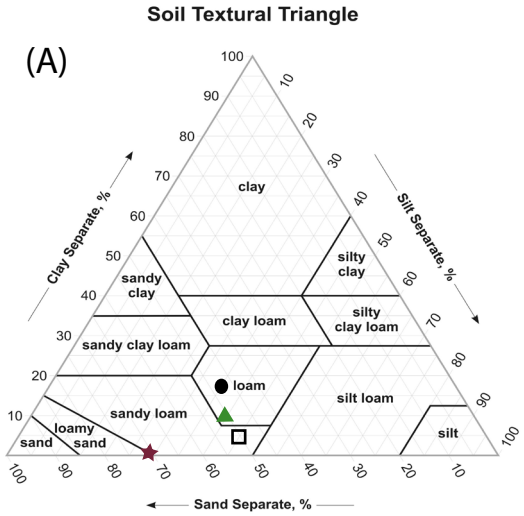

Basalt Derived. Type: Sandy Loam
Dry: 10 Yr 5/3 Brown; Wet: 10 Yr 3/3 Dark Brown

Q Alluvium Etchart Derived; Type: Loam
Dry 2.5 Yr 7/3 Pale Yellow; 10 Yr 6/3Wet Pale Brown

Q Alluvium Havallah Derived; Type: Sandy Loam
Dry 7.5 Yr 7/3 Brown; Wet: 10 Yr 3/3 Dark Brown

Q Alluvium, Cherty: Type: Loam
Dry: 10 Yr 5/3 Brown; Wet: 10Yr 3/6 Dark Yellowish Brown

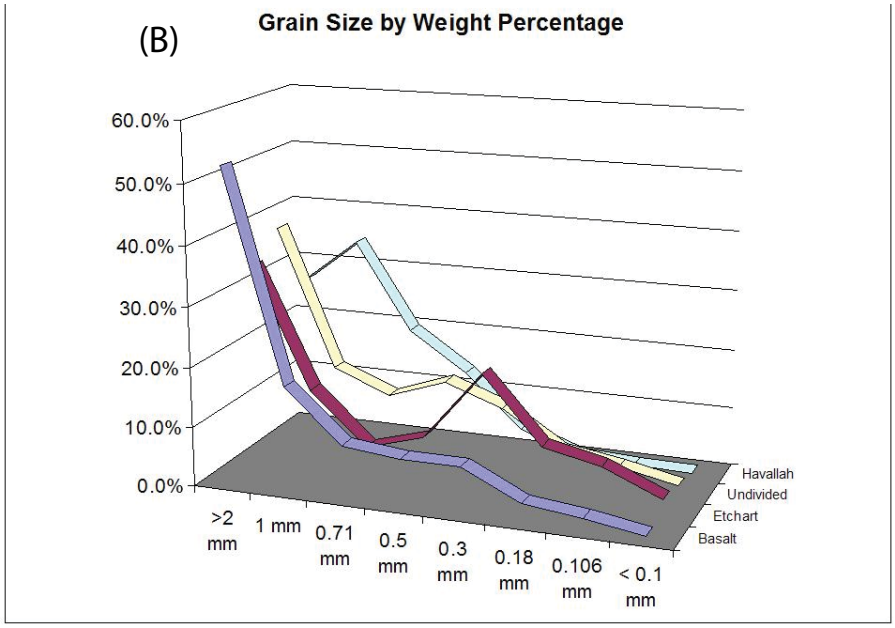

Figure 25. (A) Ternary plot of subdivided Quaternary units mapped in the Dry Hills area on a standard USDA soils textural triangle. (B) Summary of grain size distribution of Quaternary units subdivided in map by weight percentage. Data is the result of sieve analysis conducted on Quaternary units within the Dry Hills. Note the normal distribution of clasts in the undivided units between 1 mm and 0.1 mm. This distribution was identifiable in outcrop and used to sub-divide the Quaternary alluvium units in the Dry Hills as a proxy for provenance. Note the abundance of smaller particles in Etchart (Bimodal) and Havallah alluvium (Peak at 1 mm).

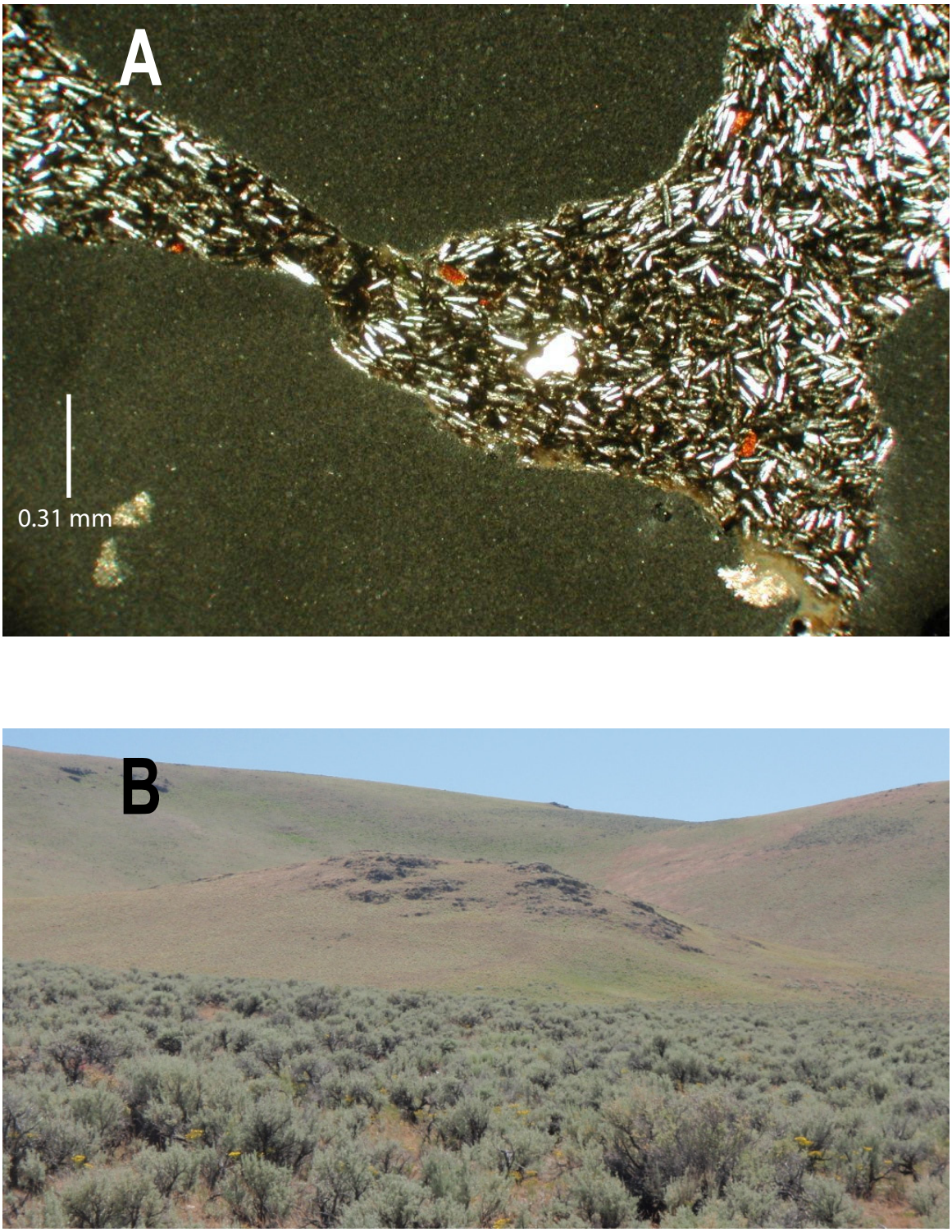

Figure 26. (A) Thin section photograph of unnamed vesicular basalt from the northern end of the Dry Hills with abundant plagioclase. 40x magnification, ppl. (B) Photograph of highly welded volcanic tuff within unnamed basalt and andesite in the northern Dry Hills. Location is sub parralel to projection of last Golconda thrust orientation.

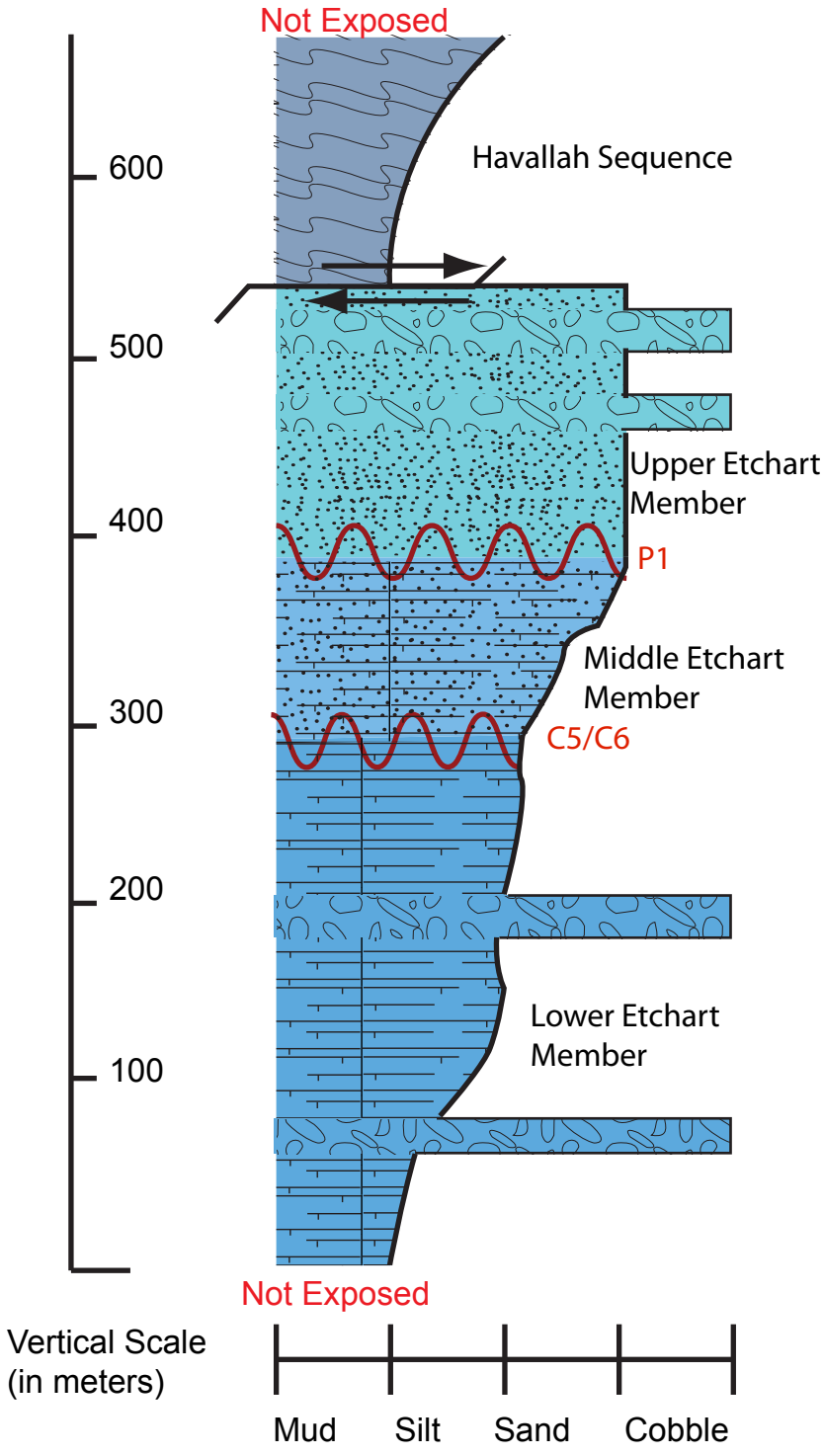

Figure 27. Stratigraphic representation of the Etchart Formation units in the Dry Hills map area. Unit thicknesses have been calculated from map data using standard methods. The lower unconformity is likely the C6 and the upper unconformity is the P1. The Etchart members are interpreted to represent increasingly shallower depositional environments due to tectonic uplifts located to the north to northwest.

Figure 28. Photograph of a Lower Etchart member outcrop, with distinctive microbial lamina in micrite. This outcrop texture is common in the Lower Etchart member, and sporadically exposed in the Middle Etchart member.

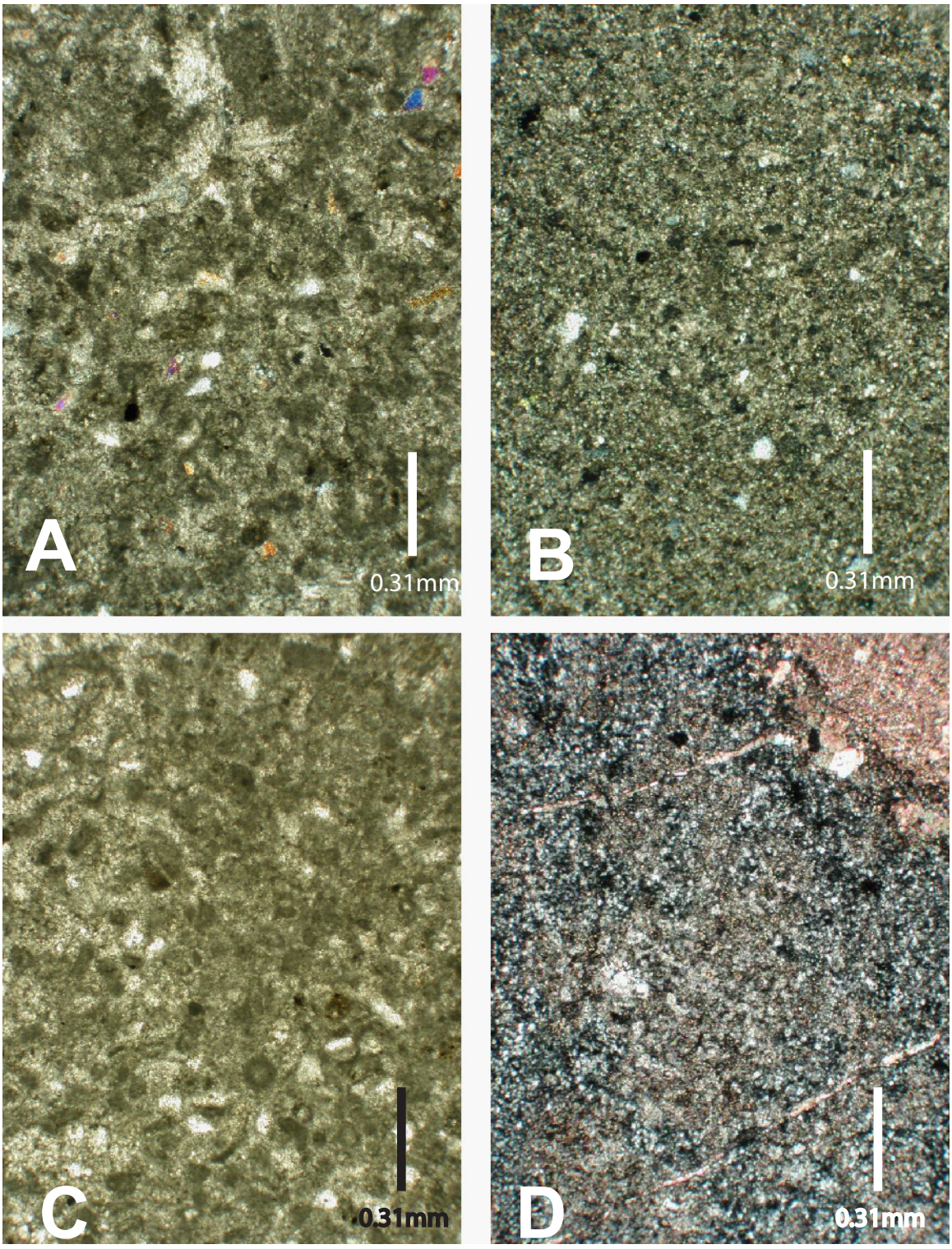

Figure 29. Thin section photographs from the Lower Etchart member wackestone-micrite taken at 40x magnification with cross-polarized light (A, B, D) and plane light (C). The lower Etchart member generally grades from silty wackestone in higher portions (A & C) to a micrite in lower exposures (B & D).

Figure 30. Photograph of exposure of Middle Etchart member. This unit characteristically weathers to smooth outcrops, lacks ledges, is light gray in color, and is thickly bedded. Hammer for scale.

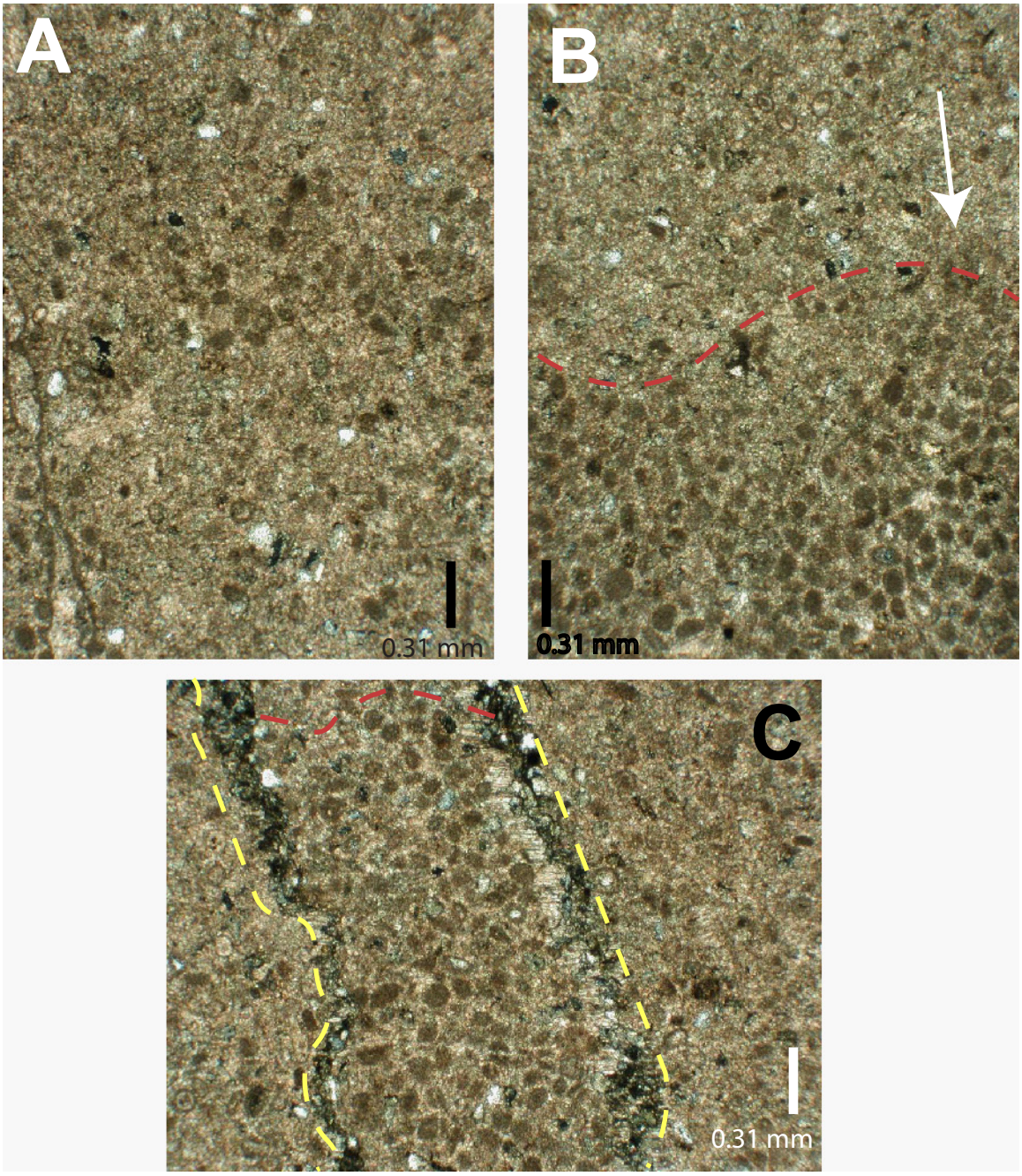

Figure 31. Photographs taken from the Midle Etchart member displaying (A) mixed packstone and wackestone, with peloid and skeletal grains; (B) which can transition abruptly along contacts (red dashed line). Unit also shows evidence of bioturbation (C) such as this vertical burrow (oulined with yellow dashed line), later filled in with carbonate grains (red dashed line), implying a high-energy, near-shore depositional setting. All photos are 40x magnification, cross-polarized light.

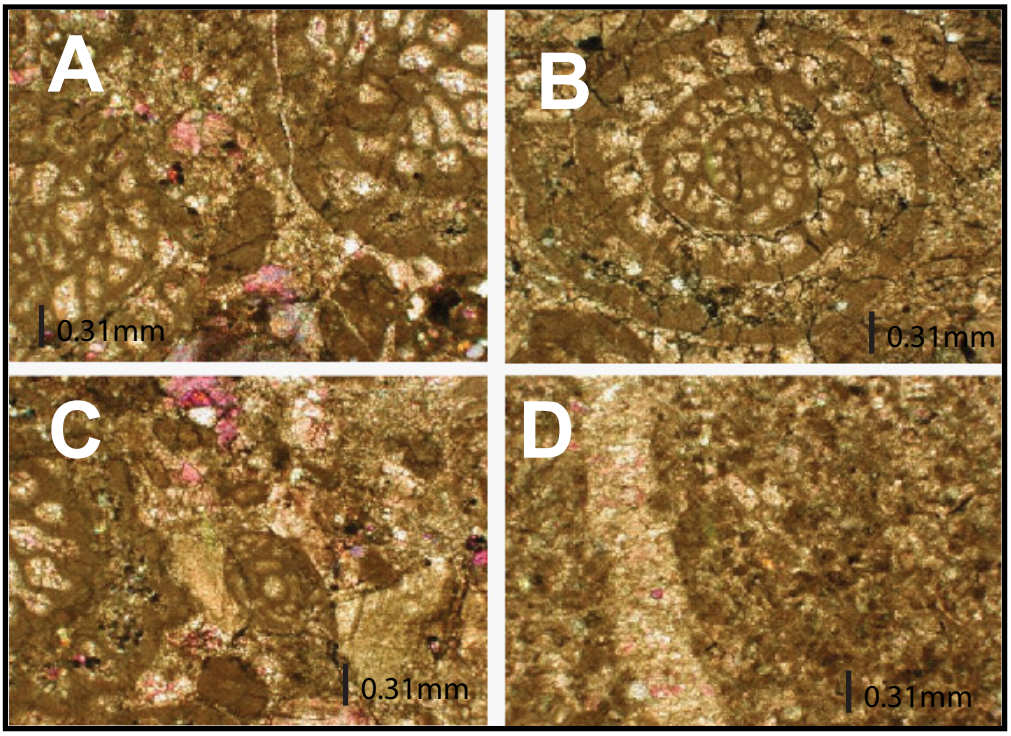

Figure 32. Thin section photographs (A, B, & C) of fossils including fusulinids from the Upper Etchart member . (D) Calcareous cement within the Upper Etchart member grainstone. Slides are stained for calcite, cross-polarized light, 40x magnification. (E) Typical Upper Etchart member exposure from the Dry Hills. Note interbedded brown chert beds. Ledges are approximately 0.5 m to 1.0 m thick.

Figure 33. (A)Typical exposure of the Havallah Sequence from the Dry Hills. This photograph displays folded mixed chert and carbonate. (B)Thin section of Havallah Sequence from the Dry Hills at 40x magnification, cross-polarized light. The Havallah Sequence is a mixed siliciclastic unit that is generally fine grained and composed of carbonate and quartz, and is commonly highly deformed.

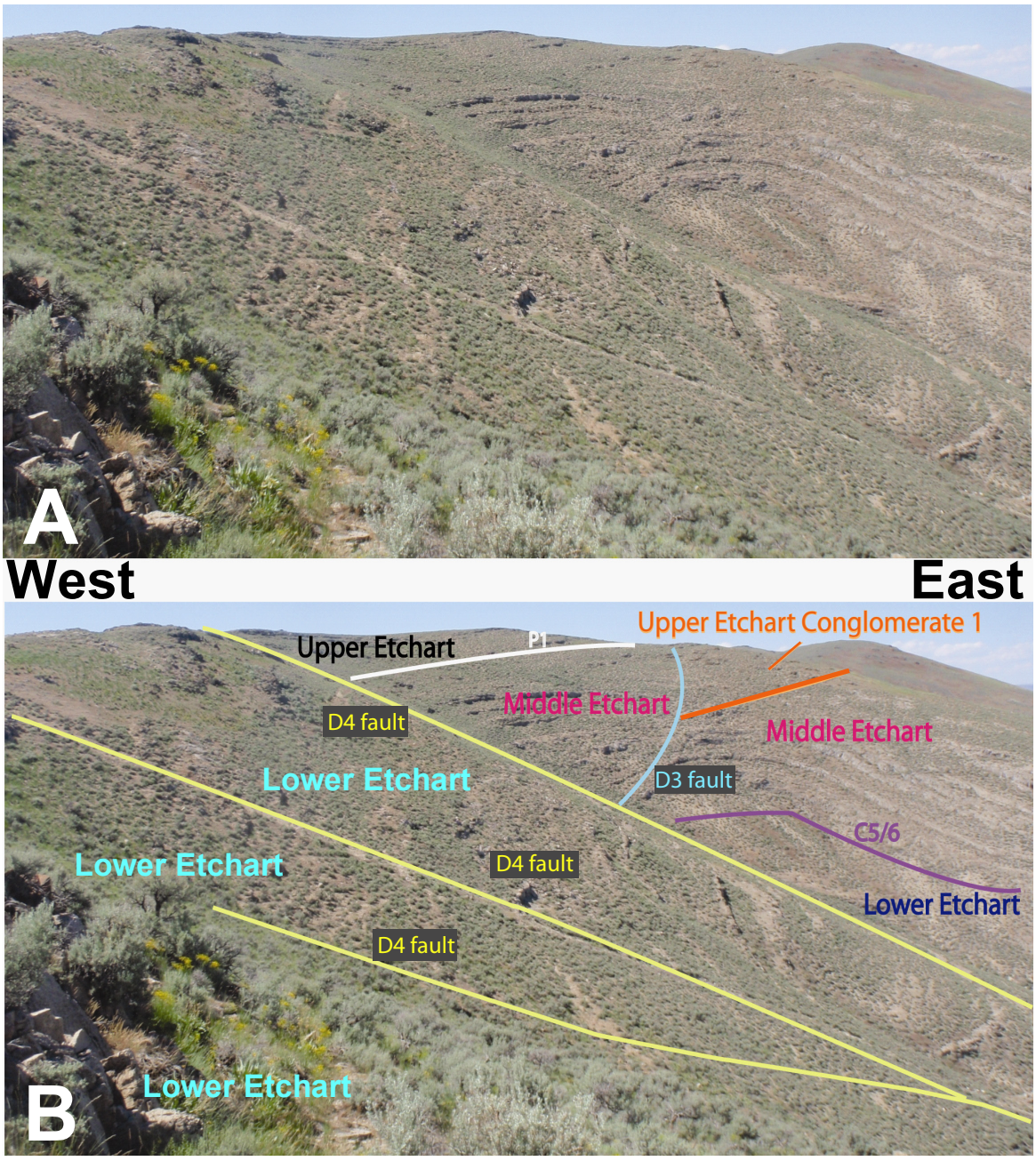

Figure 34. Photograph displaying many of the key units and features, such as the Upper, Middle, and Lower Etchart members, the P1 and C5/6 angular unconformity, and faults from fault set 1 (D3) & fault set 2 (D4). The cross cutting relationships displayed here and other locations allow for relative timing of deformations.

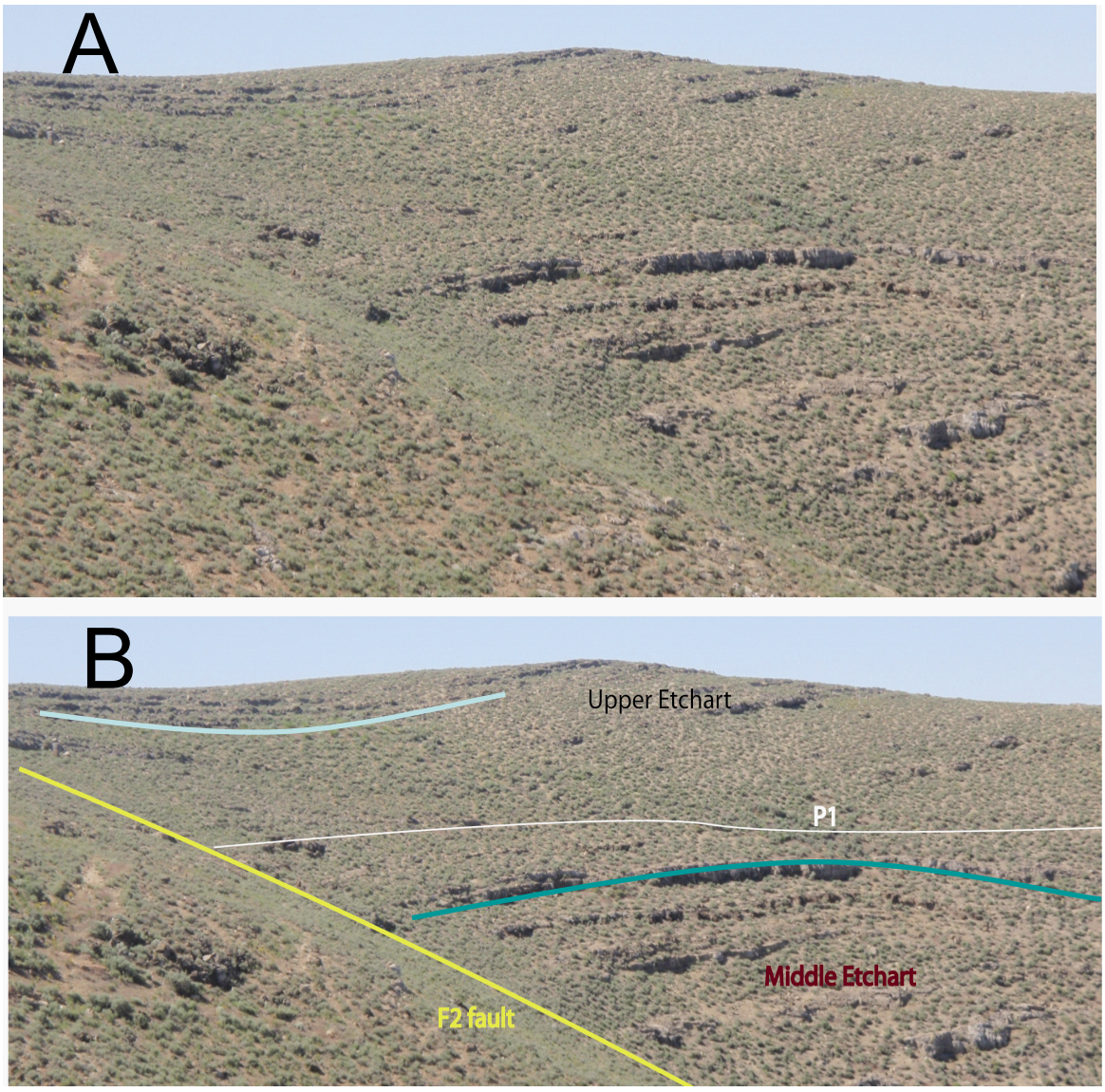

Figure 35. Exposure of the P1 angular unconformity within the Dry Hills. The Upper Etchart member displays a gentle syncline, where as the Middle Etchart member that underlies it displays an F1 anticline not located in the upper member of the Etchart Formation. The P1 unconfromity is folded by the younger syncline, although the change in orientation is not well shown in these photographs due to the angle they are taken from.

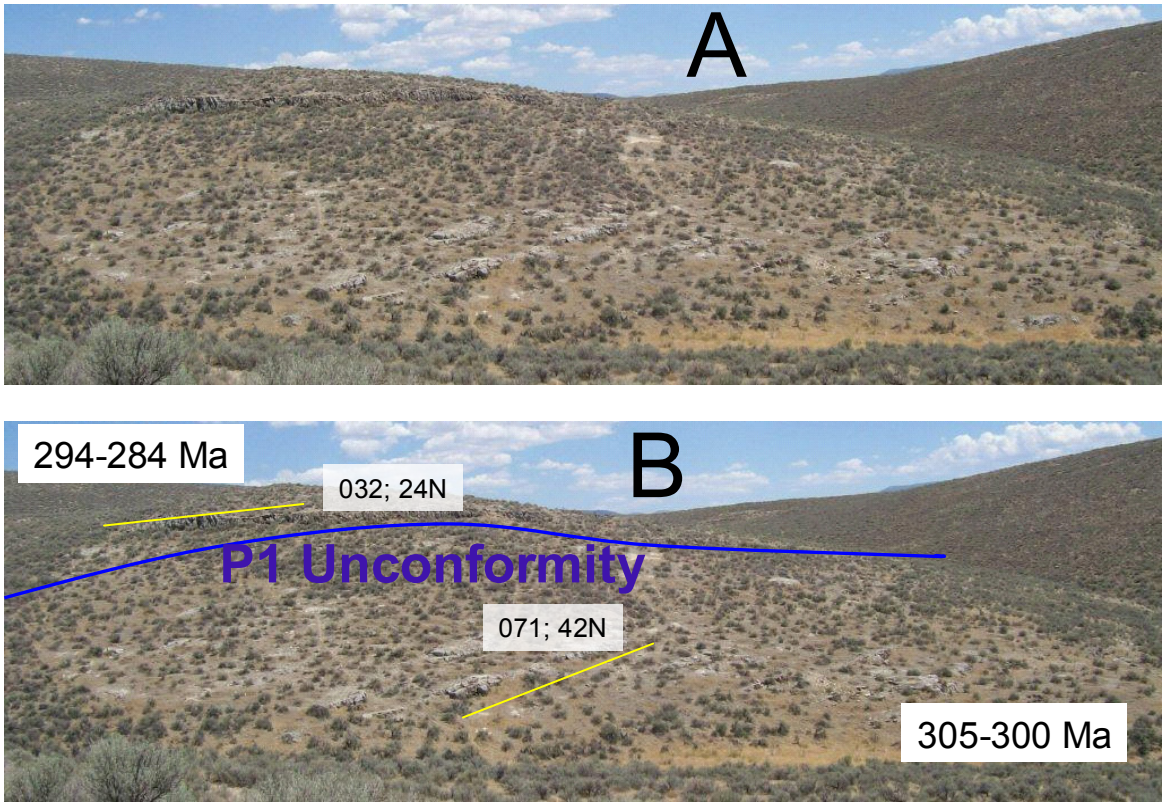

Figure 36. Figure showing angular discordance across the P1 unconformity. Note that the P1 unconformity is gently folded by F4 folds. (A) Unmodified photograph of the P1 angular unconformity taken from the Dry Hills facing NW. (B) Identical photograph with P1 angular unconformity (blue line), unit ages, and bedding orientations (yellow lines) marked.

Figure 37. (A) interbedded layers of conglomerate within the Lower Etchart member, with rock hammer for scale. Photo taken in the proximity of Lower Etchart Conglomerate 1. (B) Lower Etchart member pebble conglomerate 1 from the Dry Hills. Hammer for scale. Clasts are well rounded, well sorted, and dominantly pebble size.

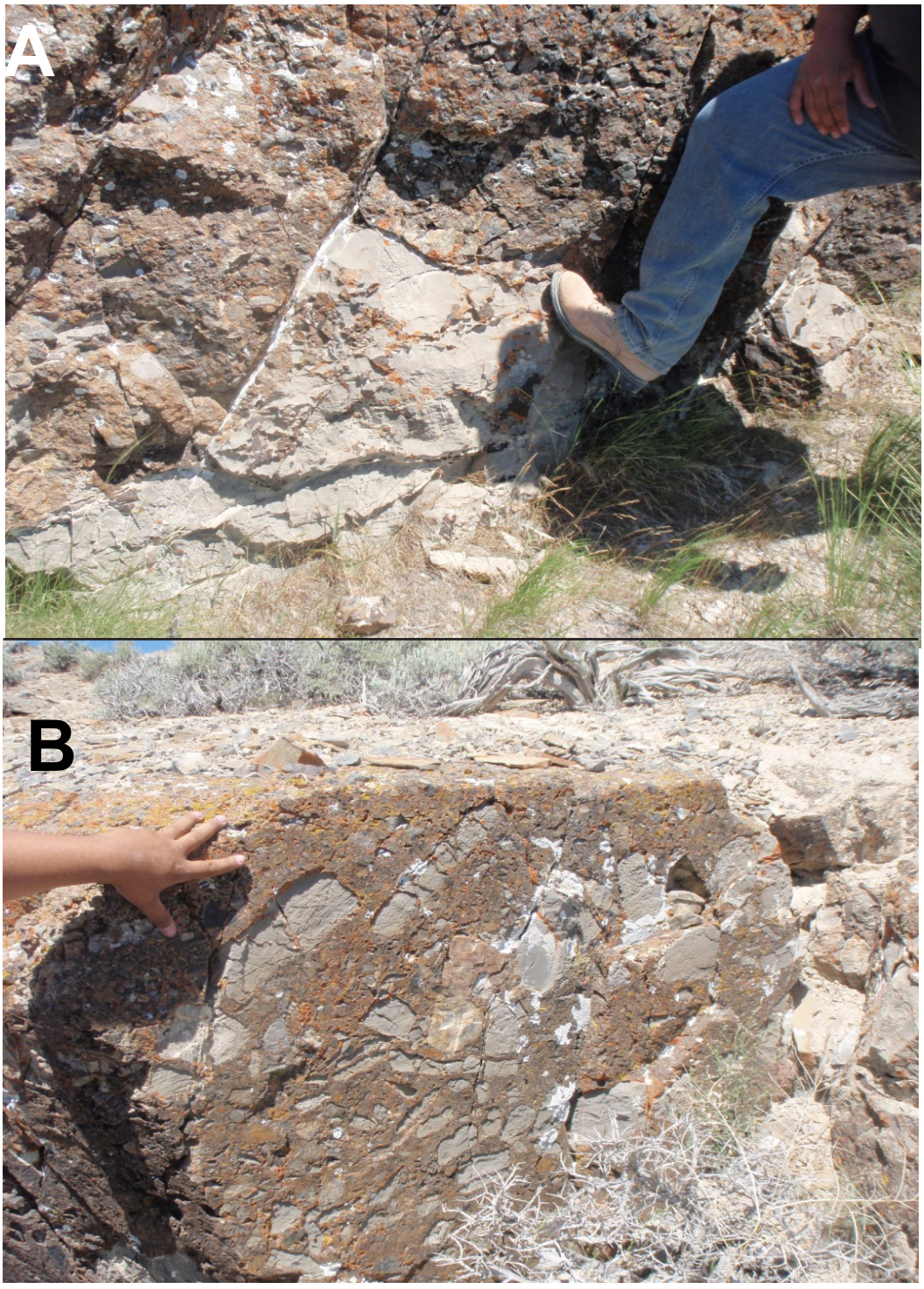

Figure 38. Photographs Upper Etchart conglomerate 1. (A) Boulder sized carbonate clasts, sheared on left side by a set 1 fault, (US size 13 boot for scale). (B) These cobble-sized carbonate clasts appear imbricated (hand for scale) and contain Atokan age fusulinids (Davydov, personal communication). Clasts of this size only occur in this conglomerate unit.

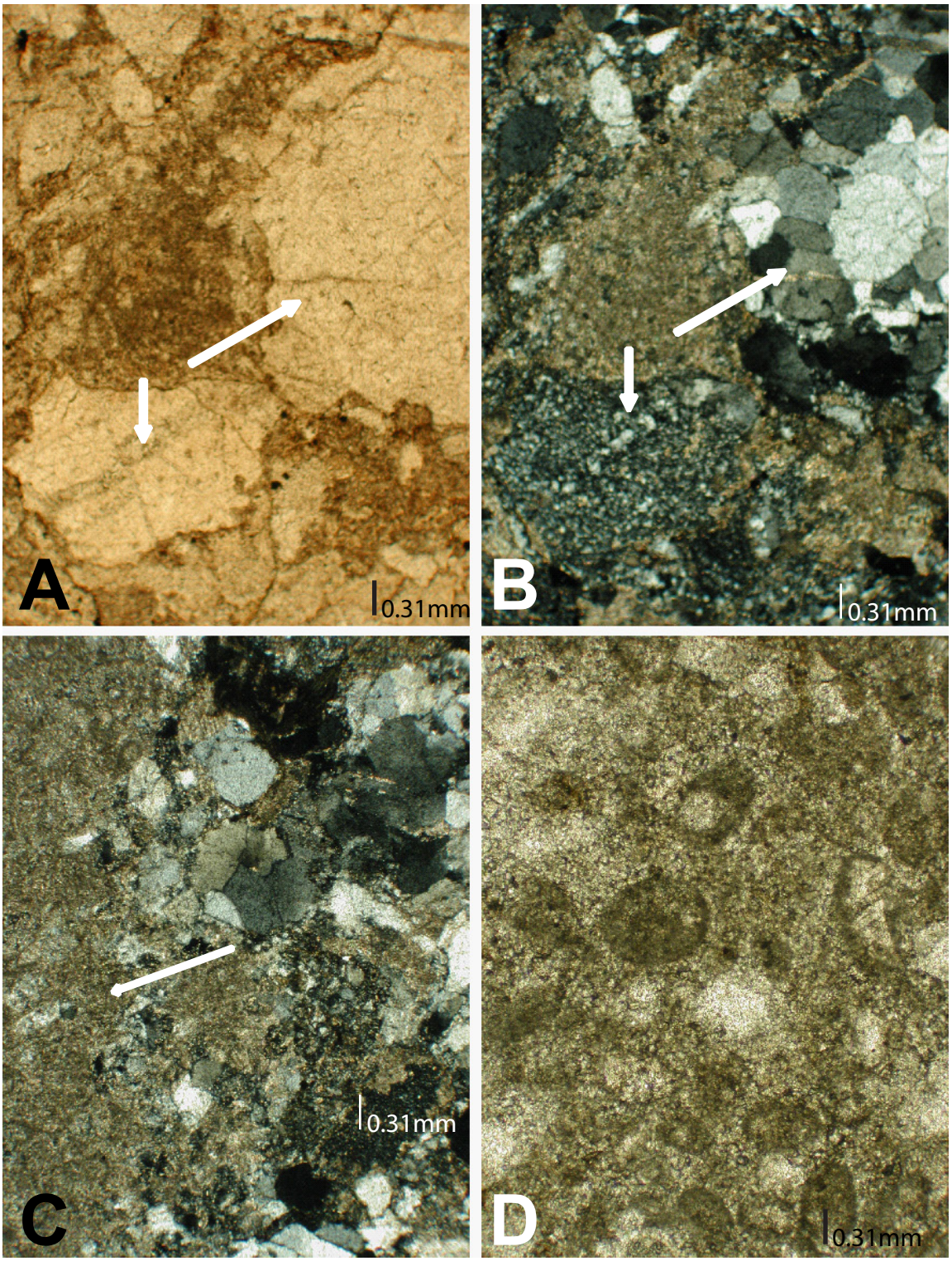

Figure 39. Photographs from the Upper Etchart Member conglomerate 1 taken at 40x magnification in PPL (A, D) and XPL (C, B). (A) and (B) are a pair of photos in PPL and XPL taken from the same location. Note polycrystaline quartz clast and carbonate dolomitized carbonate clast (white arrows). (C) Carbonate clast containing fossil fragments (white arrow). (D) fossil fragments within carbonate clasts in PPL. These clasts have been aged as Atokan.

Figure 40. (A) Close up photos of Upper Etchart Conglomerate 2. Silicious clasts within the conglomerate are pebble in size and moderately to well sorted. (B) interbedded channel of conglomerate within chert bed.

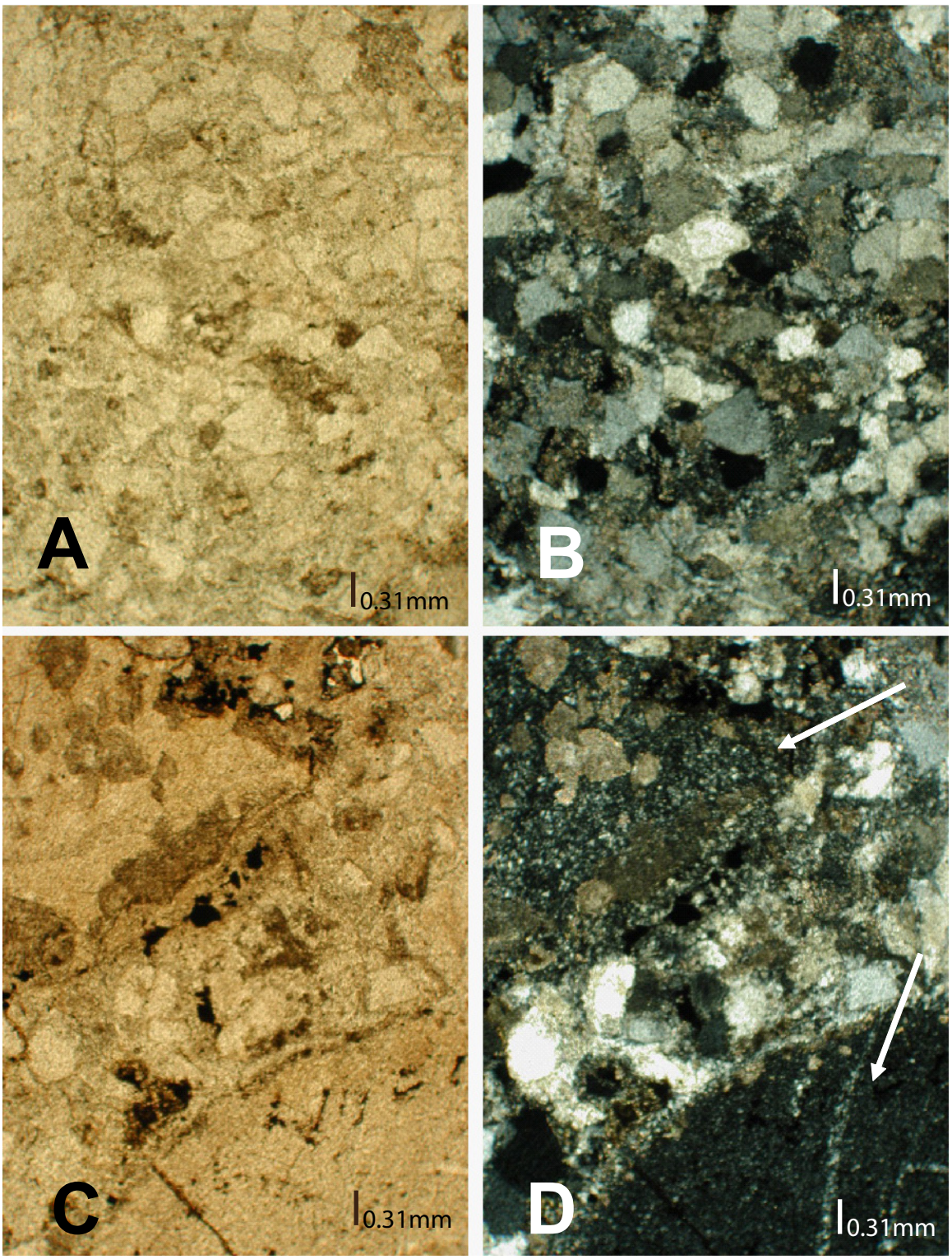

Figure 41. Photographs from the Upper Etchart member conglomerate 2 taken at 40x magnification in plane light (A, B) and cross-polarized light(C, D). The photos represent two pairs of plane light and cross-polarized shots from the same location on the thin section. The matrix is composed of sand sized quartz and carbonate grains (A&B). The carbonate clasts (C&D) are composed of two types (white arrows) of carbonate. A micrite largely unaltered (lower) and highly dolomitized micrite (upper). This conglomerate lacks fossil bearing clasts.

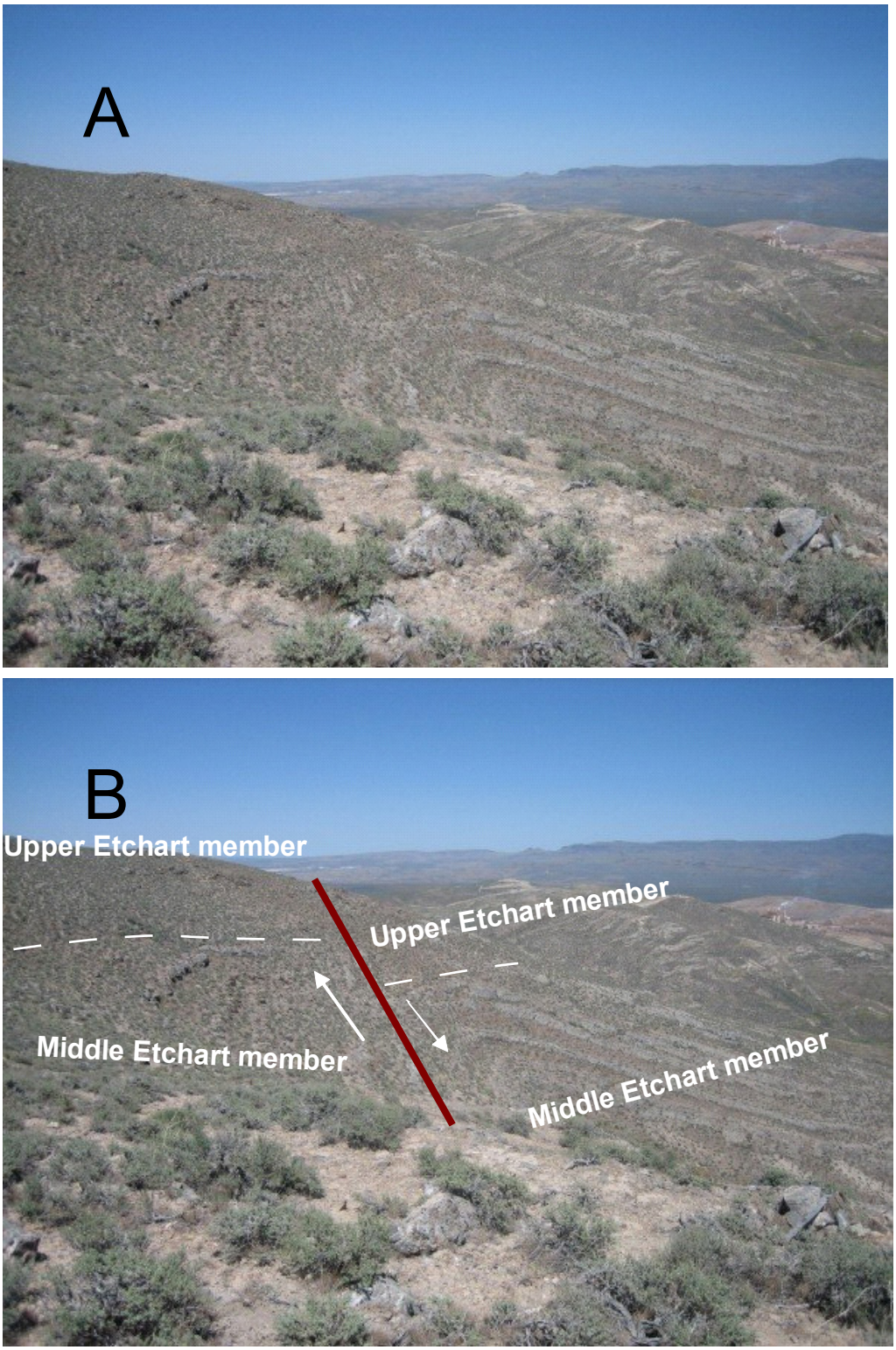

Figure 42. Example of fault set 1, N-S to SSW-NNE striking high-angle normal faults. (A) Photo of fault set 1 from Dry Hills, facing north. (B) Identical photograph as (A) with fault set 1 and motion sense identified with white arrows, fault marked in red.

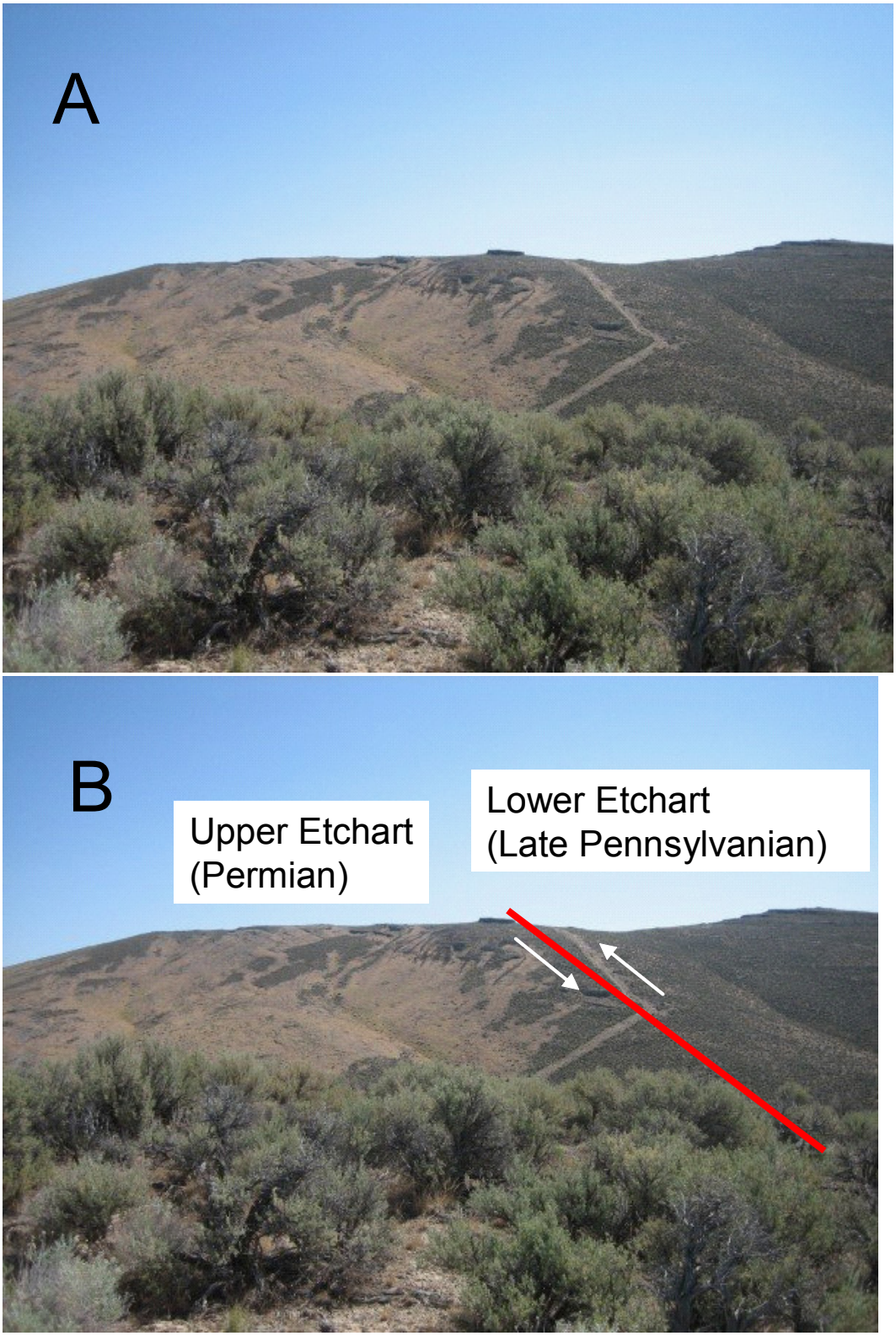

Figure 43. Example of fault set 2, ENE striking thrust faults, taken from the Dry Hills. (A) Unaltered photograph taken from the Dry Hills, facing roughly east. (B) Identical photograph with ENE striking thrust fault, motion sense, and unit names indicated.

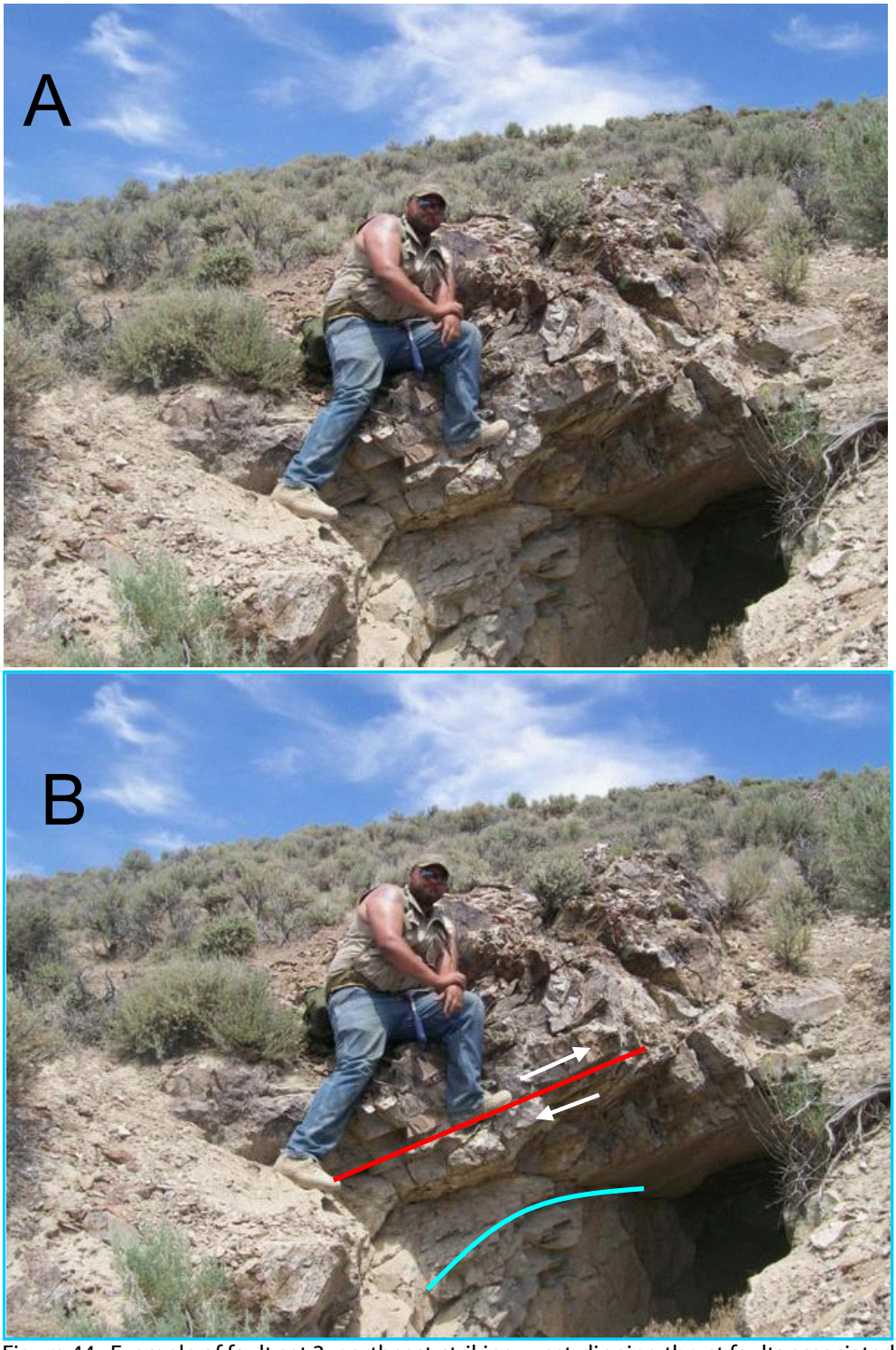

Figure 44. Example of fault set 3, northeast-striking, west-dipping thrust faults associated with the Golconda thrust. (A) Photograph of a set 3 fault from the Havallah Sequence western Dry Hills with associated fold set 4 fold under the contact. (B) identical photograph as (A) with fault set 3 (red line), fold set 4 (blue line) and motion sense indicated.

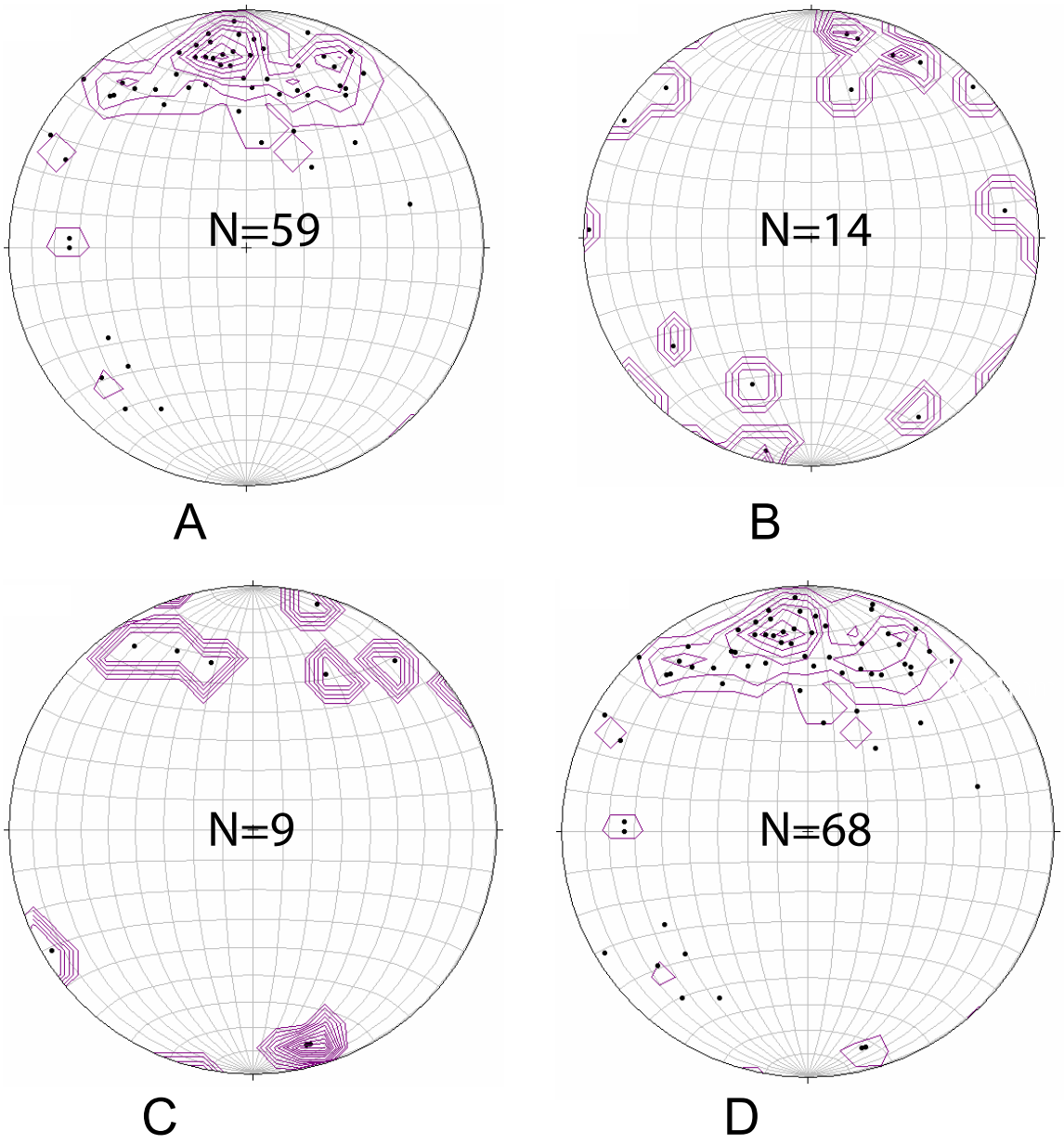

Figure 45. (A)Compilation of fold hinge orientations from the Upper Etchart member. Contour interval 2.0% per 1% area, N=59. (B)Compilation of fold hinge orientations from the Middle Etchart member, 2.0% per 1% area, N=14. (C) Compilation of fold hinge orientations from the Lower Etchart member in the Dry Hills member. Contour interval 2.0% per 1% area, N=9 Contour interval 2.0% per 1% area, N=9 (D) Compilation of hinge trend and plunge orientations from the Upper and Middle Etchart Formation in the Dry Hills. Contour interval 2.0% per 1% area, N=68

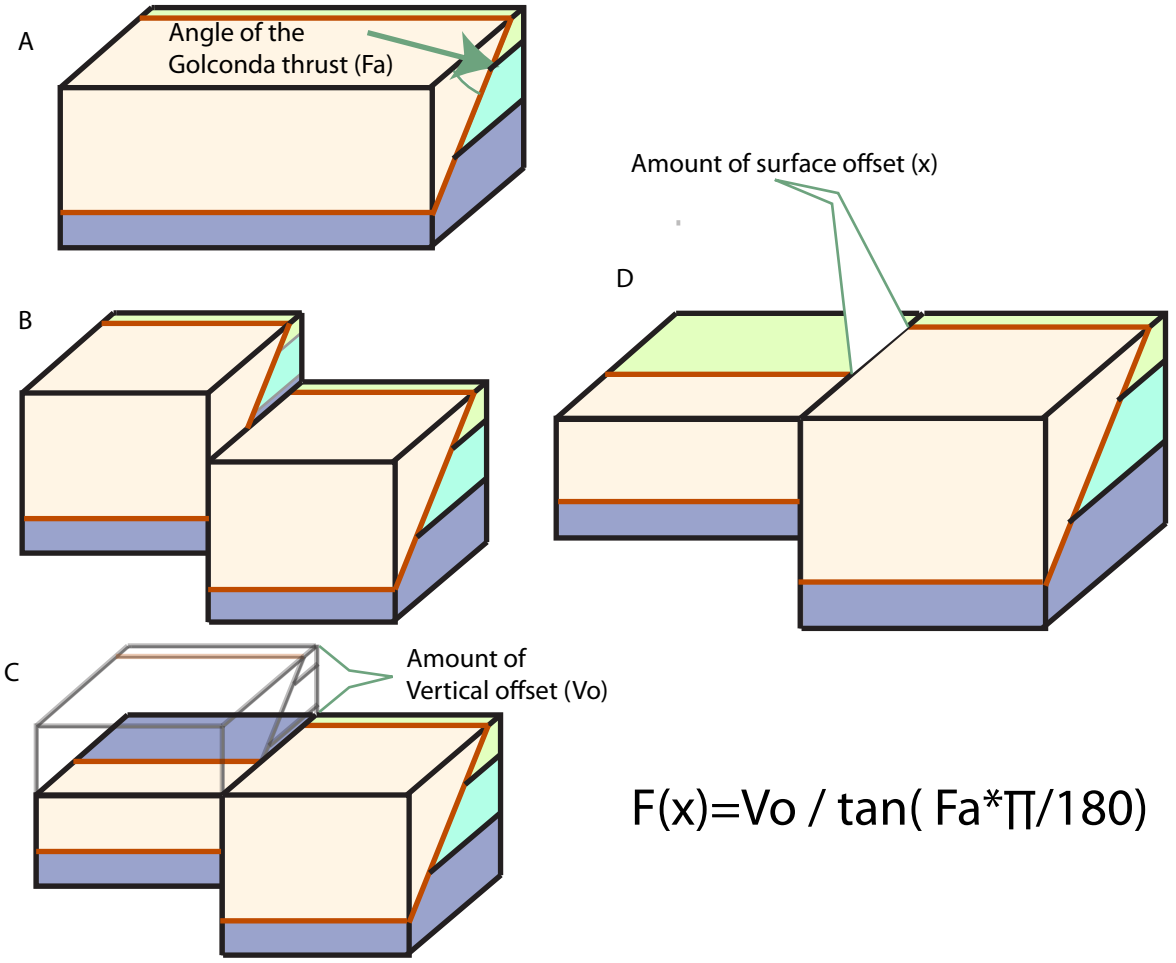

Figure 46. Block diagram that displays the method used to determine right-lateral offset of the Getchell fault.

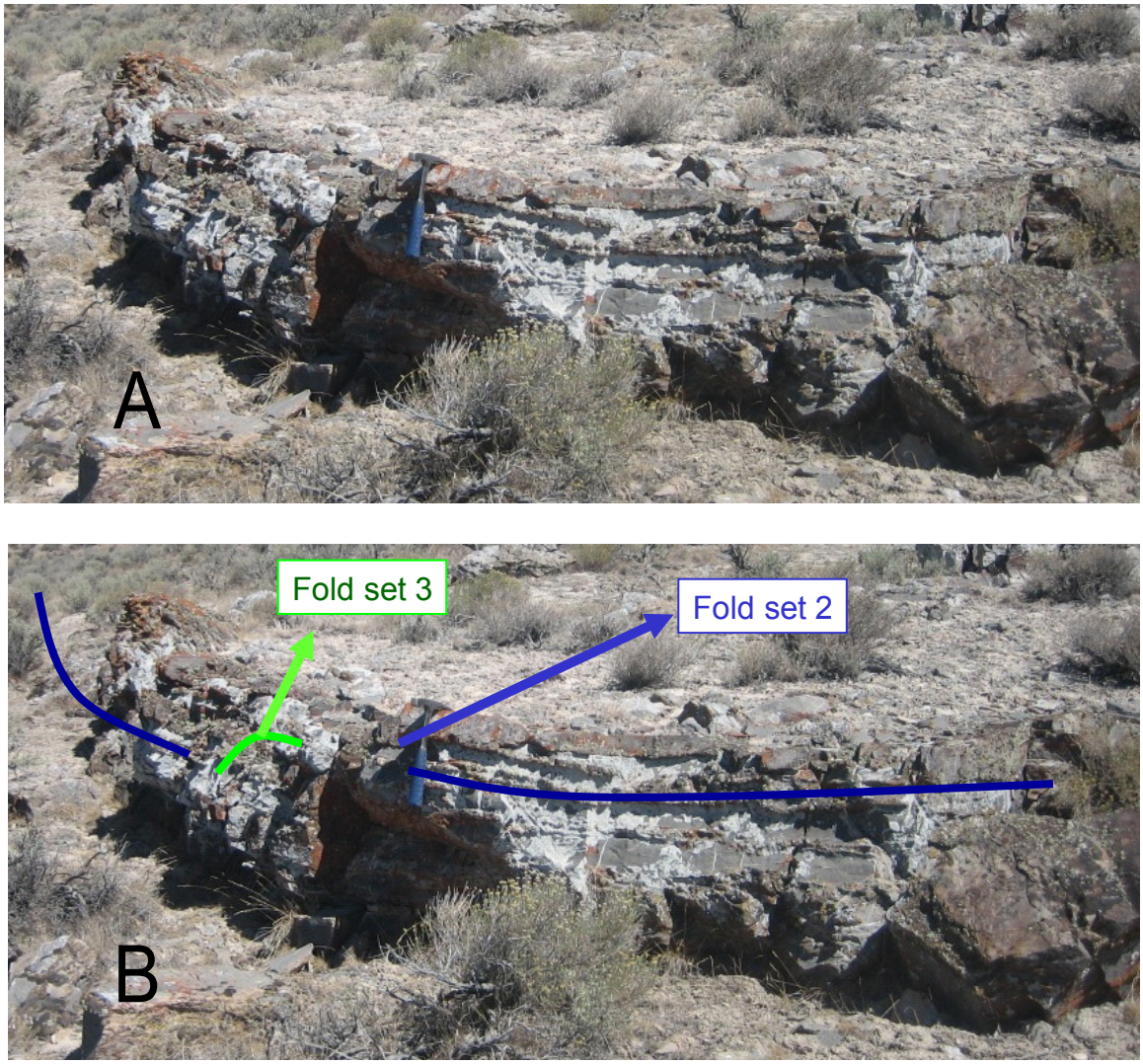

Figure 47. Example of F2 being refolded by F3, taken from the Upper Etchart member in the Dry Hills. (A) Unaltered photograph of folds taken from the Dry Hills facing roughly north. (B) Identical photograph as (A) with folds identified by green (D3) and blue (D2) lines.

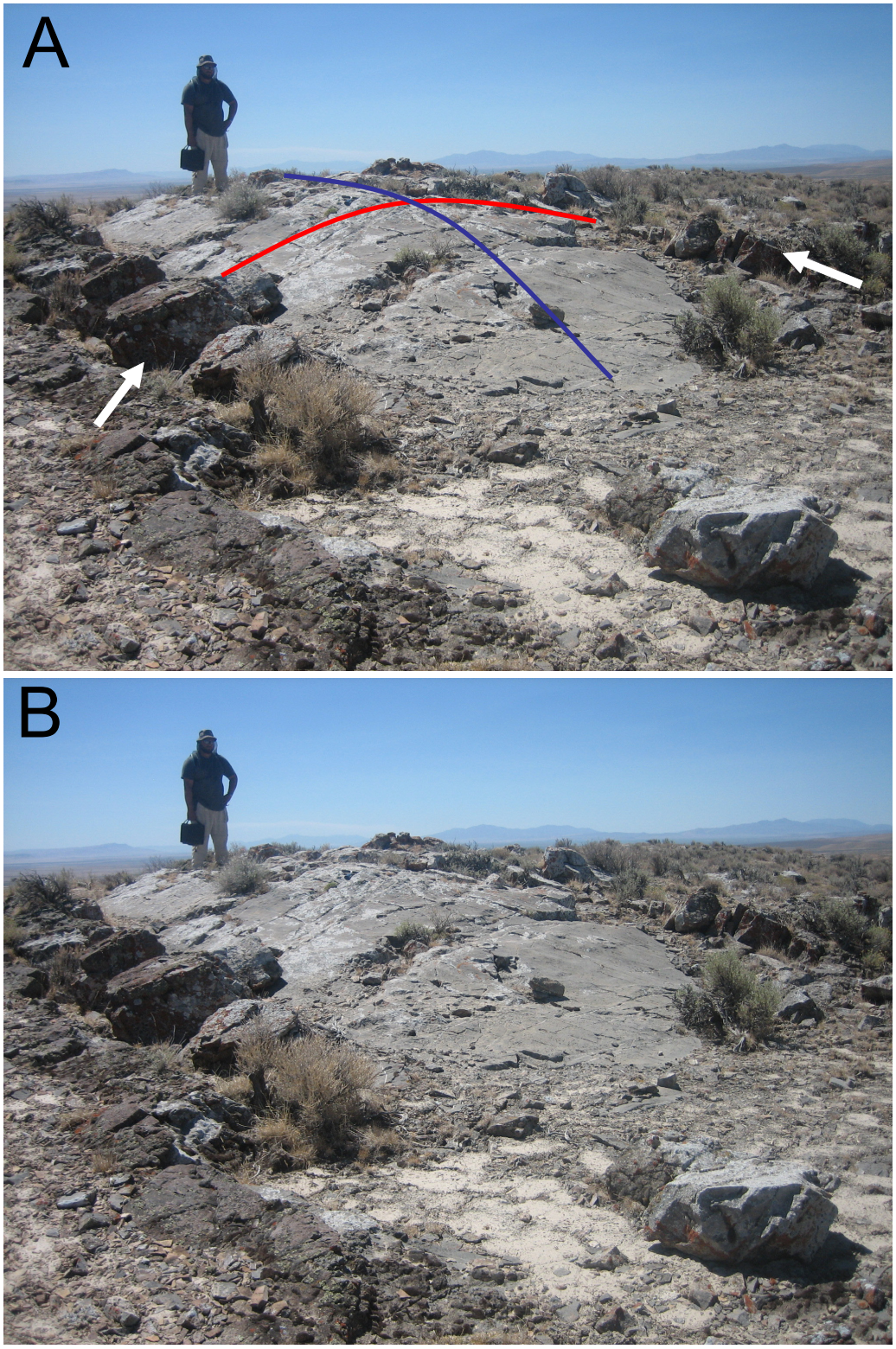

Figure 48. Figure of a refolded fold within the Upper Etchart member. Note both folds are upright and gentle. Chert beds (white arrows) reveal the first anticline. Person for scale is standing on anticlinal hinge. Second anticline folds bedding downward towards bottom of photo, with a hinge depicted with a red line. First fold (blue hinge) is a D2 fold, which is refolded by a D4 fold hinge. Photo taken facing ~ southeast.

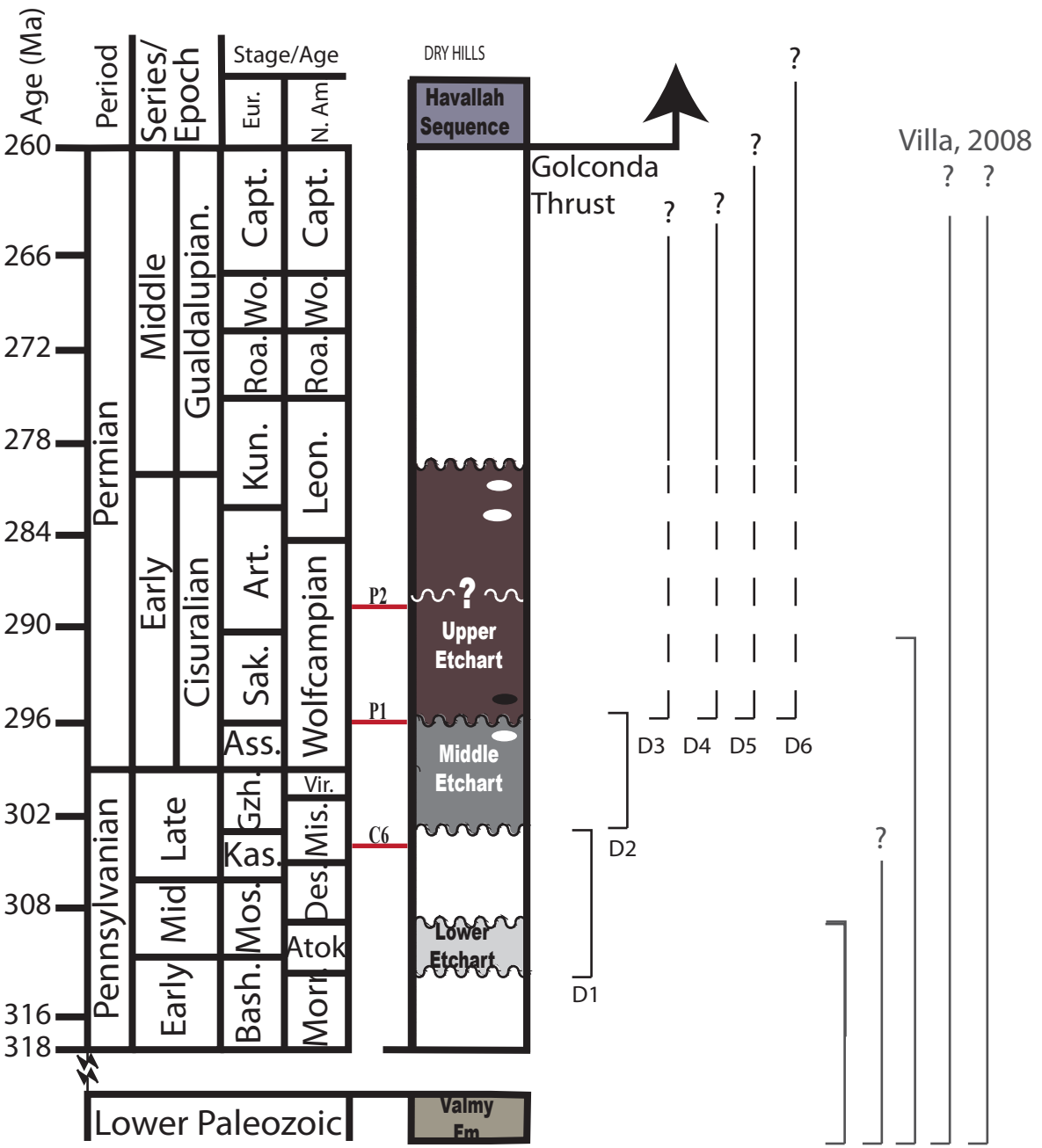

Figure 49. Tectonostratigraphic representation of the Dry Hills and the timing constraints of deformation for D1-D6. F1-F5 in light grey to the right depicts the folding deformations of Edna Mountain from Villa (2008). Structure abrievations: IPF = Iron Point Fault. Age name abrievations: Art.=Artinskian; Ass.=Asselian; Ato.=Atokan; Bash.=Bashkirian; Capt.=Capitanian; Des.=Desmoinesian; Eur.= European; Gzh.=Gzhelian; Kun.=Kasimovian; Kung.=Kungurian; Leon.=Leonardian; Mis.=Missourian; Morr.=Morrowan; Mos.=Moscovian; N. Am.= North American; Roa.=Rodian; Sak.=Sakmarian; Vir.=Virgilian; Wo.=Wordian;

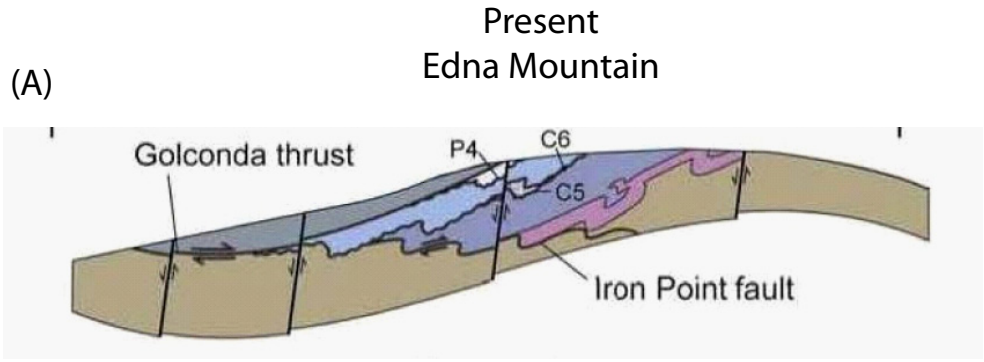

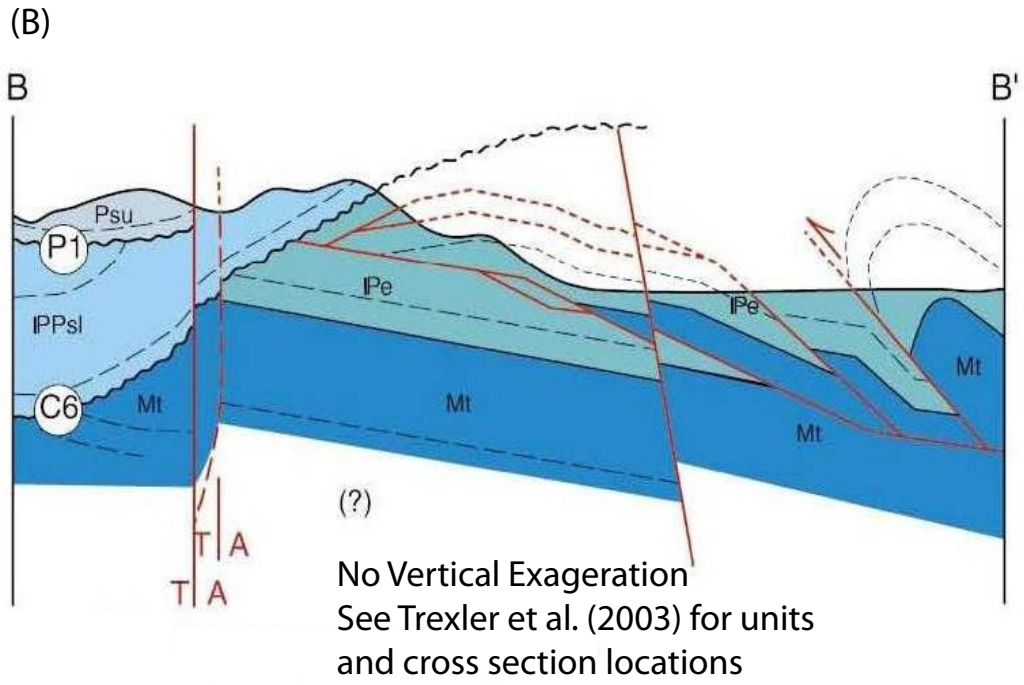

Figure 50. (A) Cross section depicting the modern location of strucures at Edna Mountain from Villa (2008). The structual history of the Dry Hills and Edna Mountain vary greatly. Depositionally, the earlier histories of both locations are similar, but vary greatly later in time. (B) Depiction of cross section at Carlin Canyon showing the P1 and C6 angular unconformities which merge at Carlin Canyon. This relationship is not recognised in the Dry Hills, as faulting leaves the distribution of the unconformities in relation to each other obscured (From Trexler et al., 2003).

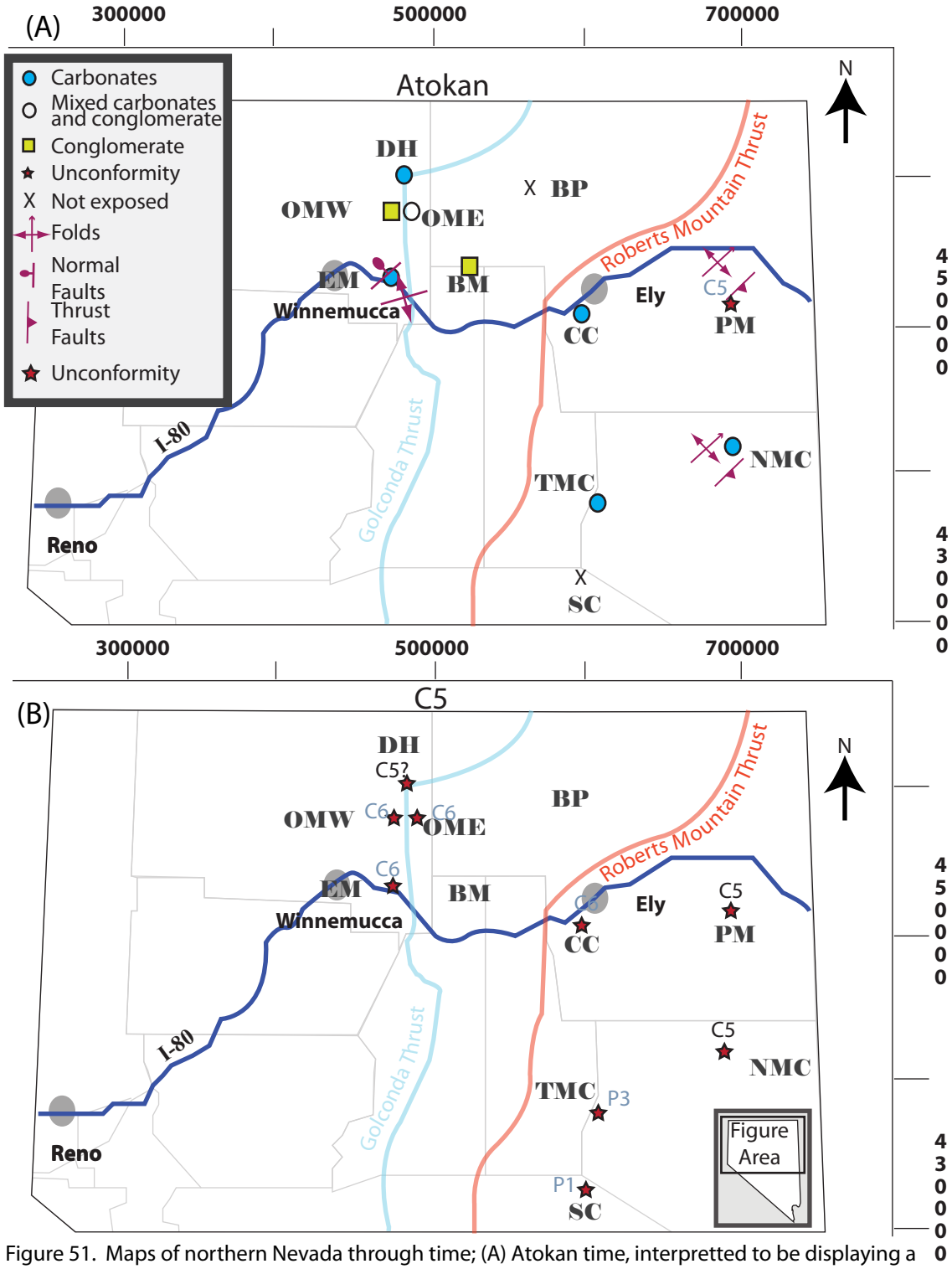

Figure 51. Maps of northern Nevada through time; (A) Atokan time, interpretted to be displaying a NW-SE shortening event with (local?) extention in the west. (B) Map displaying locations of C5 unconformities, interpretted to be the result of Atokan age driven uplift and erosion. Locations abbreviated as follows: OMW=Osgood Mountains West, OME=Osgood Mountains East, EM=Edna Mountain, BP=Beaver Peak, BM=Battle Mountain, CC=Carlin Canyon, PM=Pequop Mountian, NMC=Nine Mile Canyon, TMC=Three Mile Canyon, SC=Secret Canyon. Data from researchers cited in Fig. 12.

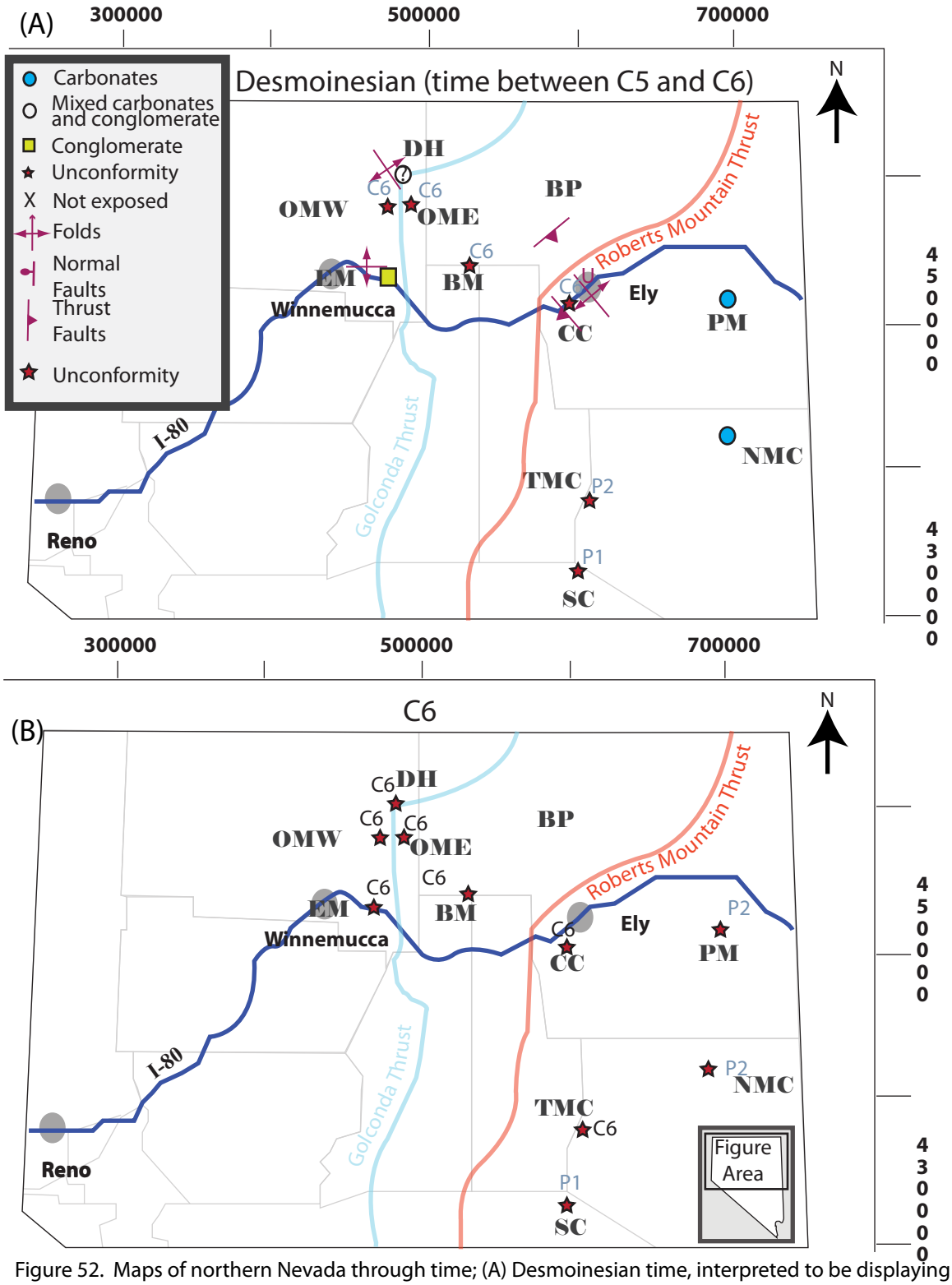

Figure 52. Maps of northern Nevada through time; (A) Desmoinesian time, interpreted to be displaying a roughly N-S shortening direction with variation in orientation of the primary stress field interrupted to be due to changes in paleotopography. (B) Map displaying locations of C6 unconformities, interpreted to be the result of Desmoinesian age driven uplift and erosion. Location abbreviations located in Fig 51. Data from researchers cited in Fig 12.

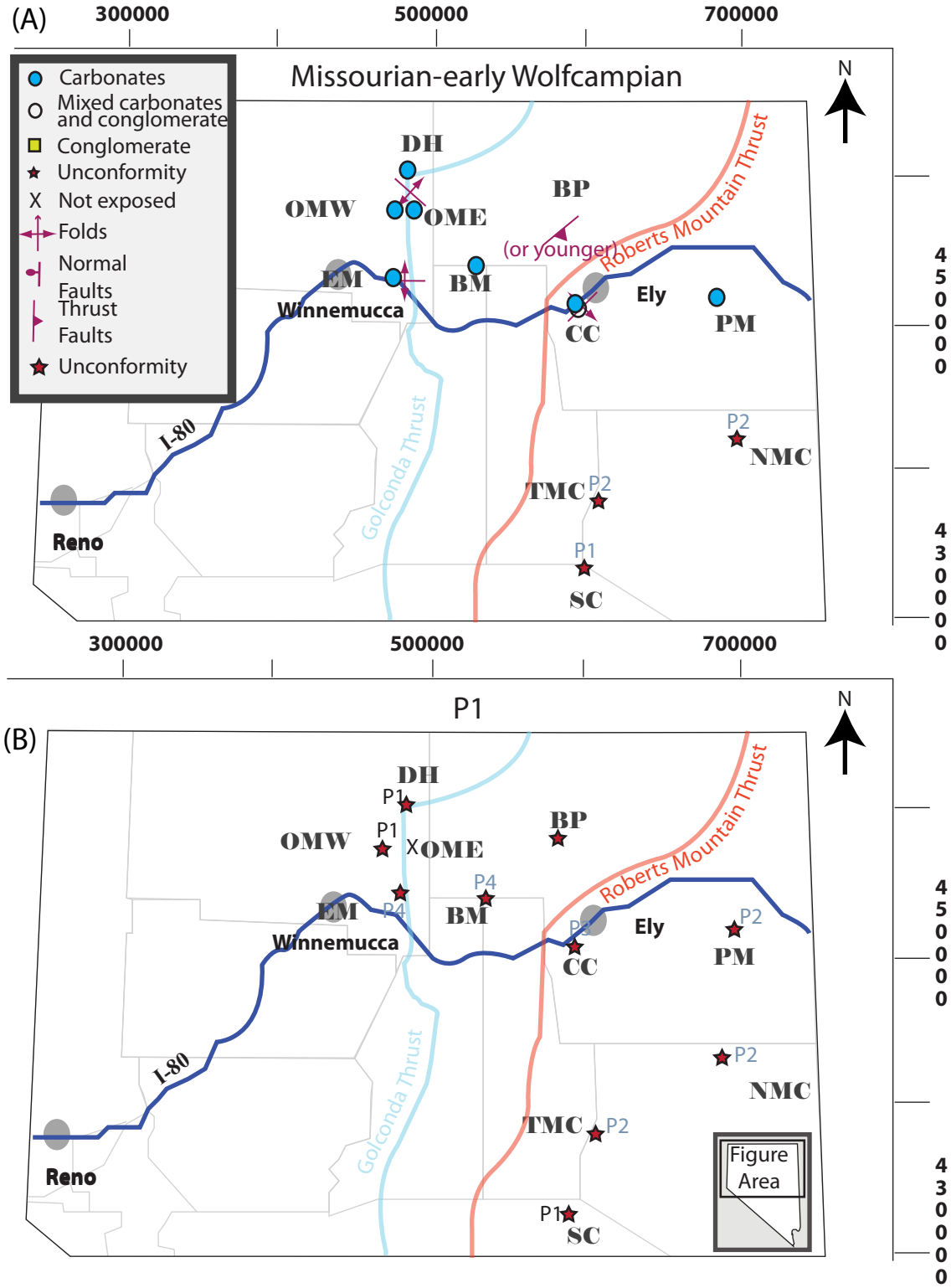

Figure 53. Maps of northern Nevada through time; (A) Missourian-Wolfcampian time, interpreted to be displaying a roughly N-S oriented tectonic event. (B) Map displaying locations of P1 unconformities, interpreted to be the result of Missourian-Wolfcampian age driven uplift and erosion. Location abbreviations listed in Fig 51. Data from researchers cited in Fig. 12.

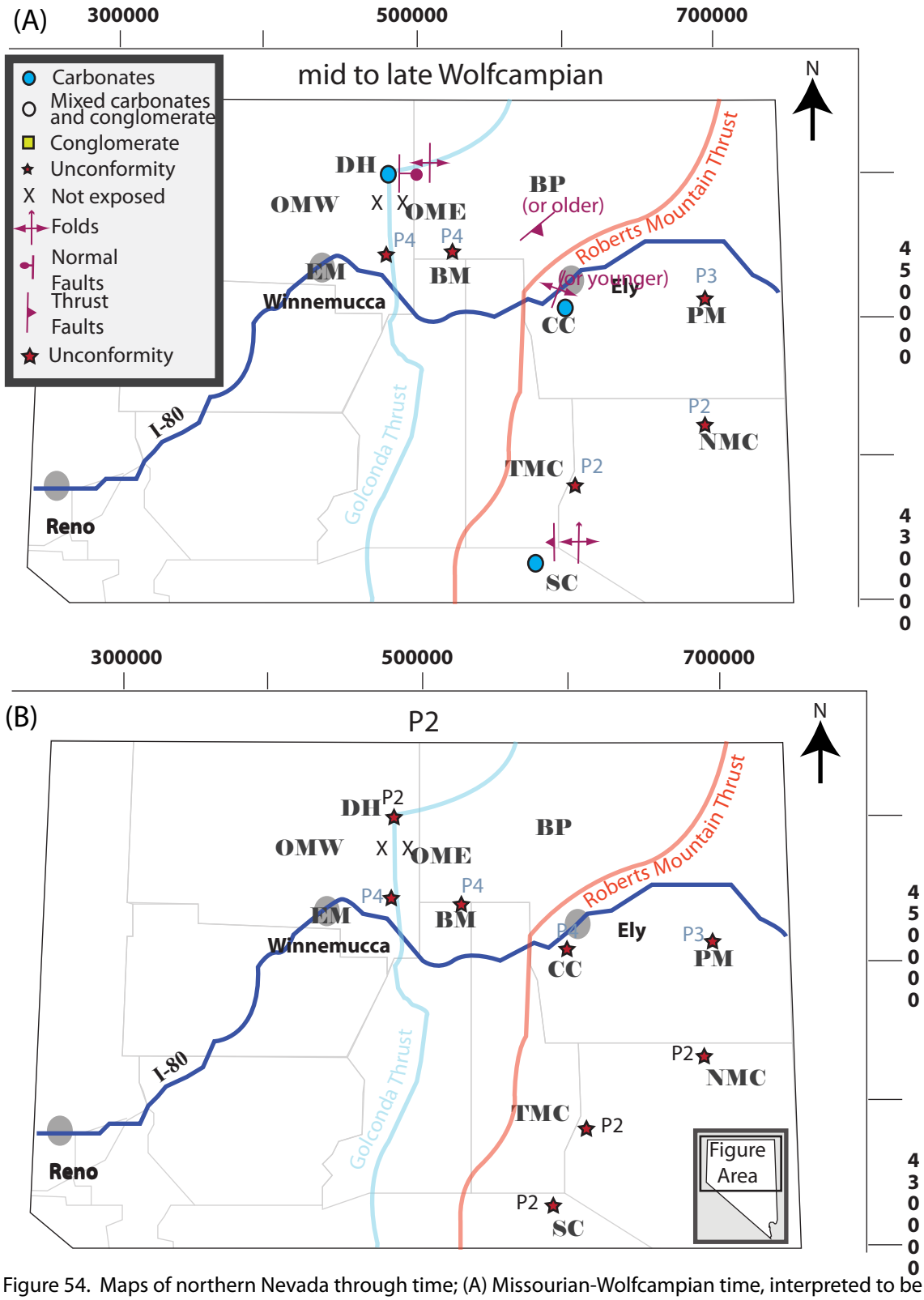

Figure 54. Maps of northern Nevada through time; (A) Missourian-Wolfcampian time, interpreted to be displaying an E-W shortening event with (local?) E-W extention in the North. (B) Map displaying locations of P1 unconformities, interpreted to be the result of Wolfcampian age driven uplift and erosion. Location abbreviations listed in Fig. 51. Data from researchers cited in Fig. 12.

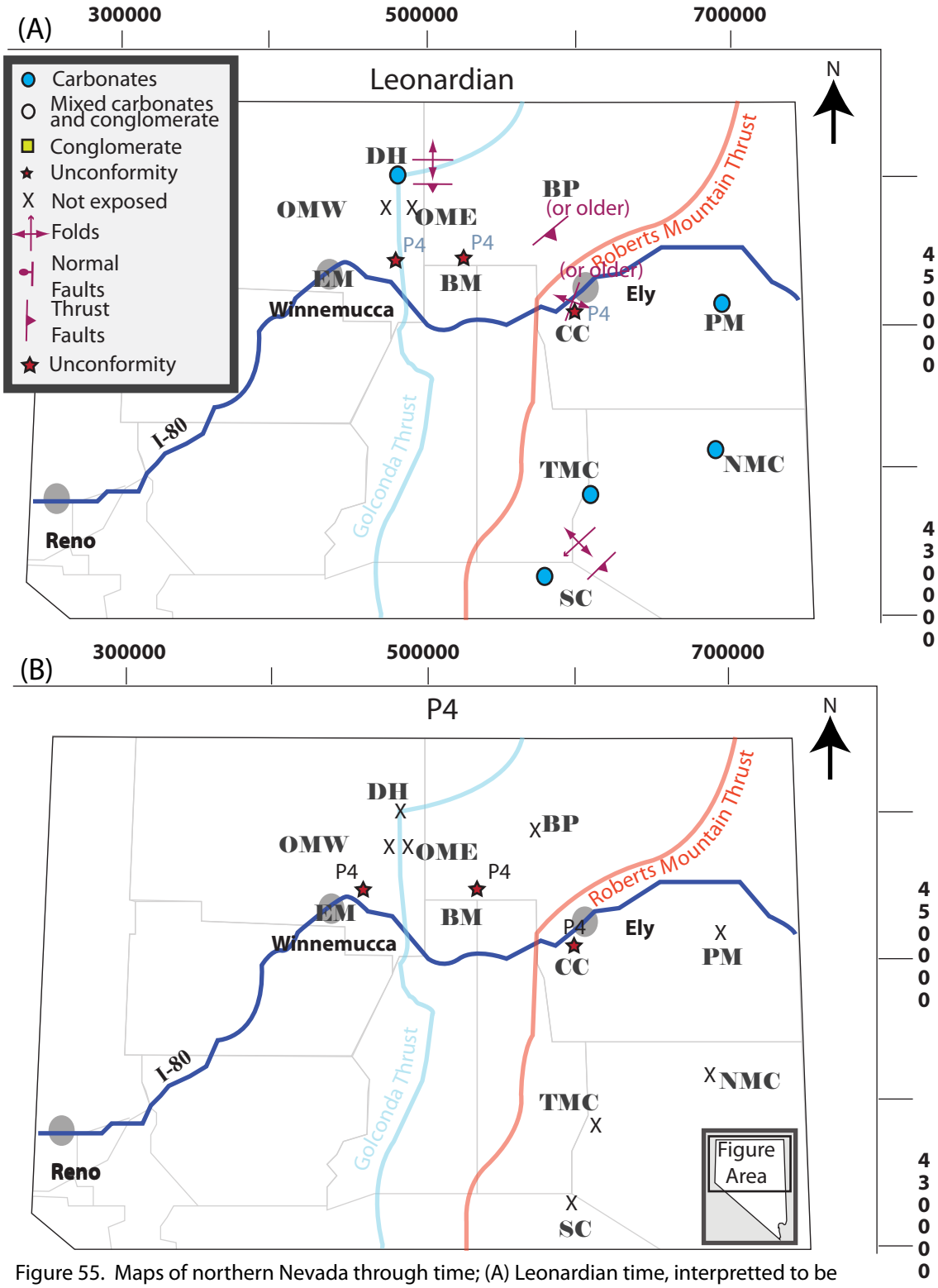

Figure 55. Maps of northern Nevada through time; (A) Leonardian time, interpretted to be displaying N-S shortening rotating to SE-NW due to paleogeography. (B) Map displaying locations of P4 unconformities, interpreted to be the result of Leonardian age uplift and erosion. Location abbreviations listed in fig 51. Data from researchers cited in Fig. 12 .

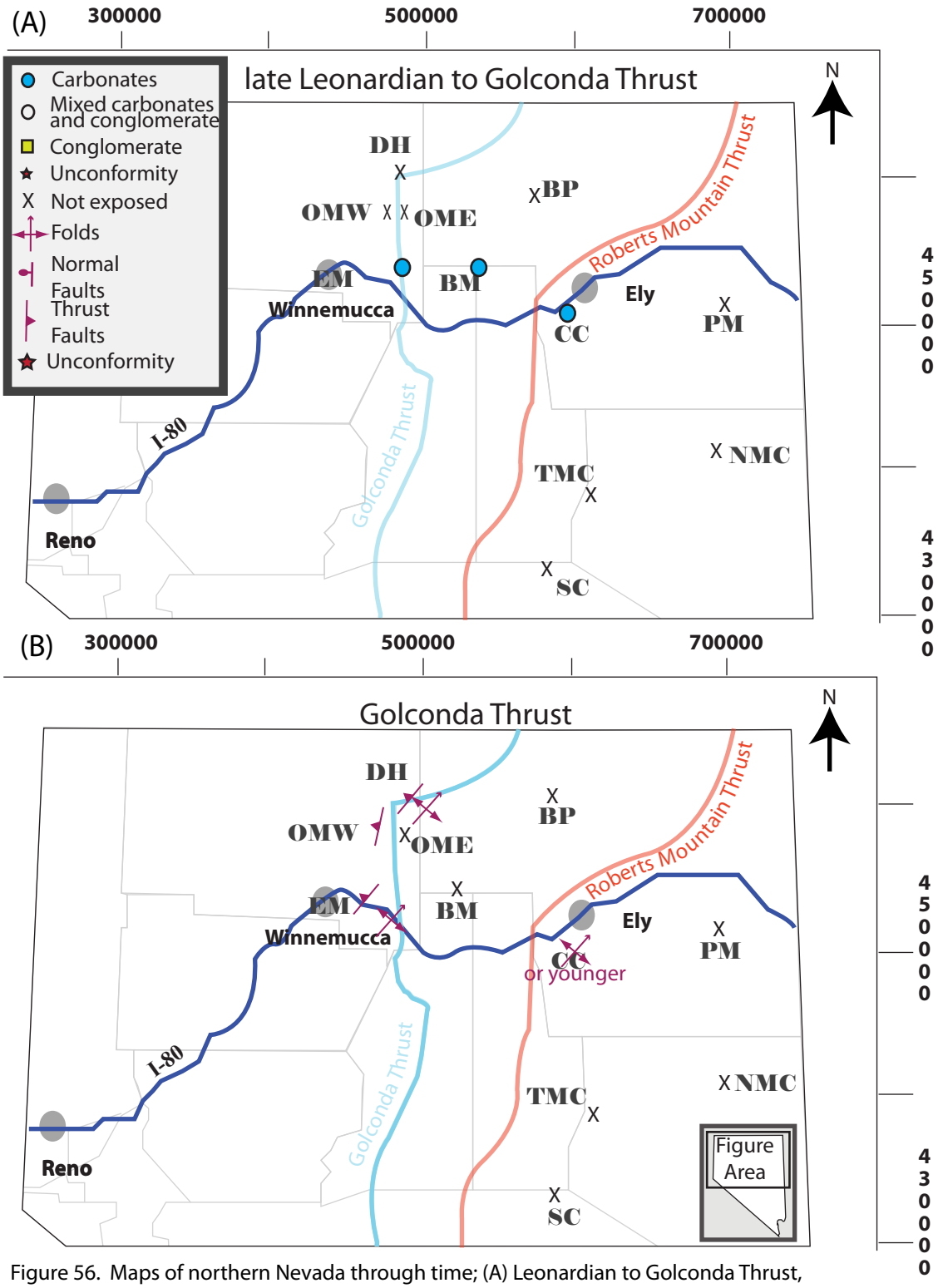

Figure 56. Maps of northern Nevada through time; (A) Leonardian to Golconda Thrust, deposition prior to Sonoma Orogeny. (B) Map displaying locations and orientation of Golconda thrust of the Sonoma Orogeny. It is interpreted to be a SE directed shortening event. Location abbreviations listed in Fig 51. Data from researchers cited in Fig. 12.

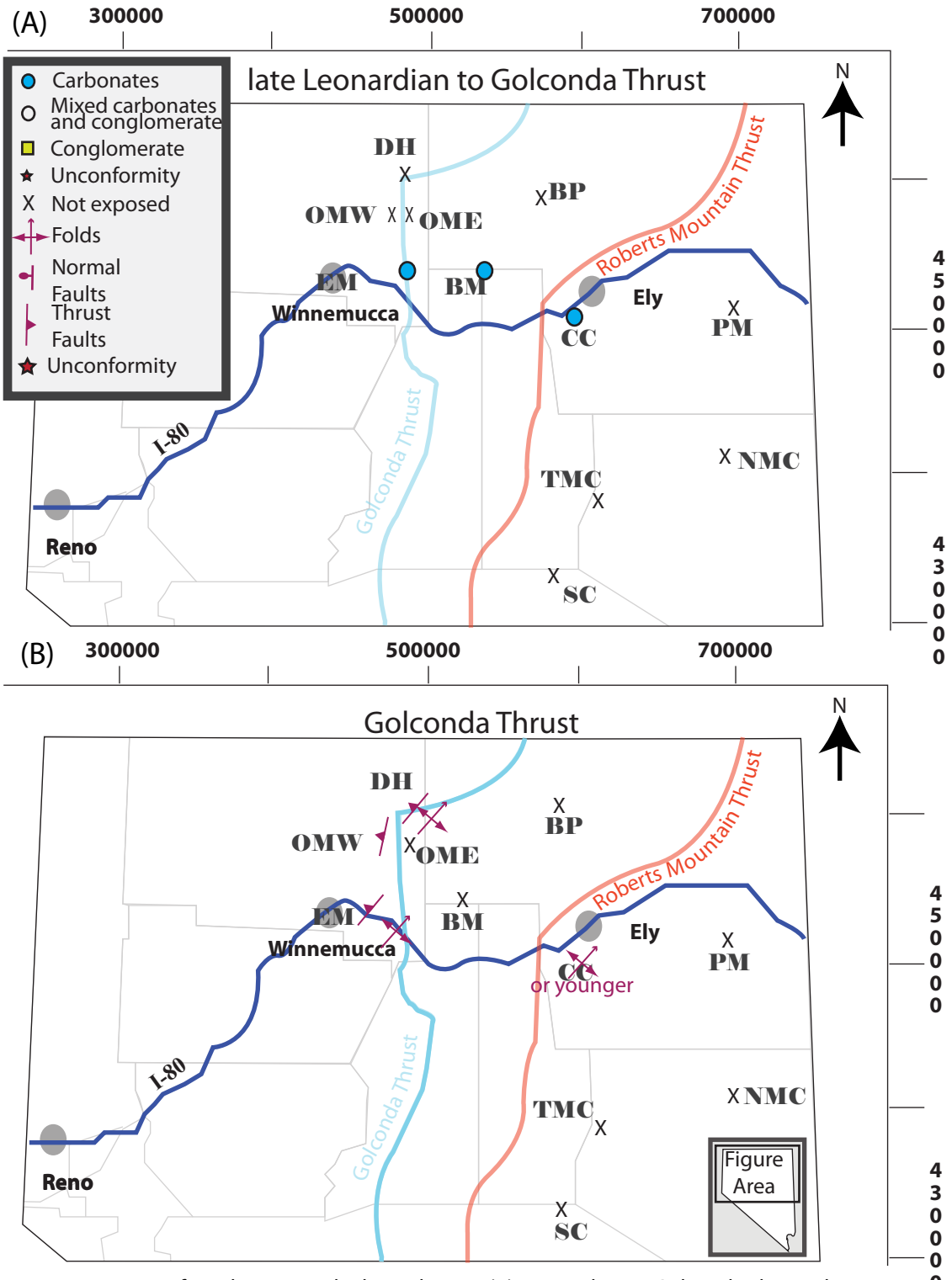

Figure 57. Maps of northern Nevada through time; (A) Leonardian to Golconda Thrust, deposition prior to Sonoma Orogeny. (B) Map displaying locations and orientation of Golconda thrust of the Sonoma Orogeny. It is interpretted to be a SE dirrected shortening event. Locations abbreviations listed in Fig 52. Data from researchers cited in Fig. 12.

APPENDIX 2

TABLES

TABLE 1. DRY HILLS STRIKE AND DIP DATA

ID #	Strike	Dip	ID #	Strike	Dip	ID #	Strike	Dip
1	358	26W	29	341	29W	57	305	08S
2	360	63W	30	343	32W	58	327	7S
3	356	73W	31	313	20W	59	299	16N
4	332	69E	32	354	31W	60	306	11S
5	358	40N	33	320	40W	61	283	21S
6	359	74E	34	304	60W	62	353	17W
7	328	49E	35	319	50W	63	304	34N
8	329	24W	36	304	24W	64	274	16N
9	304	1N	37	300	34n	65	317	24S
10	283	27N	38	297	20n	66	346	39E
11	317	29N	39	281	40N	67	354	8W
12	303	32n	40	292	29N	68	349	27W
13	337	25E	41	273	65S	69	336	11W
14	304	34N	42	360	70E	70	356	20W
15	307	32N	43	337	50E	71	308	60N
16	313	43N	44	342	10E	72	270	30N
17	324	34W	45	352	15E	73	339	22E
18	305	34N	46	272	65W	74	301	15N
19	324	62N	47	341	65W	75	356	15W
20	295	33N	48	339	18E	76	336	35W
21	349	42W	49	291	15S	77	298	40S
22	338	34W	50	357	54E	78	323	43W
23	293	31N	51	292	25N	79	337	32W
24	326	42W	52	319	25W	80	339	42E
25	324	28W	53	280	12N	81	319	29N
26	334	42W	54	310	23N	82	272	9N
27	323	42W	55	324	36E	83	320	40W
28	354	34W	56	276	38N	84	282	21N

ID #	Strike	Dip	ID #	Strike	Dip	ID #	Strike	Dip
85	357	47W	115	293	14N	145	352	18W
86	308	45W	116	345	22W	146	343	14W
87	360	35E	117	350	22W	147	277	20S
88	345	39W	118	319	10E	148	303	5S
89	348	27W	119	299	11S	149	347	2E
90	355	22E	120	305	32S	150	315	22S
91	360	40W	121	272	10S	151	354	13E
92	318	19W	122	332	5E	152	335	31E
93	347	38W	123	318	7W	153	315	26W
94	310	12S	124	347	32E	154	340	14W
95	324	20E	125	346	5W	155	336	31W
96	303	34W	126	334	18W	156	355	11W
97	286	34W	127	340	12E	157	327	11E
98	310	40W	128	336	27W	158	335	0W
99	309	56S	129	358	31W	159	310	19S
100	325	32N	130	348	9W	160	289	15N
101	292	15S	131	348	15S	161	333	50W
102	319	29E	132	312	37S	162	342	38E
103	360	47W	133	360	7W	163	278	23N
104	333	38W	134	352	14W	164	331	21W
105	352	20W	135	302	25 S	165	351	31W
106	356	15W	136	329	17S	166	345	13E
107	270	13N	137	295	22S	167	334	20W
108	345	38W	138	352	31W	168	320	50E
109	318	34E	139	339	0 N	169	348	38E
110	340	28W	140	286	17S	170	337	28E
111	298	38N	141	346	15W	171	337	17W
112	357	9W	142	307	10S	172	272	5N
113	277	16N	143	356	21W	173	352	25W

ID #	Strike	Dip	ID #	Strike	Dip	ID #	Strike	Dip
175	319	19W	205	340	22S	235	345	26W
176	355	20W	206	292	34S	236	295	34S
177	327	4W	207	307	26S	237	331	23S
178	358	32E	208	338	34S	238	307	30N
179	342	30W	209	308	20S	239	302	24S
180	302	6N	210	309	15N	240	329	38S
181	359	14W	211	341	27W	241	326	30S
182	357	27W	212	331	34W	242	328	34S
183	327	5E	213	357	21W	243	298	31S
184	360	33W	214	353	8W	244	300	24S
185	357	46W	215	334	20E	245	321	17S
186	360	23E	216	313	28S	246	323	14E
187	319	20N	217	311	19S	247	360	17W
188	321	19N	218	326	11N	248	331	80W
189	346	27W	219	298	9S	249	322	80E
190	358	20W	220	331	13S	250	349	66W
191	357	50E	221	340	13W	251	292	35S
192	339	25W	222	302	4N	252	346	26W
193	275	11N	223	317	26N	253	309	23W
194	349	25W	224	345	20W	254	289	254N
195	329	25E	225	277	7S	255	294	15N
196	323	60E	226	338	11E	256	352	43E
197	293	12S	227	345	35W	257	332	62W
198	308	5N	228	345	16W	258	358	35W
199	353	1E	229	345	13W	259	348	26W
200	326	16E	230	335	19W	260	324	24W
201	275	10N	231	295	11S	261	349	13W
202	334	10W	232	292	20S	262	333	32W
203	319	0W	233	270	0 N	263	320	45E
204	342	37E	234	337	20E	264	358	26W

ID #	Strike	Dip	ID #	Strike	Dip	ID #	Strike	Dip
265	342	13W	295	323	10W	325	311	21S
266	330	30W	296	309	22E	326	349	4W
267	327	26W	297	329	14W	327	359	22W
268	297	15N	298	297	44N	328	358	25E
269	318	32E	299	358	45E	329	319	71S
270	277	31N	300	341	15W	330	355	84E
271	290	24N	301	354	16W	331	342	71W
272	320	31N	302	340	20W	332	340	72W
273	353	30E	303	355	25W	333	343	50N
274	333	7W	304	340	17W	334	270	41E
275	348	17E	305	313	11W	335	351	71E
276	272	17N	306	353	31W	336	355	72E
277	295	17N	307	324	16W	337	342	26W
278	333	85E	308	332	21W	338	345	22E
279	320	36N	309	343	18W	339	277	24N
280	279	34N	310	350	31W	340	330	8E
281	334	16W	311	347	22W	341	279	14N
282	337	16W	312	340	53W	342	337	36E
283	355	45W	313	335	23W	343	283	11S
284	326	16W	314	337	11W	344	348	23E
285	309	20N	315	292	14N	345	285	24N
286	302	35W	316	333	10E	346	360	8W
287	355	65E	317	281	5N	347	328	11E
288	324	28N	318	349	11W	348	320	26E
289	357	15W	319	337	34W	349	360	11E
290	350	42E	320	357	26W	350	344	16E
291	352	19W	321	358	27W	351	351	78E
292	353	26W	322	328	8W	352	270	25N
293	315	6W	323	355	56W	353	343	29E
294	344	9W	324	336	51E	354	292	21N

ID #	Strike	Dip	ID #	Strike	Dip	ID #	Strike	Dip
355	335	30E	385	303	34N	415	343	34E
356	273	21N	386	306	33N	416	342	63E
357	328	50E	387	313	26N	417	306	29E
358	330	41E	388	294	45E	418	290	56N
359	302	27E	389	293	39S	419	304	41N
360	296	24N	390	317	59W	420	330	44W
361	323	52E	391	319	63E	421	347	42W
362	307	40N	392	316	44E	422	332	32E
363	325	40N	393	315	31N	423	331	25E
364	317	24N	394	310	28N	424	298	18N
365	324	42N	395	325	28N	425	297	10N
366	340	17W	396	322	44N	426	308	20N
367	319	20E	397	273	26N	427	315	16N
368	319	39E	398	274	9N	428	313	19N
369	293	11N	399	348	26E	429	324	12N
370	325	8E	400	350	26E	430	307	7N
371	325	32E	401	300	26N	431	324	19E
372	319	55E	402	306	46N	432	322	9E
373	342	60E	403	306	52N	433	325	8S
374	336	53E	404	311	24N	434	360	18E
375	339	36E	405	330	19E	435	330	17E
376	329	43E	406	292	9N	436	317	9W
377	302	60E	407	305	6N	437	289	12N
378	327	50E	408	273	29N	438	360	6E
379	317	48W	409	317	23W	439	277	21N
380	317	44N	410	309	32N	440	331	19E
381	287	44N	411	290	35N	441	307	19N
382	283	35N	412	317	31N	442	328	27E
383	290	51N	413	326	35N	443	293	41N
384	275	44N	414	332	55N	444	331	28E

ID #	Strike	Dip	ID #	Strike	Dip	ID #	Strike	Dip
445	300	66W	475	306	18N	505	278	30N
446	279	12N	476	360	80W	506	340	20W
447	280	17N	477	318	28N	507	302	25W
448	277	22N	478	337	34W	508	318	21N
449	323	11N	479	283	30W	509	303	29N
450	353	30E	480	307	21N	510	278	12N
451	275	26N	481	277	29N	511	270	27N
452	270	28N	482	278	30N	512	356	33W
453	306	38N	483	295	34N	513	360	3E
454	297	32N	484	310	44N	514	318	46N
455	292	26N	485	323	36N	515	330	38E
456	278	22N	486	311	17N	516	323	22N
457	293	13N	487	329	35W	517	288	19N
458	319	30W	488	344	14E	518	276	22N
459	304	28N	489	325		519	325	24E
460	347	23W	490	320	22W	520	359	11W
461	301	18N	491	298	24W	521	357	38E
462	302	9N	492	300	21N	522	313	30E
463	275	9N	493	310	17N	523	276	17N
464	280	20N	494	279	12S	524	315	21W
465	358	46W	495	313	16N	525	353	68E
466	307	54S	496	346	29E	526	357	58E
467	305	46E	497	357	52E	527	333	46E
468	352	58E	498	349	72E	528	339	53E
469	292	31N	499	296	19N	529	353	46E
470	279	17N	500	300	9N	530	335	53E
471	347	41E	501	286	28N	531	343	84E
472	306	41N	502	298	18W	532	343	46E
473	331	29W	503	298	20S	533	349	70E
474	315	21N	504	292	14N	534	347	41E

ID #	Strike	Dip	ID #	Strike	Dip			
535	342	36E	565	316	16S	563	357	48W
564	2	05S	536	342	74E	566	272	11S
537	346	22E	567	272	7S			
538	342	65E	568	294	1S			
539	313	20N	569	292	11N			
540	357	20W	570	298	0N			
541	356	18W	571	325	26E			
542	357	6W	572	339	35W			
543	344	6W	573	342	12E			
544	349	15E	574	314	29N			
545	322	3N	575	314	18N			
546	360	20E	576	280	8N			
547	331	19W	577	294	3S			
548	315	7N	578	276	19N			
549	310	8N	579	273	36N			
550	317	18N	580	298	19N			
551	315	14E	581	353	63E			
552	317	7S	582	355	62E			
553	284	21N	583	351	51E			
554	353	1E	584	299	28S			
555	325	14E	585	303	10N			
556	323	7E	586	354	34W			
557	284	17N	587	360	7E			
558	291	40N	588	317	38N			
559	308	32N	589	354	15W			
560	273	22N	590	309	20S			
561	322	20E	591	320	11E			
562	335	42E	114	336	44W			
144	302	1S	174	332	31W			

TABLE 2: DRY HILLS Sample Age Results

Sample #	UTM	11T 0	error	Rock
6181	484390	4569604	8	Middle Etchart
6182	484069	4569669	13	Upper Etchart
6191	483410	4569741	5	Middle Etchart
6192	483355	4569801	0	Havallah.
6193	483293	4569615	19	Havallah
6194	483293	4569615	19	Havallah
6195	483670	4569759	14	Middle Etchart?
6196a	483801	4569798	5	Middle Etchart
6197b	483801	4569798	5	Upper Etchart
6211	483032	4568288	18	Middle Etchart
6212	483032	4568288	18	Upper Etchart
6213	483189	4568237	5	Upper Etchart / Middle Etchart / New Unit
6213	483244	4568054	11	
6214	483227	4567938	9	Middle Etchart
6215	483448	4567804	9	Lower Etchart
6215	483488	4567867	0	Lower Etchart
6231	483482	4568898	29	Sil
6232	483390	4568730	10	Lower Etchart
6233	483323	4568730	10	Upper Etchart or Middle Etchart
6234	483740	4568182	8	Lower Etchart
6235	483962	4568376	5	Lower Etchart

TABLE 3: THIN SECTIONS

Name	Unit	Description
CU3	F3 fault gouge	Highly deformed, fine grained crystalline micrite with abundant dolomitatization
CU4	Havallah Formation	Finely crystalline micrite with apparent dolomitization. Contains a single pebble sized-clast of micritic limestone that contains secondary dolomite crystals.
CU6	Upper Etchart conglomerate 1	Matrix supported conglomerate. Matrix is composed of well rounded, well sorted, quartzite cemented grains. Unit contains three clast types: (1) Clasts that are highly dolomitized into large crystalline dolomite. Fine grained micrite/wackestone grains supported in an opaque black, very finely crystalline rock composed of unknown mineral type. (2) Well rounded, well sorted crypto-crystalline quartz clasts (3) Sub-angular, poorly sorted, coarsely crystalline calcite/dolomite with strain twins
CU7	Upper Etchart conglomerate 2	Possibly clast supported conglomerate with a poorly sorted matrix consisting of sand sized angular quartzite, crystalline calcite, and crystalline dolomite fragments. Quartzite cemented. Unit has three types of clasts (1) Well sorted and well rounded pebble sized chert clasts and polycrystalline quartz. (2) Angular, pebble sized wackestone containing peloids and skeletal fragments. (3) Clasts consisting of black-opaque pebble sized angular - sub-angular clasts that contain

		their own microfractures that are filling with finely crystalline calcite.
CU10	lowest portion of Lower Etchart	Finely crystalline calcite/dolomite micrite with small, broken, skeletal fragment grains. Contains microfractures filled with a crystalline calcite/dolomite. Wispy appearing inclusions of a finely grained black/opaque mineral. Member contains a single pebble-sized clast of finely crystalline dolomite that is deformed in a sigma shape.
CU12	Havallah limestone	Finely calcite/dolomite micrite. Abundant fractures filled with crystalline calcite and quartz. Strain twins present in the calcite that may show an orientation preference.
CU15	Havallah Sequence from footwall of Havallah/Havallah fault zone 3 fault	Finely laminated micrite and crystalline quartzite. Shows signs of 2cdary recrystallization, and alteration. Highly deformed, with micro folds, micro parasitic folds, micro fractures, and micro foliations all common. Micro refolded folds infer multiple deformations from multiple orientations.
CU20	Middle Etchart member	Micrite with abundant small grained peloid wackestone. Secondary re-calcification. Rare microfractures filled with crystalline cement that displays strain twins and strain fringes.
CU21	Upper Etchart member	Crystalline calcite cemented grainstone. Grains are composed of skeletal fragments, fusulinids, and coral. Cement displays strain twinning. Microfractures in calcite with associated folding, implying strike slip movement(?) Microfractures are concentrated between grains.
CU28	Lower	Peloid wackestone with

	Etchart member	microfractures filled with crystalline quartz and calcite. Calcite and quartz in factures has strain fringes and strain twins. Matrix is micrite. Some grains have been dolomitized.
CU32	Lower Etchart sandstone channels	Mixture of sand sized well rounded quartz grains and sub-rounded crystalline calcite/dolomite fragments in a micrite matrix. Calcite crystal clast record strain twinning. Pores clearly visible in slide, indicating good porosity. Sand sized clasts make up ~50-60% of sample. Clasts are ~ 85% quartz fragments.
EMC	Lower Etchart limestone conglomerate	Clast supported conglomerate. Matrix consists of a mixture quartz cemented sand-sized skeletal fragment, quartz, and peloid grains. Possible fusulinid and coral fragments in the matrix along with skeletal fragments from bryozoans, mollusks, and bivalves. Matrix is mixed siliciclastic. Strain fringes common in cement. Interpreted to be from a nearby source area due to integrity of skeletal fragments. Clasts are: (1) sub-angular to rounded packestone, wackestone, and micrite. Clasts are surrounded by a quartz “rinds” that contain strain fringes. (2) pebble sized well rounded chert clasts.
NB	Miocene Basalt	Fine grained igneous rock containing plagioclase, pyroxene, and amphibole

TABLE 4. Bedding Measured Across Dry Hills Folds

Messured Fold Number	UTM (Y)	UTM (X)	UNIT	Bedding														
1			Upper Etchart	165; 20W	342; 16W	175; 22W	20; 46W	193; 30W	196; 42W	24; 35W	005; 15W	030; 35W						
2			Upper Etchart	005; 17W	294; 11N	316; 11W	138; 14SW	135; 13N	050; 10N	113; 17NE	135; 29N							
3	483770	4569094	Middle Etchart	201; 31W	206; 26W	205; 29W	203; 46W	200; 45W	203; 32W	017; 39W	005; 38W							
4	484390	4569604	Middle Etchart	258; 33N	225; 34W	037; 14NW	055; 05NW	224; 22NW	010; 15W	215; 14 NW								
5	483410	4569741	Middle Etchart	279; 26NW	225; 35NW	190; 25NW	251; 36NW	039;11NW	205; 12NW	259; 27NW	224; 25NW	262; 14SW						
6	483270	4569580	Havallah	051; 25N	064; 46N	152; 43NE	064; 46N											
7	483270	4569580	Havallah	193; 39W	121; 52W	021; 54W	196; 47W	029; 34W	026; 31W	012; 46S	320; 45SW	350; 35SW						
8	483032	4568288	Middle Etchart	198; 50W	186; 25W	180; 76 W												
9	483189	4568237	Upper Etchart	166; 03NE	332; 01NE	330; 05NE	148; 11S	186; 21S										
10	483244	4568054	Upper Etchart	035; 50W	015; 32SW													
10	483244	4568054	Upper Etchart	015; 32SW	315; 32NE													
11	483439	4568854	Upper Etchart	197; 24W	035; 18NW	190; 21W	152; 26SW	192; 18W	211; 16W	056; 18W	012; 24W	198; 26W	196; 28W	208; 35W				
12	483500	4569276	Upper Etchart	030; 50NW	357; 40W	100; 49S	185; 36W	102; 32S										
13			Upper Etchart	192; 35W	170; 31W	020; 23W	025; 17W	029; 21W	005; 25 NW	205; 20W	350; 38NE	020; 28SE	083; 05NW	217; 04NW	180; 04W	000; 46W	191; 27W	
14	482951	4568105	Upper Etchart	329; 22NE	140; 19NE	110; 19N	105; 20N	050; 15NW	197; 22W	205; 22W								
15	482961	4568109	Upper Etchart	213; 27NW	080; 21N	285; 20N	115; 27N	133; 30N	127; 32NE	330; 45NE								
16	482920	4568091	Upper Etchart	210; 41NW	007; 29W	315; 40NE	336; 43NE	305; 30NE										
17	48294	4568101	Upper Etchart	275; 17N	230; 19NE	250; 20N	325; 12NE	166; 40E	193; 21N	192; 22NW	107; 22N	050; 40NW	178; 90					
18	482945	4568020	Upper Etchart	132; 21NE	231; 41W	195; 40W	200; 27W											
19	482616	4566922	Upper Etchart	245; 25NW	252; 21N	290; 21N	103; 21N	230; 24NW	324; 31NW									
20	482621	4566933	Upper Etchart	230; 24NW	234; 31NW	210; 34W	200; 41NW	182; 50W	193; 41NW									
21	482589	4566900	Upper Etchart	287; 15N	247; 18N	248; 14N	252; 16NW	217; 21W	222; 20NW	226; 13NW	220; 24W							
22	482483	4566799	Upper Etchart	189; 20W	208; 15W	236; 11SW	050; 11NW	010; 13W	010; 27W									
23	481993	4567863	Upper Etchart	020; 45W	305; 30N	335; 40NE												
24	481794	4567645	Upper Etchart	324; 17NE	009; 11NE	181; 13E	310; 13N	089; 11N	207; 12W	023; 23W	221; 26NW							
25	481794	4567639	Upper Etchart	305; 33NE	300; 24N	151; 33N	172; 48NE	170; 48NE	165; 44NE	341; 42NE	354; 46NE	326; 37NE	124; 33N	132; 32N				
26	481779	4567614	Middle Etchart	339; 80NE	332; 75NE	336; 87NE	289; 27N	254; 32NW	241; 19NW									
27	481588	4567340	Upper Etchart	079; 31N	286; 29N	079; 32N	251; 27N	227; 24NW	221; 26NW	230; 25NW	284; 27NW	280; 14NW	270; 20NW	306; 20NW				
28	481686	4567342	Upper Etchart	308; 43NE	118; 44NE	314; 59NE	144; 52NE	298; 35N	304; 31NE	249; 24W	018; 16W	085; 13N	117; 08NW					
30	481590	4567375	Middle Etchart	221; 22NW	090; 26N	111; 20N	111; 26N	111; 30N	125; 30NE	115; 26N	124; 21N	296; 27N	116; 27N	113; 24N	120; 26N	305; 29N	325; 60N	327; 35N
31			Lower Etchart	254; 24NW	347; 23E	291; 11W	275; 24NE											
32			Lower Etchart	032; 85SE	346; 17E	066;NW												

TABLE 5. List of Measured Folds

Fold index

Hinge Plunge	Hinge trend	UNIT	UTM (X)	UTM (Y)
1	173	Middle Etchart	4568237	483189
29	75	Upper Etchart	4568054	483244
33	15	Middle Etchart	4569580	483270
21	337	Middle Etchart	4567375	481590
24	308	Upper Etchart	4567340	481588
42	356	Middle Etchart	4568026	482953
19	353	Upper Etchart	4568026	482953
14	22	Upper Etchart	4566749	482479
29	7	Upper Etchart	4566749	482479
19	228	Upper Etchart	4566749	482479
46	22	Upper Etchart	4566749	482479
53	8	Upper Etchart	4566749	482479
13	350	Upper Etchart	4568105	482951
23	352	Upper Etchart	4568091	482920
17	5	Upper Etchart	4568101	48294
31	240	Havallah	4569746	483355
10	245	Havallah	4569236	482984
35	34	Havallah	4569510	483196
5	300	Upper Etchart	4569746	484368
11	327	Middle Etchart	4568876	484007
10	165	Middle Etchart	4568931	483799
19	325	Upper Etchart	4569004	483668
12	34	Upper Etchart	4568179	483199
24	330	Upper Etchart	4568078	483134
14	341	Upper Etchart	4568193	483016
22	32	Upper Etchart	4568371	482846
14	29	Upper Etchart	4568068	482898
31	330	Upper Etchart	4566933	482621
30	25	Middle Etchart	4567614	481779
20	1	Upper Etchart	4566922	482616
40	260	Havallah	4569580	483270
15	318	Upper Etchart	483770	4569094
7	207	Havallah	4568288	483032
7	28	Upper Etchart	4568054	483244
16	296	Upper Etchart	4568854	483439
31	237	Upper Etchart	4569276	483500
20	350	Upper Etchart	4568109	482961
11	358	Upper Etchart	4568020	482945
26	273	Upper Etchart	4568020	482945
13	2	Upper Etchart	4566900	482589
9	350	Upper Etchart	4566799	482483
24	355	Upper Etchart	4567863	481993
6	16	Upper Etchart	4567645	481794
31	22	Upper Etchart	4567639	481794
16	319	Upper Etchart	4567342	481686

Fold index

Hinge Plunge	Hinge trend	UNIT	UTM (X)	UTM (Y)
4	16	Upper Etchart	4569094	483770
4	239	Middle Etchart	4569604	484390
16	217	Upper Etchart	483770	4569094
19	348	Upper Etchart	4568089	482735
33	2	Upper Etchart	457995	482929
29	293	Upper Etchart	4567936	482884
22	338	Upper Etchart	4567912	483047
42	357	Upper Etchart	4567964	482888
30	225	Upper Etchart	4567922	482287
26	270	Upper Etchart	4567662	481764
14	323	Upper Etchart	4567399	481764
31	18	Upper Etchart	4567375	481604
18	345	Upper Etchart	4567007	481688
30	346	Upper Etchart	4566872	481767
21	16	Upper Etchart	4566934	481851
15	271	Middle Etchart	45695800	483270
6	302	Lower Etchart	4566092	481199
3	47	Lower Etchart	4565742	480769
10	10	Lower Etchart	4565915	480720
24	232	Lower Etchart	4565683	480575
16	26	Upper Etchart	4566192	480481
54	39	Upper Etchart	4566192	480421
34	12	Upper Etchart	4566259	480425
36	46	Upper Etchart	4566250	480329
29	340	Upper Etchart	4566361	480341
29	359	Upper Etchart	4566424	480397
24	33	Upper Etchart	4566456	480468
5	192	Lower Etchart	4566162	480481
11	13	Lower Etchart	4566192	480421
9	319	Lower Etchart	4566259	480425
31	202	Lower Etchart	4566250	480329
15	82	Lower Etchart	4566361	480341
13	24	Lower Etchart	4566424	480397
9	149	Lower Etchart	4566456	480468

STRATIGRAPHIC UNITS

Qau — Quaternary Alluvium, Undivided
Unit consists of unconsolidated reddish-brown, brown, to dark brown sand, silt, and clay with intermixed cobble to pebble-size basalt, carbonate, and silisiclastic clasts.

Qah — Quaternary Alluvium, Havallah Derived
Unit consists of brown to medium-brown clay-sized and silt-sized particles. Unit largely lacks clasts which is diagnostic of the unit.

Qae — Quaternary Alluvium, Etchart Derived
Unit has light-tan to brown sand, silt, and clay sized particle matrix. Abundance of reddish brown, brown, red, and orange pebble to sand sized clasts that are commonly chip shaped, and occasionally contain slickenlines are diagnostic of the unit. Unit also contains pebble to cobble sized carbonate clasts.

Qab — Quaternary Alluvium; Basalt Derived
Light tan to light reddish-brown silt, sand, clay sized particles matrix with cobble to pebble sized vesicular basalt clasts.

Qj — Jasperiod
Highly siliceous well cemented limestone/siltstone. Unit chert, quartzite and jasperiod and minor limestone inclusions. Units weathers to Reddish/Brown and is pink to light and dark gray in fresh cut. Displays many deformational characteristics, such as gash fracturing, small and large scale folding, and slicken lines. Unit is commonly found within and in close proximately to fault zones. Silica within this unit is deposited via dissolution of carbonates and replacement of silica. Unit commonly contains silica cemented highly angular breccias.

Mb — Miocene Unnamed Basalt and Andesite
Unit is dark reddish-brown weathering (Very Dusky Red; 10R 2/2) and dark gray on a fresh surface (N3). Unit consists of heavily and evenly vesiculated basalt and andesite, with no secondary mineralization within vesicles. Sporadic, thin layers and zones lacking vesicles occur locally lower in outcrops, but not laterally continuously indicative of bedding. Unit weathers to a somewhat rounded appearance in the unit. Unit is nonporphyritic. Unit is massive with no bedding horizons or visible evidence of multiple flows.

MPh — Light gray (N7) on fresh surface highly grainstone, packestone, wackestone, and micrite that weather to yellowish gray (5Y 7/2). Unit is interbedded commonly with siltstone, silty limestone, chert, argillite, sandstone, and jasperiod. Bedding thickness varies, but is usually thin to moderate thick, and very well bedded. Commonly unit displays extensive secondary silisiclastic alteration and extreme structural deformation. Unit is consistent with descriptions of the Mills Canyon or Trenton members of the Havallah Formation.

Pc1 — Upper Etchart Conglomerate 1
Clasts supported conglomerate consisting of pebble-to-boulder sized clasts. Clasts consist of Atokan-age sub-angular limestone clasts, and sub-rounded to rounded chert, and lithic clasts. Average clast size is pebble. Chert and sandstone clasts are moderate-to-well sorted. Limestone clasts are poorly-sorted. Limestone clasts range in size from cobble-to-boulder, where as most other clasts are pebble sized. Matrix is reddish-to-orange (5YR 5/6) weathering and gray to light gray on a fresh surface. Matrix consists of sand and silt sized carbonate and siliceous particles abundant within interstitial spaces. Poor to moderate imbrication of clasts occurs uncommonly.

Pc2: — Upper Etchart Conglomerate2

Pue — Upper Etchart member
Fresh surface is light to medium gray (5b 5/1 – N1) weathers to medium gray (N6-N7) well-bedded packestone/grainstone composed of well-sorted, sand-sized, pelletiod and skeletal grains. Matrix material is crystalline dolomite and calcite, with rare amounts of secondary chert solidification. Contains sporadic, very thin (< 1 cm thick) interbeds of siliceous and calcareous siltstone/mudstone. Member commonly contains medium to thickly inner-bedded ribbon chert layers and chert nodules. Interbedded, very thin, silty-sandy stingers are common. Member displays pinches and swells and sporadic cross trough stratification. Fossils within member include large amounts of fusulinids, conodant, crinoids, brachiopods, and corral fragments.

IPPme — Member is a dark gray (N6) weathering, dark gray (N6) on a fresh surface, silty packestone to micrite. Packestone and wackestone grains are peliods in a calcite and dolomite mud matrix. Thick beds are poorly-bedded. Weathered surface uncommonly displays a textural surface that resembles corral. Contains interbedded chert beds up to 30 cm thick, silty-sized calcite sand grains, cemented with calcite and dolomite, with rare fossils, including fusulinids, coral, and crinoids. Member weathers to smooth edges, and commonly breaks into small lithics or powder when struck. Member is very difficult to break into large pieces. Fossils within member include moderate to small amounts of fusulinids, conodant, crinoids, corral fragments, pellets, and peliods.

IPs — Lower Etchart Interbedded Chert
2-5 meter thick beds of massive chert beds

IPst — IPs: Lower Etchart Sandstone
Sandstone in channels is white, off-white, to light tan, fine-grained, well cemented, well sorted with cross trough stratification visible locally. Some sandstone channels contain wackestone-grainstone carbonate grainstone cut and fill channels.

IPlec1 — Lower Etchart Conglomerate 1
Clasts supported conglomerate consisting of pebble sized, rounded to well rounded dark to light gray chert, and reddish to pink quartzite clast. Clasts are very well sorted and are very well cemented by a crystalline gray calcite.

IPlec2 — Lower Etchart Conglomerate 2
Unit is conglomerate with pebble to cobble sized, gray crystalline limestone clasts supported by crystalline calcite and quart matrix. Small secondary chert nodules are common as is re-solidification around clasts. Clasts are sub-angular to sub-rounded and moderately sorted.

IPle — Pennsylvanian (Atokan) Lower Etchart Formation
Very thin to thick-bedded, dark gray (N3) silty dolostone, wackestone, and micrite that weathers to dark gray, medium gray, and light gray, with the dominate color being medium gray (N4). Fresh surface can also appear speckled white and medium gray, due to extensive secondary calcite recrystallization. Sporadic grains are peliods, and are commonly dolomitized. Member is generally moderately-to-poorly bedded. Member is massive in areas, but commonly poorly bedded, and locally contains rare cross trough stratification. Weathered surface commonly displays a texture that resembles coral. Member also sporadically contains alternating dark and light bands of micrite. Lower section conformability transitions to thick (10's of meters scale) massive black micrite. Member generally lacks fossils.

GN MN
0°20'
6 MILS
17°
320 MILS

N

Nevada

Quadrangles (7.5')
1
2
1. Dry Hills North
2. Dry Hills South

Symbols

Stratigraphic contact, dashed where approximately located

Plunging fold(s), calculated from strike and dip messurements of bedding along fold limbs and across hinge; Fold orientation geometricly calculated

Plunging fold(s), fold geometry messured in the field

Thrust Fault showing dip where messured, dashed where approximately located, dotted where concealed; triangle on the up-thurst side

Normal Fault showing dip where messured, dashed were approximately located, dotted where concealed; ball and bar on the down-thrown side

Strike and dip of bedding

0 250 500 750 1000
Scale in Meters

Drafted by
Samuel Siebenaler,

484 485 485

B'

Plate 1


481000mE
45 74
45 73
45 72
45 71
45 70
45 69
45 68
45 67
45 66
45 65
45 64
482
483
BM4928
BM 5352
HILLS
TRAIL
JEEP
A
A'
B
D
D'
E
E'
H

Plate 2

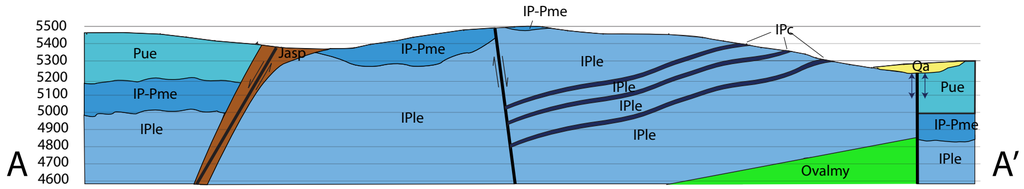
A
A′
IP-Pme
IPc
Pue
Jasp
IP-Pme
IPle
IPle
IPle
IPle
IPle
Qa
Pue
IP-Pme
IPle
Ovalmy
5500
5400
5300
5200
5100
5000
4900
4800
4700
4600

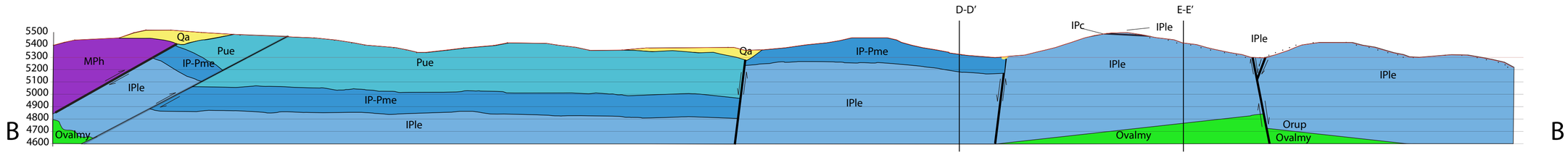
B
B
D-D′
E-E′
Qa
MPh
Pue
IP-Pme
IPle
Pue
IP-Pme
IPle
Ovalmy
Qa
IP-Pme
IPle
IPc
IPle
IPle
IPle
IPle
Ovalmy
Orup
Ovalmy
5500
5400
5300
5200
5100
5000
4900
4800
4700
4600

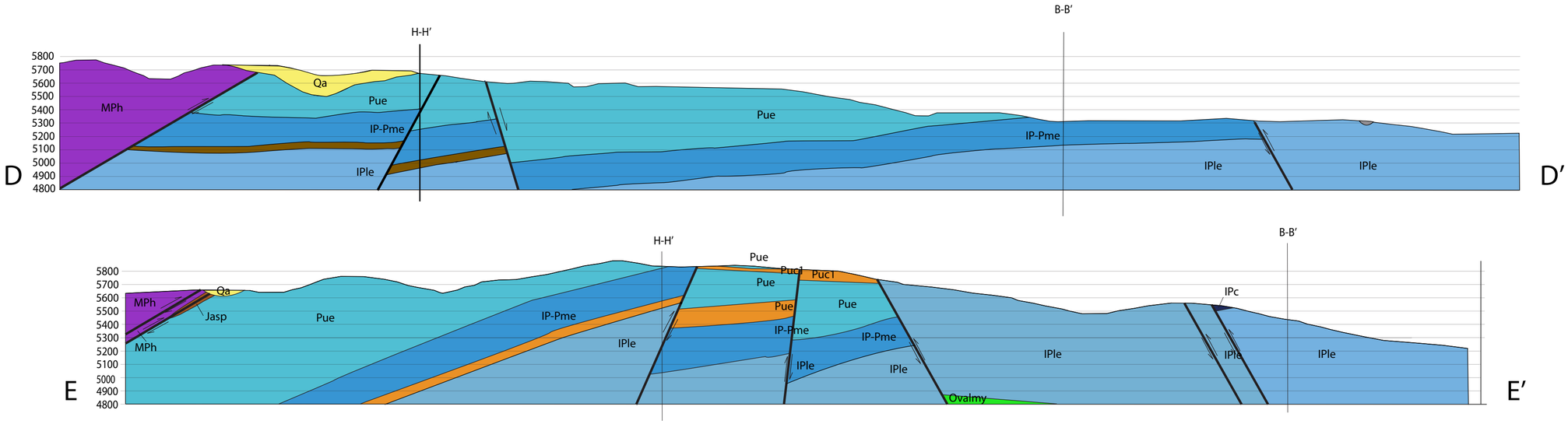
D
D′
H-H′
B-B′
Qa
MPh
Pue
IP-Pme
IPle
Pue
IP-Pme
IPle
IPle
5800
5700
5600
5500
5400
5300
5200
5100
5000
4900
4800

E
E′
H-H′
B-B′
MPh
Qa
Jasp
MPh
Pue
IP-Pme
IPle
Pue
Puc1
Puc1
Pue
Pue
Pue
IP-Pme
IP-Pme
IPle
IPle
IPle
IPle
IPc
IPle
IPle
Ovalmy
5800
5700
5600
5500
5400
5300
5200
5100
5000
4900
4800

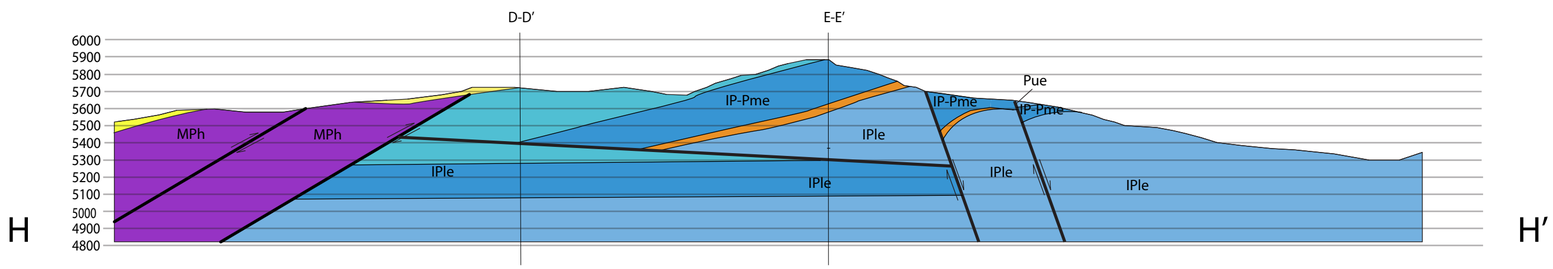
H
H′
D-D′
E-E′
MPh
MPh
IP-Pme
IPle
IPle
IPle
IP-Pme
IP-Pme
IP-Pme
Pue
IPle
IPle
IPle
6000
5900
5800
5700
5600
5500
5400
5300
5200
5100
5000
4900
4800

Plate 3

VITA

Graduate College
University of Nevada, Las Vegas

Samuel Anthony Siebenaler

Degrees:
Bachelor of Science, Geosciences; Geology, 2007
Winona State University

Publications:

Siebenaler, S. Vore, J., Grey, Z., and Briggs, T., 2010, Newmont Geologic Mapping in the Surface Pit Mining Environment of Northern Nevada; Examples from Carlin, Phoenix, and Twin Creeks Mine Sites: Geological Society of America Abstracts with Programs, v. 42, no. 5, p. 581.

Siebenaler, S. A., Taylor, W.J., Cashman, P.H., Trexler, J.H., and Davydov, V.I., 2008, Structural and biochronologic analysis of the northern Dry Hill, Humboldt County, Nevada [abs.]: Geological Society of America Rocky Mountain Section Meeting, v.40, p. 39.

Taylor, W. J., Siebenaler, S., Cashman, P., Trexler, J., Davydov, V., 2008, Seven post-Pennsylvanian structural events in the Dry Hills and Northern Osgood Mountains: Evidence of Late Paleozoic tectonism and new Getchell fault offset data [abs.]: American Geophysical Union, #T21B-1972.

Siebenaler, S. A. and Taylor, W.J., 2007, Structural analysis of the Pennsylvanian to Permian Etchart Formation in the northern Dry Hills, Humboldt County, Nevada [abs.]: University Of Nevada Las Vegas Geosynposium.

Anderson J. L. B.; Cintala, M. J.; Siebenaler, S. A.; Barnouin-Jha, O. S., 2007, Ejecta- and Size-Scaling Considerations from Impacts of Glass Projectiles into Sand [abs.]: Lunar and Planetary Science Conference, No. 1338, p.2266

Awards:
Geological Society of Nevada scholarship
Brenada E. French Scholarship in Geology
Geological Society of Nevada Foundation Fund Scholarship
UNLV Graduate & Professional Student Association grant

Military Medals/Awards:
Army Commendation Medal

Good Conduct Medal
Army Achievement Medal
Global War on Terror Service Medal
Army Service Ribbon
Overseas Service Ribbon

Thesis Title: Late Paleozoic Deformation in the Osgood Mountains and Dry Hills, Northern Nevada

Thesis Examination Committee:

Chairperson, Dr. Wanda Taylor, Ph.D.
Committee Member, Dr. Patricia Cashman, Ph.D.
Committee Member, Dr. Andrew Hanson, Ph.D.
Committee Member, Dr. Eugene Smith, Ph.D.
Committee Member, Chih-Hsiang Ho, Ph.D.